University of the Witwatersrand

Doctoral Thesis

SYMBOL LEVEL DECODING OF REED-SOLOMON CODES WITH IMPROVED RELIABILITY INFORMATION OVER FADING CHANNELS

Author:

Olayinka Olaolu Ogundile

A thesis submitted in fulfilment of the requirements for the degree of Doctor of Philosophy

in the

School of Electrical and Information Engineering

March 2016

The financial assistance of the National Research Foundation (NRF) towards this research is hereby acknowledged. Opinions expressed and conclusions arrived at, are those of the author and are not necessarily to be attributed to the NRF.

Declaration

I, Ogundile, Olayinka Olaolu, declare that this thesis titled, "Symbol Level Decoding of Reed-Solomon Codes with Improved Reliability Information Over Fading Channels" and the work presented in it are my own. I confirm that:

- This work was done wholly or mainly while in candidature for a research degree at this University.
- Where any part of this thesis has previously been submitted for a degree or any other qualification at this University or any other institution, this has been clearly stated.
- Where I have consulted the published work of others, this is always clearly attributed.
- Where I have quoted from the work of others, the source is always given. With the exception of such quotations, this thesis is entirely my own work.
- I have acknowledged all main sources of help.

Signed: _____

Date: _____

UNIVERSITY OF THE WITWATERSRAND

Abstract

Engineering and the Built Environment
School of Electrical and Information Engineering

Doctor of Philosophy

SYMBOL LEVEL DECODING OF REED-SOLOMON CODES WITH IMPROVED RELIABILITY INFORMATION OVER FADING CHANNELS

by Olayinka Olaolu Ogundile

Supervisor: Dr. D.J.J. Versfeld

Reliable and efficient data transmission have been the subject of current research, most especially in realistic channels such as the Rayleigh fading channels. The focus of every new technique is to improve the transmission reliability and to increase the transmission capacity of the communication links for more information to be transmitted. Modulation schemes such as M-ary Quadrature Amplitude Modulation (M-QAM) and Orthogonal Frequency Division Multiplexing (OFDM) were developed to increase the transmission capacity of communication links without additional bandwidth expansion, and to reduce the design complexity of communication systems.

On the contrary, due to the varying nature of communication channels, the message transmission reliability is subjected to a couple of factors. These factors include the channel estimation techniques and Forward Error Correction schemes (FEC) used in improving the message reliability. Innumerable channel estimation techniques have been proposed independently, and in combination with different FEC schemes in order to improve the message reliability. The emphasis have been to improve the channel estimation performance, bandwidth and power consumption, and the implementation time complexity of the estimation techniques.

Of particular interest, FEC schemes such as Reed-Solomon (RS) codes, Turbo codes, Low Density Parity Check (LDPC) codes, Hamming codes, and Permutation codes, are proposed to improve the message transmission reliability of communication links. Turbo and LDPC codes have been used extensively to combat the varying nature of communication channels, most especially in joint iterative channel estimation and decoding receiver structures. In this thesis, attention is focused on using RS codes to improve the message reliability of a communication link because RS codes have good capability of correcting random and burst errors, and are useful in different wireless applications.

This study concentrates on symbol level soft decision decoding of RS codes. In this regards, a novel symbol level iterative soft decision decoder for RS codes based on parity-check equations is developed. This Parity-check matrix Transformation Algorithm (PTA) is based on the soft reliability information derived from the channel output in order to perform syndrome checks in an iterative process. Performance analysis verify that this developed PTA outperforms the conventional RS hard decision decoding algorithms and the symbol level Koetter and Vardy (KV) RS soft decision decoding algorithm.

In addition, this thesis develops an improved Distance Metric (DM) method of deriving reliability information over Rayleigh fading channels for combined demodulation with symbol level RS soft decision decoding algorithms. The newly proposed DM method incorporates the channel state information in deriving the soft reliability information over Rayleigh fading channels. Analysis verify that this developed metric enhances the performance of symbol level RS soft decision decoders in comparison with the conventional method. Although, in this thesis, the performance of the developed DM method of deriving soft reliability information over Rayleigh fading channels is only verified for symbol level RS soft decision decoders, it is applicable to any symbol level soft decision decoding FEC scheme.

Besides, the performance of the all FEC decoding schemes plummet as a result of the Rayleigh fading channels. This engender the development of joint iterative

channel estimation and decoding receiver structures in order to improve the message reliability, most especially with Turbo and LDPC codes as the FEC schemes. As such, this thesis develops the first joint iterative channel estimation and Reed-Solomon decoding receiver structure. Essentially, the joint iterative channel estimation and RS decoding receiver is developed based on the existing symbol level soft decision KV algorithm. Consequently, the joint iterative channel estimation and RS decoding receiver is extended to the developed RS parity-check matrix transformation algorithm. The PTA provides design ease and flexibility, and lesser computational time complexity in an iterative receiver structure in comparison with the KV algorithm.

Generally, the findings of this thesis are relevant in improving the message transmission reliability of a communication link with RS codes. For instance, it is pertinent to numerous data transmission technologies such as Digital Audio Broadcasting (DAB), Digital Video Broadcasting (DVB), Digital Subscriber Line (DSL), WiMAX, and long distance satellite communications. Equally, the developed, less computationally intensive, and performance efficient symbol level decoding algorithm for RS codes can be use in consumer technologies like compact disc and digital versatile disc.

Dedicated to God Almighty.

Acknowledgements

All praises be to God Almighty for His Love and Mercy over my life, most especially for giving me the strength throughout this PhD programme.

My profound gratitude goes to my supervisor, Dr. D.J.J. Versfeld, whose wealth of knowledge, experience, suggestions, and guidance has facilitated the fruitful completion of this PhD programme. I am surprised as every day passes at his sincere integrity, and commitment towards my research. His advice, encouragements, and corrections toward this work are outstanding. God bless you Sir! Amen.

Special thanks to my loving parents Col. S.O. Ogundile (rtd) and Mrs. R.O. Ogundile, my brother Capt. E.O. Ogundile, and the entire Ogundile's family for their uncompromising support during this programme. I love you all.

I am extremely grateful to the School of Electrical and Information Engineering, University of the Witwatersrand. The financial support of the Centre for Telecommunication Access and Services (CeTAS), the University of the Witwatersrand, Johannesburg, South Africa is also acknowledged. Besides, am deeply grateful to the CeTAS group for sponsoring my conference trips.

I want to also thank my home University, Tai Solarin University of Education, Ijagun, Ijebu-ode, Ogun state, Nigeria, for entrusting in me. Most especially, I am grateful to my colleagues in the Department of Physics and Telecommunications for their support towards the successful completion of my programme.

Finally, I am grateful to all other people who have contributed in one way or the other to the success of this PhD programme, most especially, the past and present CeTAS group members. May the Almighty God bless you all! Amen

Contents

List of Figures

List of Tables

CHAPTER 1

Introduction

Since early times, people endlessly created new techniques and technologies to communicate their messages and ideas to each other. Consequently, over the years, different types of increasingly complex communication systems have been devised for people to communicate or transmit their messages. The concept behind each new technique is to improve the transmission reliability and to increase the transmission capacity of the communication links for more information to be transmitted [1]. In the past decades, modulation techniques were developed to improve the transmission capacity, compatibility, message security and quality of the communication system. Modulation techniques provide more flexibility and trade-offs to optimize the efficiency of the communication system design. Fig. 1.1 shows a basic block diagram of a simple communication system.

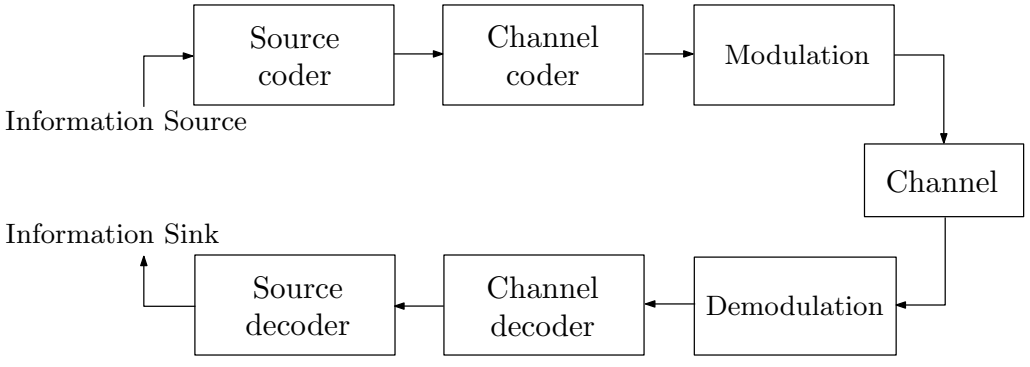

FIGURE 1.1: Block diagram of a communication system [1].

However, developers of communication systems face different challenges using these modulation techniques. Most common is the bandwidth limitations in transmitting the data, and the data transmission rate of the systems. Due to the transmission bandwidth limitations and high data transmission rate demand, higher

order modulation schemes are needed in order to optimise the spectral efficiency. Modulation schemes such as M-ary Quadrature Amplitude Modulation (M-QAM) and Orthogonal Frequency Division Multiplexing (OFDM) systems are capable of achieving better transmission bit rates with little or no bandwidth expansion. These modulation systems provide developers with design flexibility, high spectral efficiency and narrow power spectrum [2]. Accordingly, attention is focused on these modulation schemes because of their aforementioned advantages. In particular, this thesis concentrates on rectangular 16-QAM (M =16) systems. Fig. 1.2 shows the rectangular 16-QAM signal constellation with the sequence of information bit to symbol mapping used in this thesis. In the thesis, it is assumed that the modulated transmitted 16-QAM sequence is $S = S_{Re} + jS_{Im}$, with $S_{Re}, S_{Im} \in \{\pm 1, \pm 3\}$ [1 ,2]. Each of the modulation symbol is derived from the information bits $b = \{b_1, b_2, b_3, b_4\}$ as shown in Table 1.1.

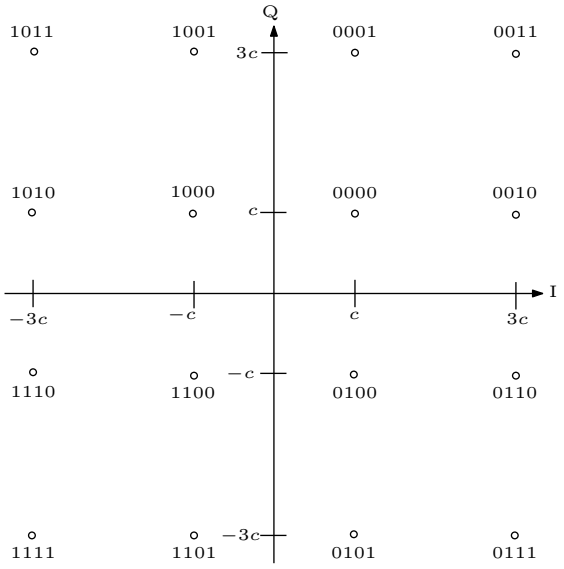

FIGURE 1.2: Rectangular 16-QAM constellation diagram.

TABLE 1.1: 16-QAM information bit to symbol mapping.

b_1b_3	Re	b_2b_4	Im
10	-1	10	-1
11	-3	11	-3
01	+3	01	+3
00	+1	00	+1

Notwithstanding, improving the message reliability (in other words, improving the probability of detecting the correct message) of a communication link using these modulation schemes have been a major challenge due to the varying properties of communication channels. The most common and realistic channel to model a wireless communication link is the Rayleigh fading channel. Accordingly, the thesis assumed Jakes's isotropic scattering model [3] for the complex Rayleigh fading with zero mean and unit variance (variance = 1). Variations in the channel properties due to multipath propagation and Doppler effects can distort the structure of the transmitted message prior to detection. In return, this plummets the performance of modulation schemes and the overall communication system. Therefore, it is important to properly estimate and compensate for these channel errors in order to enhance the probability of a correct message detection. Many channel estimation techniques have been proposed independently, and in combination with different Forward Error Correction (FEC) schemes in order to improve the message reliability. The emphasis have been to improve the channel estimation performance, bandwidth and power consumption, and the implementation time complexity of the estimation techniques.

With respect to the channel estimation techniques, FEC schemes such as Reed-Solomon (RS) codes, Turbo codes, Low Density Parity Check (LDPC) codes, Hamming codes, and Permutation codes, are used to improve the message reliability of a communication link. FEC schemes automatically correct errors detected at the receiver of a communication system. Error correcting codes are used in state of the art wireless applications in order to provide efficient data transmission over fading channels. With error correcting codes, the performance of the modulation schemes can be improved in a couple of ways. Of particular interest, error correcting codes are deployed in joint iterative channel estimation and decoding receiver structures in order to improve the message reliability. Thus, construction of good FEC decoding schemes to combat these mitigating channel conditions in whichever capacity have been the subject of recent research.

When transmitting over Rayleigh fading channels, Turbo and LDPC codes have been used extensively to combat the varying nature of communication channels,

most especially in joint iterative channel estimation and decoding receiver structures. In this thesis, attention is focused on using RS codes introduced in [4] to improve the message reliability of a communication link because RS codes have good capability of correcting random and burst errors [5, 6], and are useful in different wireless applications. More so, the study is centred on symbol level soft decision decoding of RS codes. Additionally, since the thesis concentrates on 16-QAM systems, $GF(2^4)$ (GF-Galois Field) is assumed. However, most of the results in this thesis can be extended to longer codes (for example, $GF(2^6)$ and $GF(2^8)$, where higher M-QAM systems such as 64-QAM and 256-QAM can be adopted.

1.1 Research Question

Although FEC schemes have been used extensively over fading channels to improve the message reliability of communication links, RS codes have not been widely used partly because it exhibits high decoding complexity. RS codes form an important class of linear block codes capable of correcting random symbol errors, as well as burst errors [5, 6]. As such, extensive investigation on improving the message reliability over Rayleigh fading channels using RS codes is extremely important because RS codes are useful in numerous wireless applications (see Section 1.5). For example, extensive investigations on improving the message reliability using Turbo and LDPC codes over Rayleigh fading channels have revealed the strong error correcting capabilities of these FEC schemes. Aside the efficient decoding algorithms proposed for these FEC schemes (Turbo and LDPC codes) in literature, the investigations also engender the development of joint iterative channel estimation and decoding receiver structures in order to combat the mitigating Rayleigh fading channel conditions. Therefore, extensive investigations on improving the message reliability using RS codes in severe Rayleigh fading channel conditions can guarantee better message transmission success.

Accordingly, in this thesis, the broad research question is stated as:

- *Can the performance of communication systems with Reed-Solomon codes be enhanced over Rayleigh fading channels such that the probability of correct message detection is significantly improved?*

1.2 Research Hypotheses

Koetter and Vardy [7] proposed a symbol level soft RS decoder applied to the Guruswami and Sudan (GS) RS list decoding algorithm [13, 14]. The work in [7] was verified to reduce errors in Additive White Gaussian Noise (AWGN) channels and Rayleigh fading channels using M-QAM. Results in [7] shows significant performance improvement (between 1-3dB gain) in the Codeword Error Rate (CER - is the probability of the decoder making an incorrect codeword decision) over Rayleigh fading channels in comparison to previous RS decoding algorithms [13-19]. Other important soft decoding algorithms for RS codes are found in [20, 21]; however, they are bit level based soft decoding algorithms. Soft FEC decoders basically use reliability information from the channel output to improve the message reliability over Rayleigh fading channels. Nevertheless, most soft FEC decoders do not take into account the CSI when deriving these reliability information. Take for example, the KV decoder proposed in [7] do not incorporate the CSI while deriving the soft reliability information from the channel output. The performance of the KV algebraic soft decision decoding algorithm or most soft decision decoding algorithms can further be improved if the CSI is taken into consideration while deriving the reliability information. Hence, this thesis is first focused at incorporating the CSI in deriving soft reliability information over Rayleigh fading channels for symbol level soft decision decoders.

In addition, the KV algorithm or any viable RS soft decoder can be deployed in a joint iterative channel estimation and decoding receiver structure to enhance its performance over Rayleigh fading channels. Besides, from literature, see for instances [8-12], the performance of Turbo and LDPC codes are improved over Rayleigh fading channels when deployed in a joint iterative channel estimation and decoding receiver structure. Consequently, this thesis proposes to enhance

the performance of *RS* codes over Rayleigh fading channels in a similar approach. In return, this will improve the message reliability over Rayleigh fading channels in comparison with when the symbol level *RS* soft decision decoding algorithms are only combined with the demodulator. Note, the primary aim of deploying *RS* codes in an iterative receiver structure in this thesis is not to compare between codes (*RS* codes, Turbo codes, or LDPC codes), rather, the introduction of *RS* codes in an iterative receiver structure because of its numerous advantages in wireless applications.

Finally, the combined soft decision decoder based on the *KV* algorithm [7] applied to the *GS* decoder [13, 14] exhibits very high computational time complexity. As such, the computational time complexity worsen when deployed in an iterative receiver structure. In this regard, a less computationally intensive, and performance efficient symbol level soft decision decoding algorithm for *RS* codes is developed. Essentially, the symbol level *RS* soft decision decoding algorithm is developed to improve the message reliability of communication links at reduced computational time complexity. This developed algorithm provides design ease and flexibility, and lesser computational time complexity in an iterative receiver structure in comparison with the *KV* algorithm.

Therefore, as a starting point for investigations, three key hypotheses are stated in order to answer this research question.

1. *Incorporating the channel state information in deriving soft reliability information over Rayleigh fading channels will yield better performance in comparison with when the CSI is not taken into consideration.*

2. *A symbol level iterative soft decision decoder for RS codes based on parity-check equations will outperform the conventional RS hard decision decoding algorithms and the symbol level Koetter and Vardy RS soft decision decoding algorithm.*

3. *Adapting symbol level RS soft decision decoding algorithms in a joint iterative channel estimation and decoding receiver structure will yield a better*

performance in comparison with when the symbol level RS soft decision decoding algorithms are only combined with the demodulator.

1.3 Research Aim and Objectives

The development of a reliable and efficient technique of improving the message reliability of a communication link is paramount in today's communication society. In this regard, this study is aimed at enhancing the message reliability over Rayleigh fading channels using FEC schemes, in particular, the *RS* codes. To achieve the aim of this study, the following objectives are highlighted.

1. *To develop a reliable and efficient way of deriving soft reliability information over Rayleigh fading channels for symbol level soft decision decoding FEC schemes.*

2. *To develop a joint iterative channel estimation and decoding receiver based on the existing symbol level Koetter and Vardy RS algorithm.*

3. *To develop a novel, less computationally intensive, and performance efficient symbol level soft decision decoding algorithm for RS codes*

4. *To adapt the the novel symbol level RS soft decision decoding algorithm in a joint iterative channel estimation and decoding receiver structure.*

5. *To model and simulate the proposed algorithms in (1)-(4) using Matrix Laboratory (MATLAB) software.*

1.4 Research Argument

As expounded in Section 1.2, the thesis arrived at three key hypotheses based on the broad research question in Section 1.1. Consider the simple joint iterative channel estimation and *RS* decoding receiver structure shown in Fig. 1.3. Assume the input to the receiver experiences fading as a result of the Rayleigh channel.

With respect to the channel estimation technique employed, the combined demodulation and *RS* decoder (Fig. 1.3 without the dotted lines) requires reliability information from the channel output in order to efficiently demodulate and decode the received signal. In most cases, the reliability information fed into the soft decoder determines the performance of the decoder. With this in mind, devising a reliable and efficient way of deriving reliability information over Rayleigh fading channels is paramount towards improving the performance of the *RS* decoder. This thesis proposes an efficient method of deriving reliability information over Rayleigh fading channels by incorporating the estimated channel state information. It is proven in this thesis that this method improves the message reliability over Rayleigh fading channels in comparison with the conventional method in [5, 6, 22]. Chapters 2 and 3 give the CER performance proof, subsequently verifying Hypothesis (1) of this thesis.

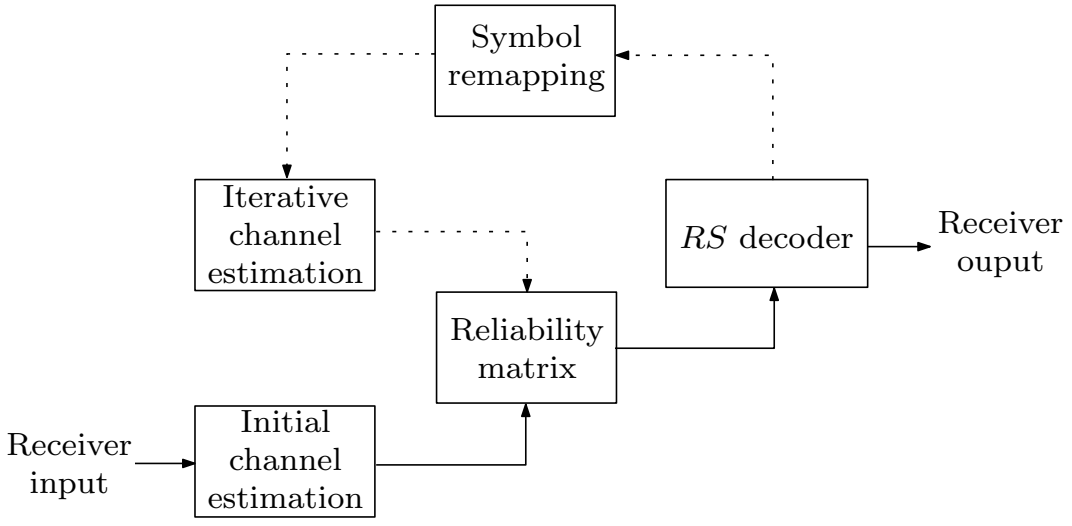

FIGURE 1.3: Simple block diagram of a joint iterative channel estimation and *RS* decoding receiver structure.

Additionally, as shown in Fig. 1.3, the *RS* decoder forms an important block for the successful transmission of the messages over Rayleigh fading channels. Consequently, developing a less computationally intensive, and performance efficient symbol level soft decision decoding algorithm for *RS* codes is essential. With good reliability information from the channel output, an efficient *RS* decoding algorithm will further improve the performance of the combined demodulation and decoding receiver (Fig. 1.3 without the dotted lines). In this regard, a symbol level *RS* soft

decision decoding algorithm is developed in Chapter 5. Performance evaluations show that this newly developed symbol level RS soft decision decoding algorithm yields better performance than the RS hard decision decoding algorithms found in literature, and the popular KV algebraic soft decision decoding algorithm. Results in Chapter 5 verify this performance analysis, and confirm Hypothesis (2) of this thesis. Thus, a combination of the proposed method of deriving reliability information (Chapters 2 and 3), and the novel symbol level RS soft decision decoding algorithm proposed in Chapter 5 will enhance the message transmission success over Rayleigh fading channels.

Moreover, for severe Rayleigh fading conditions, the performance of the combined demodulation and decoding receiver plummets (Fig. 1.3 without the dotted lines). Therefore, a joint iterative channel estimation and RS decoding receiver structure is desirable (Fig. 1.3 with the dotted lines). Chapters 4 and 6 verify the performance increase offered by joint iterative channel estimation and RS decoding receiver structures in comparison with the combined demodulation and RS decoding receivers (Fig. 1.3 without the dotted lines). Accordingly, the results in Chapters 4 and 6 assert Hypothesis (3) of this thesis.

Summarily, for a desirable performance or improved message reliability over Rayleigh fading channels using RS codes, this thesis investigated these three hypotheses. The finding of this study indicates that the combination of these hypotheses satisfy the thesis research question. A good reliability information from the channel output enhances the performance of the RS soft decoder (refer to Chapters 2 and 3). Nevertheless, a good reliability information from the channel output will only guarantee successful message transmission if the RS soft decoder is dependable. Also, a combination of good reliability information and dependable RS soft decoder in an iterative receiver structure as presented in Chapters 4, 5 and 6 enhances the probability of a correct message detection.

1.5 Research Relevance and Applications

Despite the fact that a number of studies have been undertaken on joint iterative channel estimation and decoding receivers over Rayleigh fading channels, most especially with Turbo and LDPC codes, none has been carried out using *RS* codes. *RS* codes form an important class of linear block codes capable of correcting random symbol errors, as well as burst errors [5, 6]. They are used in wireless communication systems such as Digital Audio Broadcasting (DAB), Digital Video Broadcasting (DVB), Digital Subscriber Line (DSL), WiMAX, and long distance satellite communications. The European Telecommunications Standards Institute (ETSI) encourages the use of *RS* codes in DAB and DVB applications [23, 24]. Also, the Consultative Committee for Space Data Systems (CCSDS) proposed the adoption of *RS* codes in the data link because of its efficient error correcting capabilities [25, 26]. Therefore, the work in this thesis will be useful in enhancing the performance of *RS* codes when used in these aforementioned wireless applications. Equally, the developed less computationally intensive, and performance efficient symbol level decoding algorithm for *RS* codes can be used in consumer technologies like compact disc and digital versatile disc.

This study also divulges the importance of reliability information in symbol level *RS* soft decision decoding algorithms, most especially over Rayleigh fading channels. The combined demodulation with symbol level *RS* soft decision decoding algorithms in the literature do not efficiently take the estimated CSI into account while deriving the soft reliability information over Rayleigh fading channels. This remains a fundamental limitation to the performance of symbol level *RS* soft decision decoding algorithms over Rayleigh fading channels. As such the developed DM method of deriving soft reliability information over Rayleigh fading channels will enhance performance of symbol level *RS* soft decision decoding algorithms. The beauty of this proposed DM is that it can be deployed with any symbol level soft decision decoding FEC scheme.

Besides, the findings of this study are verified using higher order modulation

schemes such as M-QAM and OFDM. As known from literature, M-QAM and OFDM are capable of achieving better transmission bit rates without any bandwidth expansion. Also, these modulation schemes offers more design flexibility than other modulation schemes, high spectral efficiency and narrow power spectrum [2]. Therefore, the work in this thesis proffer solutions in improving the performance of these modulation schemes over Rayleigh fading channels in wireless applications like DAB, and DVB.

1.6 Thesis Organization

This thesis consists of seven chapters. Chapter 1 presents the general introduction, research question and hypotheses, research aim and objectives. Other details provided in Chapter 1 include the research relevance and applications, and the set of reasons in support of the research hypotheses. From the findings of this study, Chapters 2-5 are formatted as published in peer-reviewed conference and journal papers. As well, Chapter 6 is formatted as submitted for publication in a peer-reviewed journal paper. Finally, Chapter 7 summarizes the study with regards to the results and analysis from the peer-reviewed conferences and journals presented in Chapters 2-6 of this thesis. Some recommendation for future research possibilities are also presented in Chapter 7. The synopsis of Chapters 2-6 are as follows.

In Chapter 2, an improved DM method of deriving soft reliability information over flat Rayleigh fading channels for combined demodulation with symbol level RS soft decision decoding algorithms is developed. The performance of the developed metric is verified using rectangular M-QAM systems as the modulation scheme, and the KV algorithm as the symbol level soft decoding FEC scheme. Performance analysis of this proposed DM method with the conventional DM method in [5, 7, 22] are also presented in this chapter. The CER results show significant improvement in the proposed DM method of deriving soft reliability information over flat Rayleigh fading channels in comparison with the conventional method. Although, in this chapter, the performance of the developed DM method of deriving soft

reliability information over Rayleigh fading channels is only verified for symbol level *RS* soft decision decoders, it is applicable to any symbol level soft decision decoding FEC scheme. For example, it is applicable to any symbol level decoding algorithm for LDPC codes.

Chapter 3 extends the work in Chapter 2 to OFDM systems on time-varying frequency-selective fading channels. M-QAM is adapted as the modulation scheme in the OFDM system structure design. Similarly, CER performance comparison is presented in this chapter between the proposed DM method and the conventional DM method used in [5, 6, 22]. The proposed DM method is extended to OFDM systems on time-varying frequency-selective fading channels in order to verify the proposed metric for different Rayleigh fading conditions.

A decision directed iterative channel estimation and Reed-Solomon decoding over flat Rayleigh fading channels is presented in Chapter 4. The joint iterative channel estimation and decoding receiver structure employs the *KV* soft decision decoding algorithm as the FEC scheme. A key feature in this chapter is the proposal of the Distance Metric (DM) method of deriving the *a priori* information used in the feedback process of the iterative receiver. The chapter also proves that the DM method exhibit less computational delay and time complexity in comparison with the widely use Log Likelihood Ratio (LLR) method. In addition, performance comparison is presented in this chapter between the *KV* algorithm without iterative feedback and the *KV* algorithm with iterative feedback for both the DM and LLR *a priori* information derivation methods. Firstly, the *KV* iterative receiver structure achieves a significant Symbol Error rate (SER - is the probability of the detector making an incorrect symbol decision) performance improvement compared to the *KV* receiver without feedback. These results indicate that *RS* codes can be used in a joint iterative channel estimation and decoding receiver structure over flat Rayleigh fading channels in order to improve the message reliability. Secondly, the proposed DM method achieves the same SER performance in comparison with the widely used LLR method at lower computational delay

and time complexity. This implies that the proposed DM method is a suitable replacement for the widely used LLR method because it has the advantage of lower computational delay and time complexity.

Chapter 5 develops a novel symbol level iterative soft decision algorithm for Reed-Solomon codes based on parity-check equations. This Parity-check matrix Transformation Algorithm (PTA) is based on the soft reliability information derived from the channel output in order to perform syndrome checks in an iterative process. Performance analysis verify that this developed PTA outperforms the conventional RS hard decision decoding algorithms and the symbol level Koetter and Vardy RS soft decision decoding algorithm. This portrays the proposed PTA for RS codes as a robust symbol level FEC decoding scheme, and it can be implemented on real time coding systems to improve the message reliability of communication links.

In Chapter 6, a low complexity iterative channel estimation and decoding receiver is developed based on the Reed-Solomon PTA. The Reed-Solomon PTA is adapted in an iterative receiver structure because it offers design ease and flexibility, and lesser computational time complexity in comparison with the KV algorithm. A key feature of this iterative receiver structure is the simple symbol remapping process used to refine the previous estimate of the channel after each iterative Reed-Solomon PTA decoding. Simulation results show significant SER improvement in the iterative receiver in comparison with the receiver without iterative feedback. Besides, the Reed-Solomon PTA provides design ease and flexibility, and lesser computational time complexity in an iterative receiver structure in comparison with the first Reed-Solomon KV iterative receiver structure.

1.7 Conclusion

This chapter introduces the general scope, the challenges and accomplishments of this study. The research question and hypotheses, and the aim and objectives of this study are clearly pointed out in this chapter. Importantly, Chapter 1 divulges

the set of reasons in support of the research hypotheses. Besides, the relevance of this study and applications are also emphasized in this chapters. Finally, Chapter 1 summarises the specific achievements and contributions of the remaining chapters of this thesis.

1.8 References

[1] G. Keiser, *Optical Communication Essentials.* Tata McGraw-Hill Companies, 4th edition, 2008.

[2] B. Sklar, *Digital Communication.* Prentice Hall, 2nd edition, Jan 2001.

[3] W. C. Jakes, *Mobile microwave communication.* New York: Wiley, 1974.

[4] I. S. Reed and G. Solomon, "Polynomial codes over Certain Finite fields," J. Soc.Ind. Appl. Maths., 8:300-304, June 1960.

[5] T. K. Moon, *Error Correction Coding: Mathematical Methods and Algorithms.* John Wiley & Sons, 2005.

[6] S. Lin and D. J. Costello, *Error Control Coding,* 2nd ed. Prentice Hall, June 2005.

[7] R. Koetter and A. Vardy, "Algebraic soft-decision decoding of Reed-Solomon codes," *Information Theory, IEEE Transactions on*, vol. 49, no. 11, pp. 2809-2825, Nov 2003.

[8] M. Valenti and B. Woerner, "Iterative channel estimation and decoding of pilot symbol assisted turbo codes over flat-fading channels," *Selected Areas in Communications, IEEE Journal on,* vol. 19, no. 9, pp. 1697–1705, Sep 2001.

[9] T. Zemen, M. Loncar, J. Wehinger, C. Mecklenbrauker, and R. Muller, "Improved channel estimation for iterative receivers," in *Global Telecommunications Conference, 2003. GLOBECOM '03. IEEE,* vol. 1, Dec 2003, pp. 257–261 Vol.1.

[10] H. Niu and J. Ritcey, "Iterative channel estimation and decoding of pilot symbol assisted LDPC coded QAM over flat fading channels," in *Signals, Systems and Computers, 2004. Conference Record of the Thirty-Seventh Asilomar Conference on,* vol. 2, Nov 2003, pp. 2265-2269 Vol.2.

[11] M.-K. Oh, H. Kwon, D.-J.Park, and Y. H. Lee, "Iterative Channel Estimation and LDPC Decoding With Encoded Pilots," *Vehicular Technology, IEEE Transactions on,* vol. 57, no. 1, pp. 273-285, Jan 2008.

[12] O. Oyerinde and S. Mneney, "Iterative receiver with soft-input-based-channel estimation for orthogonal frequency division multiplexing-interleave division multiple access systems" *Communications, IET,* vol. 8, no. 14, pp. 2445-2457, Sept 2014.

[13] V. Guruswami and M. Sudan, "Improved decoding of Reed-Solomon and algebraic-geometry codes," *Information Theory, IEEE Transactions on*, vol. 45, no. 6, pp. 1757-1767, Sep 1999.

[14] M. Sudan, "Decoding of Reed Solomon codes beyond the error-correction bound," *Journal of Complexity,* vol. 13, pp. 180-193, 1997.

[15] E. R. Berlekamp, *Algebraic Coding Theory.* New York: McGraw-Hill, Inc., 1968.

[16] J. Massey, "Shift-register synthesis and bch decoding," *Information Theory, IEEE Transactions on,* vol. 15, no. 1, pp. 122-127, Jan 1969.

[17] R. Welch and R. Berlekamp, "Error Correction for Algebraic Block Codes," Patent US 4 633 470, Dec. 30, 1986.

[18] A. Vardy and Y. Be'ery, "Bit-level soft-decision decoding of Reed-Solomon codes," *Communications, IEEE Transactions on,* vol. 39, no. 3, pp. 440-444, Mar 1991.

[19] Ray-Chaudhuri and H. Chan, "Bit-level parallel decoding of Reed-Solomon codes," in *Proc. 31st Allerton Conf. Communications, Control, and Computing*, Sept 1993.

[20] J. Jiang and K. Narayanan, "Iterative Soft-Input Soft-Output Decoding of Reed amp; #8211;Solomon Codes by Adapting the Parity-Check Matrix," *Information Theory, IEEE Transactions on,* vol. 52, no. 8, pp. 3746–3756, Aug 2006.

[21] O. Ur-rehman and N. Zivic, "Soft decision iterative error and erasure decoder for Reed #8211;Solomon codes," *Communications, IET,* vol. 8, no. 16, pp. 2863–2870, 2014.

[22] W. Phoel, J. Pursley, M. Pursley, and J. Skinner, "Frequency-hop spread spectrum with quadrature amplitude modulation and error-control coding," *in Military Communications Conference, 2004. MILCOM 2004. 2004 IEEE*, vol. 2, Oct 2004, pp. 913-919 Vol. 2.

[23] ETSI EN 300 744 V1.6.1 (2009-01), "DVB; Framing structure, channel coding, and modulation for digital terrestrial television".

[24] ETSI TS 102 563 V1.2.1 (2010-05), "DAB; Transport of AAC audio".

[25] CCSDS, "TM Synchronization and Channel Coding, Recommendation for Space Data Systems Standards." CCSDS 131.0-B-1, Blue Book, Issue 1, September 2003.

[26] Y. Liu, Y. Guan, J. Zhang, *et al.*, "Reed-Solomon Codes for Satellite Communications," in *Control, Automation and Systems Engineering, 2009. CASE 2009. IITA International Conference on*, July 2009, pp. 246-249.

-

CHAPTER 2

Improved Reliability Information for Rectangular 16-QAM Over Flat Rayleigh Fading Channels

In this chapter, an improved DM method of deriving soft reliability information over flat Rayleigh fading channels for combined demodulation with symbol level *RS* soft decision decoding algorithms is developed. The performance of the developed metric is verified using a rectangular M-QAM system as the modulation scheme, and the *KV* algorithm as the symbol level soft decoding FEC scheme. Computer simulation results show the importance of incorporating the CSI in deriving soft reliability information over flat Rayleigh fading channels. The results of this finding have been published in a peer-reviewed conference paper. Therefore, this chapter is structured in line with this published paper. The paper detail is as follows:

- **O. Ogundile** and D. Versfeld, "Improved reliability information for rectangular 16-QAM over flat Rayleigh fading channels," in *Computational Science and Engineering (CSE), 2014 IEEE 17th International Conference on,* Dec 2014, pp. 345–349.

O. Ogundile conceptualised and implemented the model, as well as obtained all the results presented in this conference paper. Also, the manuscript was prepared by **O. Ogundile**. The research and manuscript preparation was supervised by D. Versfeld.

Abstract

Reliability information derived from the channel output in the form of a Log Likelihood Ratio or a Distance Metric (DM) have been proposed in literature for M-ary Quadrature Amplitude Modulation systems. Reliable soft information from the channel output improves the performance of the forward error correction decoding algorithm. This paper proposes an improved method of extracting reliability information in the form of a DM for rectangular 16-QAM over flat Rayleigh fading channels. The reliability information is obtained from the derived *scaled* Channel State Information (CSI), and the estimated CSI which result due to variations in the Rayleigh fading channel gain. The Koetter and Vardy, Reed-Solomon (KV-RS) algebraic soft-decision decoding algorithm is used to verify the performance of this proposed method. The performance of this proposed method is documented through computer simulation. From the simulation results, the proposed method achieves significant improvement in Codeword Error Rate (CER) performance in comparison with the conventional DM method in literature with no additional computational time complexity.

Index Terms

CSI, DM, KV-RS soft decision decoder, Rayleigh fading Channel, rectangular 16-QAM, reliability information.

2.1 Introduction

Due to transmission bandwidth limitations and high data transmission rate demand in wireless technology, higher order modulation schemes are required in order to allow more data per bandwidth to be transmitted. M-ary Quadrature Amplitude Modulation (M-QAM) systems achieve better transmission bit rate without

any bandwidth expansion. M-QAM provide communication developers with better design flexibility than other modulation schemes, high spectral efficiency, and narrow power spectrum [1].

However, the performance of M-QAM over Rayleigh fading channels depend on effective channel estimation and compensation techniques. Channel estimation for M-QAM over Rayleigh fading channels have been the subject of recent research. Channel estimation techniques have been proposed independently, and in combination with different Forward Error Correction (FEC) algorithms. Emphasis have been on improving the channel estimation performance, bandwidth and power consumption, and the implementation time complexity of the estimation techniques.

With respect to the channel estimation technique used, soft-decision decoding requires reliability information from the channel output to accurately decode the encoded transmitted data. The reliability information can be in the form of a Log Likelihood Ratio or a Distance Metric (DM). In [2-4], the conventional DM method of extracting reliability information for M-QAM was analysed. The metric compares the distances from all the symbols in the output M-QAM constellation to the received QAM points. This paper proposes an improved method of extracting reliability information in the form of a DM for rectangular 16-QAM over flat Rayleigh fading channel with Additive White Gaussian Noise (AWGN). In this case, the metric compares the distances from the estimated Channel State Information (CSI) to all the entries in the *scaled CSI* as derived in Section 2.3.

The derived reliability information is fed into the Koetter and Vardy, Reed-Solomon (KV-RS) soft decision decoder [3] to compare its performance with the method analysed in [2-4]. The performance comparisons are documented through computer simulation assuming different values of normalized Doppler f_DT, and frame length size L. The CSI is estimated using the Pilot Symbol Assisted Modulation (PSAM) cubic interpolation channel estimation technique proposed in [5]. The simulation results shown in Fig. 2.3-2.5 verify the performance of both DM methods of extracting soft reliability information. This work have applications in

wireless communication, specifically in most M-QAM systems and forward error correction schemes.

The remainder of the paper is organized as follows. Section 2.2 gives a description of the system model and the PSAM cubic interpolation channel estimation technique. In Section 2.3, the conventional method, and the proposed improved method of extracting reliability information for rectangular 16-QAM are analysed. Performance comparisons and discussion are presented in Section 2.4. We summarize the paper with concluding remarks in Section 2.5.

2.2 System Model

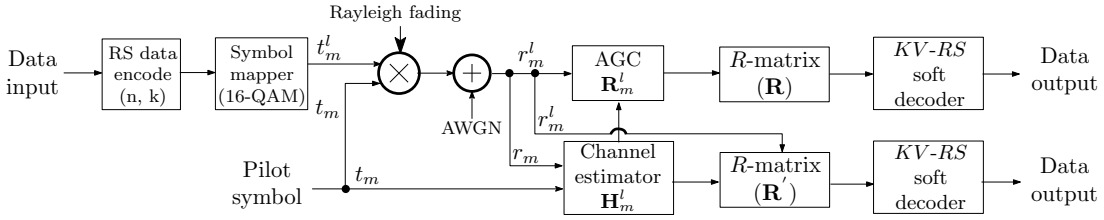

FIGURE 2.1: Simulation setup

Consider the simulation setup of Fig. 2.1. The input data is encoded using a (n, k) Reed-Solomon (RS) code. The RS codeword and information symbol lengths are defined by n and k respectively. The encoded data is mapped to rectangular 16-QAM complex data symbols in which both the real and imaginary parts take values from a set $(\pm 1c, \pm 3c, ... \pm (\bar{m}-1)c)$, where $\bar{m}$ is of the form $M = \bar{m}^2$ [6]. Known pilot symbols are periodically inserted to the mapped input data as shown in Fig. 2.2 (we assume all pilot symbols take on the same values). The data and pilot symbols are divided into frames of equal length L with each frame beginning with a pilot symbol followed by L-1 data symbols. The frame structures are transmitted over a flat Rayleigh fading channel with normalized Doppler $f_D T$ (where f_D is Doppler frequency, and T is the symbol period), and distorted with Additive White Gaussian Noise. Note, we assume Jakes's isotropic scattering model [7] for the complex Rayleigh fading.

The faded received signal corrupted with AWGN in the current *m-th* frame after down-converting and matched filtering is given as:

$$r_m^l = \mathbf{H}_m^l t_m^l + z_m, \quad l = 1, ..., L-1, \tag{2.1}$$

where $\mathbf{H}_m^l$ is the complex zero mean Gaussian variables denoting the fading distortion at the data symbol positions, z_m is the complex AWGN with variance $N_o/2$, and t_m^l is the transmitted QAM symbols.

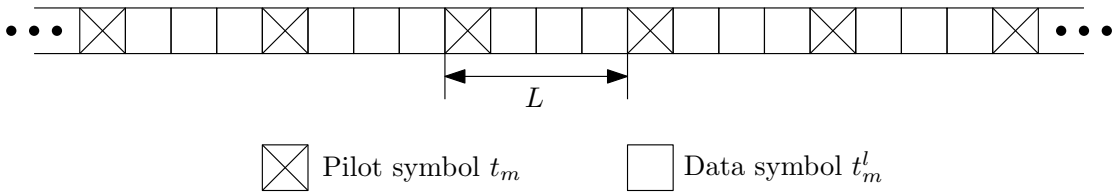

FIGURE 2.2: Transmitted frame structure.

The noisy fading estimates at the *m-th* pilot symbol positions is obtained by dividing the received pilot symbols by the known transmitted pilots as:

$$\mathbf{h}_m = \frac{r_m}{t_m} = \hat{h}_m + \frac{z_m}{t_m}, \tag{2.2}$$

where t_m and r_m are the transmitted and received pilot symbols respectively, and $\hat{h}_m$ is the complex zero mean Gaussian variables representing the fading distortion at the pilot symbol positions. The CSI $\mathbf{H}_m^l$ in the current *m-th* frame at the *l-th* data symbol position is derived by interpolating the known pilot symbol fading estimates $\mathbf{h}_m$.

2.2.1 CSI Computation

The CSI $\mathbf{H}_m^l$ in the current *m-th* frame at the *l-th* data symbol position is computed by interpolating the four nearest pilot symbol fading estimates $\mathbf{h}_m$. Given that $(\mathbf{h}_m, \ldots, \mathbf{h}_{m+3})$ are the four nearest pilot symbol fading estimates to the *l-th* data symbol, and $(\beta_m, \ldots, \beta_{m+3})$ are the known positions of the pilot symbols in

the transmitted frame structure. The CSI $\mathbf{H}_m^l$ is derived using the cubic interpolation technique as [5]:

$$\mathbf{H}_m^l = \sum_{l=1}^{L-1} \gamma_1 + \gamma_2(l) + \gamma_3(l)^2 + \gamma_4(l)^3, \tag{2.3}$$

where $(\gamma_1, \ldots, \gamma_4)$ are the cubic filter coefficients which is defined as [5]:

$$\begin{bmatrix} \gamma_1 \\ \gamma_2 \\ \gamma_3 \\ \gamma_4 \end{bmatrix} = \begin{bmatrix} 1 & \beta_m & \beta_m^2 & \beta_m^3 \\ 1 & \beta_{m+1} & \beta_{m+1}^2 & \beta_{m+1}^3 \\ 1 & \beta_{m+2} & \beta_{m+2}^2 & \beta_{m+2}^3 \\ 1 & \beta_{m+3} & \beta_{m+3}^2 & \beta_{m+3}^3 \end{bmatrix}^{\mathbf{-1}} \begin{bmatrix} \mathbf{h}_m \\ \mathbf{h}_{m+1} \\ \mathbf{h}_{m+2} \\ \mathbf{h}_{m+3} \end{bmatrix}. \tag{2.4}$$

The cubic interpolation technique exhibits high computational complexity for large input data. As derived in Eqn. (2.4), matrix inversion is required every time to compute the filter coefficient for each data symbol position. Therefore, we assume a sliding window approach in computing the filter coefficients in order to reduce the computational time complexity.

The four nearest pilot symbols positions are fixed as ($\beta_1, \beta_{1+L}, \beta_{1+2L}$, and β_{1+3L}), and we shift the fading estimates at the pilot symbol positions in order to compute the filter coefficients at each data symbol position. We hereby modify Eqn. (2.4) as:

$$\begin{bmatrix} \gamma_1 \\ \gamma_2 \\ \gamma_3 \\ \gamma_4 \end{bmatrix} = \begin{bmatrix} 1 & 1 & 1 & 1 \\ 1 & \beta_{1+L} & \beta_{1+L}^2 & \beta_{1+L}^3 \\ 1 & \beta_{1+2L} & \beta_{1+2L}^2 & \beta_{1+2L}^3 \\ 1 & \beta_{1+3L} & \beta_{1+3L}^2 & \beta_{1+3L}^3 \end{bmatrix}^{\mathbf{-1}} \begin{bmatrix} \mathbf{h}_m \\ \mathbf{h}_{m+1} \\ \mathbf{h}_{m+2} \\ \mathbf{h}_{m+3} \end{bmatrix}. \tag{2.5}$$

As shown in Fig. 2.2, each frame starts with a pilot symbol, so β_1 is always equal to one ($\beta_1 = 1$) while computing the fading distortion at each data symbol position. In Eqn. (2.5), the matrix inversion operation is performed once and used in computing the filter coefficient for each of the data symbol positions. We only adjust the column vector representing the fading estimates at the pilot symbol position; ensuring that the four nearest fading estimates at the pilot symbol

position to the *l-th* data symbol are used in the interpolation process. Thus, computing the CSI $\mathbf{H}_m^l$ using Eqns. (2.3) and (2.5) is straightforward and less computationally intensive.

2.3 Reliability Matrix

The estimated CSI $\mathbf{H}_m^l$ is conventionally used to scale the received data symbol r_m^l only in order to compensate for the fading channel errors in a process called Automatic Gain Control (AGC). The reliability information matrix (**R**-matrix) is thus extracted directly from the scaled received data symbol $\mathbf{R}_m^l$, and the symbols in the output 16-QAM constellation in the form of a DM as proposed [2-4]. Alternatively, the **R**-matrix can be extracted directly from the estimated CSI $\mathbf{H}_m^l$, and the derived *scaled* CSI as we propose in this paper.

2.3.1 Existing Method

Given that the estimated CSI $\mathbf{H}_m^l$, and noisy received QAM symbols r_m^l in the simulation setup of Fig. 2.1 are defined by Eqns. (2.6) and (2.7) respectively.

$$\mathbf{H}_m^l = [\eta_0, \eta_1, \ldots \eta_{n-1}], \tag{2.6}$$

$$r_m^l = [r_0, r_1, \ldots r_{n-1}] \tag{2.7}$$

Conventionally, the estimated CSI $\mathbf{H}_m^l$ is used to scale the noisy received QAM symbols r_m^l to obtained the scaled received QAM symbol $\mathbf{R}_m^l$ as:

$$\mathbf{R}_m^l = \frac{r_{m_j}^l}{\mathbf{H}_{m_j}^l} \qquad j = 0 \ldots n-1. \tag{2.8}$$

Thus, the reliability matrix (**R**-matrix) is computed from the scaled received QAM symbols $\mathbf{R}_m^l$, and the symbols in the output 16-QAM constellation in the form of a DM as [4]:

$$\mathbf{D} = \sqrt{(\mathbf{R}_{m_x}^l - Z_x)^2 + (\mathbf{R}_{m_y}^l - Z_y)^2}, \tag{2.9}$$

where $\mathbf{R}^l_{m_x}$ and $\mathbf{R}^l_{m_y}$ are the real and imaginary part of the scaled received QAM symbol $\mathbf{R}^l_m$ respectively, and $Z_{xy} = (Z_x,\ Z_y)$ are the symbols in the output 16-QAM constellation. Eqn. (2.9) measures the distance from the scaled received QAM symbols $\mathbf{R}^l_m$ to all the output 16-QAM constellation points Z_{xy} to form an $\mathbf{M} \times \mathbf{n}$ **R**-matrix (**R**) as [2-4]:

$$\mathbf{R} = \begin{bmatrix} \alpha_{0,0} & \alpha_{0,1} & \dots & \alpha_{0,n-1} \\ \alpha_{1,0} & \alpha_{1,1} & \dots & \alpha_{1,n-1} \\ \vdots & \vdots & \ddots & \vdots \\ \alpha_{M-1,0} & \alpha_{M-1,1} & \dots & \alpha_{M-1,n-1} \end{bmatrix}. \tag{2.10}$$

The entries of the **R**-matrix (**R**) derived in Eqn. (2.10) are normalized and quantized to $\log_2(M)$ bits of precision.

2.3.2 Proposed Method

We propose an improved method of extracting reliability information for 16-QAM over flat Rayleigh fading channels using the distance metric method. In this case, the **R**-matrix is derived directly from the estimated CSI $\mathbf{H}^l_m$, and the derived *scaled CSI* in the form of a DM. To this effect, we scale the received QAM symbols r^l_m by all the output 16-QAM constellation points (Z_{xy}) to form an $\mathbf{M} \times \mathbf{n}$ *scaled CSI* matrix defined as:

$$\mathbf{H}^{'l}_m = \{h_{i,j}\}, \tag{2.11}$$

where

$$h_{i,j} = \frac{r^l_{m_j}}{Z_{xy_i}}, \quad i = 0 \dots M-1 \ \text{ and } \ j = 0 \dots n-1.$$

Therefore, the **R**-matrix is derived from the *scaled CSI* $\mathbf{H}^{'l}_m$, and the estimated CSI $\mathbf{H}^l_m$ in the form of a DM as:

$$\mathbf{D}^{'} = \sqrt{(\mathbf{H}^l_{m_x} - \mathbf{H}^{'l}_{m_x})^2 + (\mathbf{H}^l_{m_y} - \mathbf{H}^{'l}_{m_y})^2}, \tag{2.12}$$

where $\mathbf{H}_{m_x}^{'l}$ and $\mathbf{H}_{m_y}^{'l}$ are the real and imaginary part of the *scaled CSI* $\mathbf{H}_{m}^{'l}$ respectively. Similarly, $\mathbf{H}_{m_x}^{l}$ and $\mathbf{H}_{m_y}^{l}$ are the real and imaginary part of the estimated CSI $\mathbf{H}_{m}^{l}$ respectively. Eqn. (2.12) measures the distance from the estimated CSI $\mathbf{H}_{m}^{l}$ to all the entries in the *scaled CSI* $\mathbf{H}_{m}^{'l}$ to form an $\mathbf{M} \times \mathbf{n}$ $\mathbf{R}$-matrix ($\mathbf{R}^{'}$) defined as:

$$\mathbf{R}^{'} = \begin{bmatrix} \alpha_{0,0}^{'} & \alpha_{0,1}^{'} & \cdots & \alpha_{0,n-1}^{'} \\ \alpha_{1,0}^{'} & \alpha_{1,1}^{'} & \cdots & \alpha_{1,n-1}^{'} \\ \vdots & \vdots & \ddots & \vdots \\ \alpha_{M-1,0}^{'} & \alpha_{M-1,1}^{'} & \cdots & \alpha_{M-1,n-1}^{'} \end{bmatrix}. \tag{2.13}$$

Also, the entries in Eqn.(2.13) are normalized and quantized to $\log_2(M)$ bits of precision.

2.4 Results and Discussion

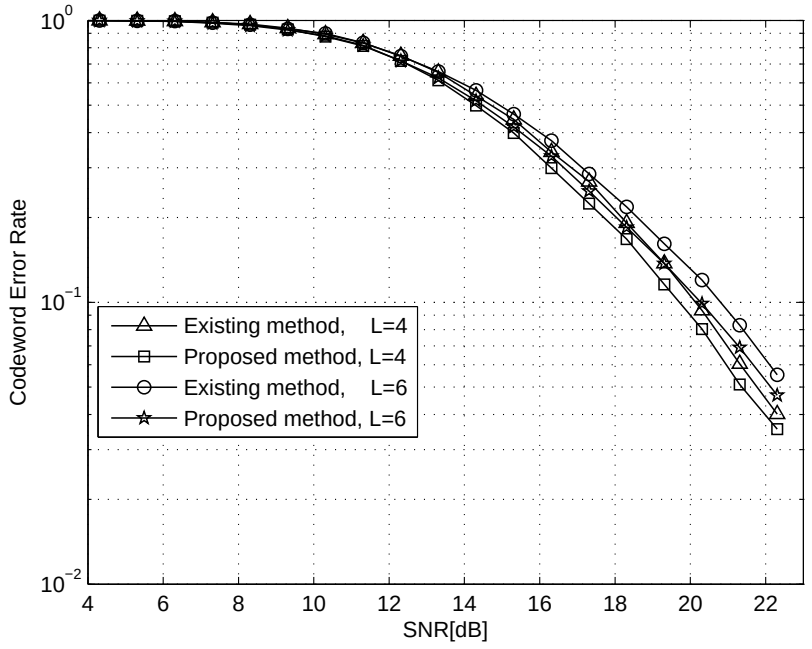

FIGURE 2.3: System performance in terms of CER versus SNR for normalize Doppler $f_D T$=0.0100

A simulation study was carried out to investigate the Codeword Error Rate (CER) performance of the existing and proposed methods. The computed $\mathbf{R}$-matrices ($\mathbf{R}$

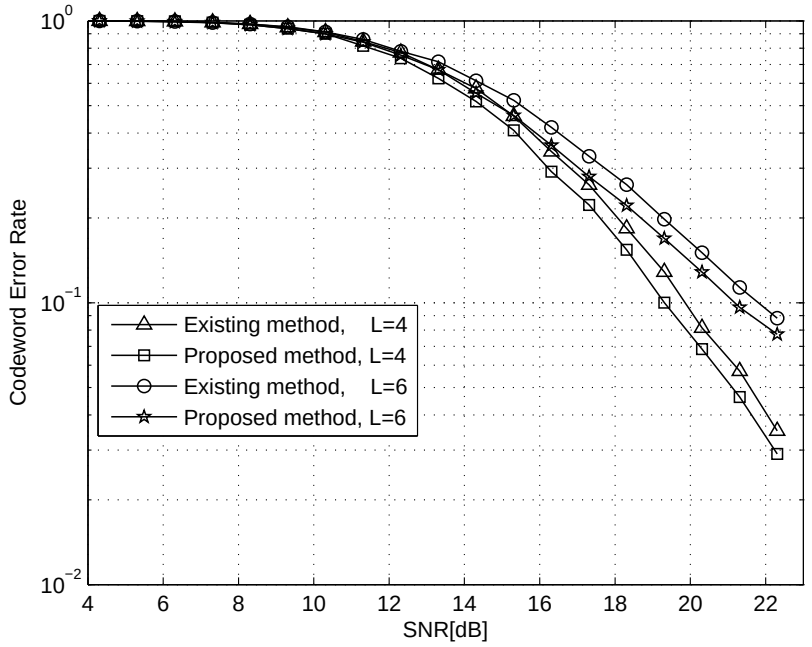

FIGURE 2.4: System performance in terms of CER versus SNR for normalize Doppler $f_D T$=0.0125

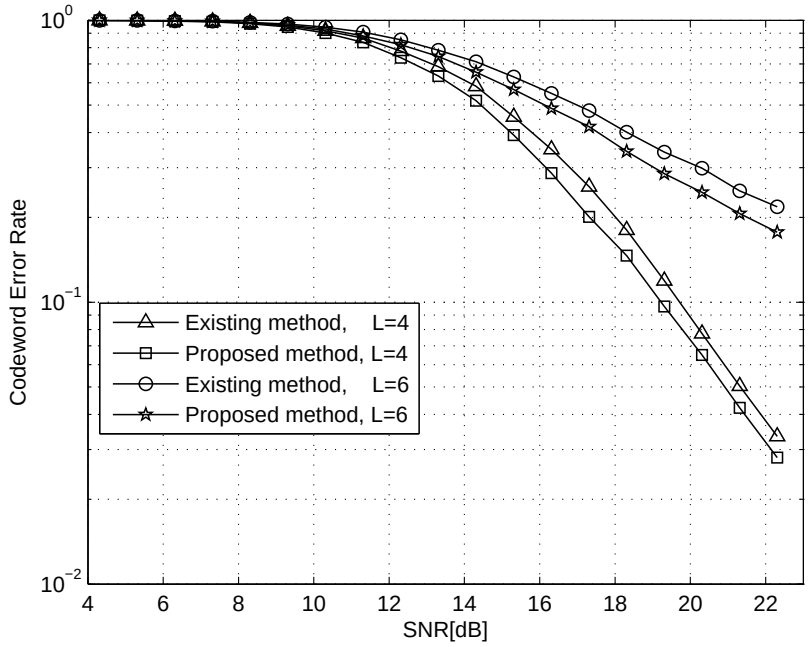

FIGURE 2.5: System performance in terms of CER versus SNR for normalize Doppler $f_D T$=0.0150

and $\mathbf{R}^{'}$) are fed into the *KV-RS* soft decision decoder which converts this reliability information into a choice set of interpolation points along with their multiplicities. The *KV-RS* soft decision algorithm inherits the interpolation and factorization properties of the Guruswami and Sudan algorithm [8]. An RS codeword length n=15, and information symbol length k=7 are assumed in the simulation setup of Fig. 2.1. A list size L_s=4 is used for the *KV-RS* soft decoder in order to reduce the simulation complexity. The list size L_s ($L_s \geq 1$) determines the decoding performance of the *KV-RS* soft decision decoder. The higher the value L_s the better the decoding performance of the *KV-RS* soft decoding algorithm but at the price of increased decoding time complexity.

The performance of the $\mathbf{R}$-matrices ($\mathbf{R}$ and $\mathbf{R}^{'}$) are documented using the same input data as shown in the simulation setup of Fig. 2.1. Frame length sizes L=4 and L=6 are assumed for the PSAM cubic interpolation channel estimation technique [5] for three different normalized Doppler f_DT=0.0100, f_DT=0.0125, and f_DT=0.0150. Fig. 2.3-2.5 shows the CER performance of the proposed method compared with the existing method analysed in [2-4]. As shown in the figures, the proposed method of extracting the $\mathbf{R}$-matrix from the *scaled* CSI, and the estimated CSI offers significant improvement in CER performance ($+0.5dB$) with no additional computational time complexity.

As also shown in Fig. 2.3-2.5, the CER performance of both methods of extracting reliability information for rectangular 16-QAM over flat Rayleigh fading channels drop with increase in the normalized Doppler f_DT but the proposed method still offer superior CER performance to the conventional method. The channel state information is difficult to obtain as the fading rate (f_DT) of the channel increases. Thus, the information metric derived in Eqns. 2.10 and 2.13 using the conventional and proposed method respectively is unreliable. This results in the significant CER performance reduction as the the fading rate increases from $f_DT = 0.0100 - f_DT = 0.0150$. Furthermore, as the frame length size L increases from L=4 to L=6, the CER performance of both methods degrade, nevertheless, the proposed method exhibits significant improvement in CER performance compared to the conventional method. Note that the performance of the cubic channel estimator

depends on the frame length L. The smaller the frame length size, the better the performance of the cubic channel estimator.

This proposed method introduces little or no bias in computing the reliability values for each output QAM symbol. It assigns the closest symbols to the received QAM points with roughly the same reliability values. Thus, it gives enough freedom to the FEC soft decoder to prioritize more symbols with good reliability values. On the other hand, we observe that the conventional method assigns very high reliability value to potential symbol compared to other nearby symbols on the output QAM constellation. This may result in decoding failure if the potential symbol with high reliability value is not the transmitted symbol. The FEC soft decoder in this case has fewer symbols to prioritize; as such, the decoding performance of the soft decoder is degraded.

2.5 Conclusion

In this paper, an improved distance metric method of extracting soft reliability information for rectangular 16-QAM over flat Rayleigh fading channel has been proposed. The reliability information is obtained from the derived *scaled* CSI, and the estimated CSI in the form of a DM. The performance of this proposed method is documented through computer simulation assuming three different normalized Doppler f_DT and frame length L=4 and L=6. The KV-RS soft decision decoder is used to verify the performance of this proposed method. Results show that this method achieves significant improvement in CER performance. Also, we noted that as the normalized Doppler f_DT increases, this proposed method displays significant CER performance compared to the conventional DM method, even at fairly low Signal-to-Noise Ratios (SNR). Simulation results shown in Fig. 2.3-2.5 confirm our analysis. Although, results are shown for rectangular 16-QAM, this proposed method can be extended to higher rectangular QAM signal constellations and Reed-Solomon codes because the estimated CSI $\mathbf{H}_m^l$ (using the cubic estimator or any optimum channel estimation technique) do not depend on the order of signal constellation (M).

2.6 References

[1] B. Sklar, *Digital Communication.* Prentice Hall, 2nd edition, Jan 2001.

[2] T. K. Moon, *Error Correction Coding: Mathematical Methods and Algorithms.* John Wiley & Sons, 2005.

[3] R. Koetter and A. Vardy, "Algebraic soft-decision decoding of Reed-Solomon codes," *Information Theory, IEEE Transactions on*, vol. 49, no. 11, pp. 2809-2825, Nov 2003.

[4] W. Phoel, J. Pursley, M. Pursley, and J. Skinner, "Frequency-hop spread spectrum with quadrature amplitude modulation and error-control coding," *in Military Communications Conference, 2004. MILCOM 2004. 2004 IEEE*, vol. 2, Oct 2004, pp. 913-919 Vol. 2.

[5] L. Erup, F. M. Gardner, and R. Harris, "Interpolation in digital modems. ii. implementation and performance," *Communications, IEEE Transactions on*, vol. 41, no. 6, pp. 998-1008, Jun 1993.

[6] M. K. Simon and J. Smith, "Carrier Synchronization and Detection of QASK Signal Sets," *Communications, IEEE Transactions on*, vol. 22, no. 2, pp. 98-106, Feb 1974.

[7] W. C. Jakes, *Mobile microwave communication.* New York: Wiley, 1974.

[8] V. Guruswami and M. Sudan, "Improved decoding of Reed-Solomon and algebraic-geometry codes," *Information Theory, IEEE Transactions on*, vol. 45, no. 6, pp. 1757-1767, Sep 1999.

CHAPTER 3

Improved Reliability Information for OFDM Systems On Time-Varying Frequency-Selective Fading Channels

This chapter extends the study in Chapter 2 to OFDM systems on time-varying frequency-selective fading channels. In this case, the frequency domain CSI is incorporated in deriving the soft reliability information on time-varying frequency-selective fading channels. M-QAM is adapted as the modulation scheme in the OFDM system structure design. Also, the KV Reed-Solomon algorithm is employed as the symbol level soft decision decoding FEC scheme. Computer simulation results verify that the proposed metric offers significant performance increase in comparison with the conventional method at reasonable computational time complexity. Similarly, this finding have been been published in a peer-reviewed conference paper. Thus, this chapter is organised in line with this published paper. The paper detail is as follows:

- **O. Ogundile** and D. Versfeld, "Improved reliability information for OFDM systems on time-varying frequency-selective fading channels," in *Wireless Telecommunications Symposium (WTS), 2015,* April 2015, pp. 1–7.

The model and idea in this conference paper was developed by **O. Ogundile**, as well as all the results produced. Besides, **O. Ogundile** prepared the manuscripts. D. Versfeld supervised the research and the manuscript preparation.

Abstract

Recently, soft reliability information derived from the Channel State Information (CSI) using Distance Metric (DM) method was shown to improve the performance of rectangular M-ary Quadrature Amplitude Modulation (M-QAM) systems over flat Rayleigh fading channels. In this paper, we extend this method to Orthogonal Frequency Division Multiplexing (OFDM) systems on time-varying frequency-selective Rayleigh fading channels. In particular, we derive the soft reliability information from the frequency domain CSI. The performance of the OFDM system is verified using the Koetter and Vardy, Reed-Solomon (KV-RS) algebraic soft decision decoding algorithm. We compare the Codeword Error Rate (CER) performance of the OFDM system with 16-QAM as the modulation schemes. In addition, the OFDM system performance is documented for different values of normalized Doppler frequency, and frame length size. From the computer simulation results, the proposed method offers superior CER performance in comparison with the conventionally used DM method in the literature with no significant increase in computational time complexity.

Index Terms

Cubic estimator, CSI, DM, KV-RS soft decision decoder, LMMSE, OFDM, reliability information.

3.1 Introduction

High data transmission rate demand in wireless communication technology motivated the use of Orthogonal Frequency Division Multiplexing (OFDM) in different wireless communication applications. Also, OFDM offers other advantages which include its effective and efficient use of the limited spectrum resource, and its robustness against multipath fading which is the main contributor of Inter Symbol

Interference (ISI) [1-5]. However, the efficient use of OFDM over wireless communication systems require effective channel estimation because of the time-varying properties of the channel. This has resulted in extensive investigations on different channel estimation techniques by researchers in order to improve the performance of OFDM systems on time-varying frequency-selective Rayleigh fading channels.

OFDM have been deployed with different soft decision Forward Error Correction (FEC) schemes (such as Turbo codes, Low Density Parity Check (LDPC) codes, Reed-Solomon codes etc) over time-varying frequency-selective channels. The emphasis have been to improve the performance of the OFDM systems with these soft decision error correcting schemes in comparison with the hard decision FEC schemes. However, these soft decision FEC schemes require soft reliability information from the channel output to effectively decode the encoded information. The soft reliability information can be derived in the form of a Distance Metric (DM) or a Log likelihood Ratio (LLR).

References [6-8] analyse the conventional DM method of deriving soft reliability information from the channel output for rectangular M-ary Quadrature Modulation systems (M-QAM). The metric in [6-8] measures the distances from the output M-QAM constellation points to the received QAM point. Recently, [9] proposed an improved method of extracting soft reliability information also in the form of a DM for rectangular M-QAM over flat Rayleigh fading channels. They derived their reliability information from the estimated Channel State Information (CSI), and the "scaled CSI". Their results show significant performance improvement in comparison with the conventional DM method with no significant increase in computational time complexity. However, they did not present any analytical computational time complexity result to buttress their analysis.

In this paper, the work in [9] is extended to OFDM systems. We derive the soft reliability information from the estimated frequency domain CSI in the form of a DM. 16-QAM is used as the modulation scheme in the OFDM system structure assuming time-varying frequency-selective Rayleigh fading channels. The frequency

domain CSI is derived using the Pilot Symbol Assisted Modulation (PSAM) Linear Minimum Mean Square Error (LMMSE) criterion [4, 10], and the PSAM cubic channel estimation method [9, 11] for different frame length size F_L. Two different PSAM channel estimators are used in this work in order to give substantial concluding remarks on this proposed method of extracting soft reliability information for OFDM systems. The channel estimation is based on block type pilot arrangement [4]. The Koetter and Vardy, Reed-Solomon (KV-RS) decoder [7] is used as the soft decision FEC scheme in the OFDM system structure. The system performance is documented through computer simulation for different values of normalized Doppler F_dT because the channel impulse response $\bar{H}(F)$ depends on F_dT. Fig. 3.3 and Fig. 3.4 verify the OFDM system performance. Furthermore, the paper presents a simple comparative computational time complexity analysis between the proposed and existing DM methods as shown in Table 3.1. Although, results of this work are shown for rectangular 16-QAM as the modulation scheme in the OFDM system, this work can be extended if other rectangular QAM signal constellations (M=8, 32, 64, 128, etc) are used as the modulation scheme in the OFDM system.

The relevance and contribution of this paper is as follow. The paper presents a simple way of improving the performance of OFDM systems combined with soft decision FEC schemes on time-varying frequency-selective Rayleigh fading channels. More so, the performance of the OFDM system is analysed employing Reed-Solomon (RS) codes as the FEC scheme. OFDM systems are used with RS codes in different wireless communication application such as DVB, WIMAX, ADSL, LTE, etc. Thus, this work is useful for these wireless applications in order to further improve the OFDM system performance with soft decision FEC schemes on time-varying frequency-selective Rayleigh fading channels.

The rest of this paper is organized as follows. Section 3.2 gives a description of the system and channel model. In Section 3.3, the PSAM channel estimators employ to derive the frequency domain CSI are briefly described. The existing and proposed DM methods of extracting soft reliability information are analysed in Section 3.4. In Section 3.5, we present a simple analytical computational time

complexities of the existing DM method in comparison with the proposed DM method. Section 3.6 presents and discusses the comparative computer simulation results. The paper is summarized with concluding remarks in Section 3.7.

3.2 System and Channel Model

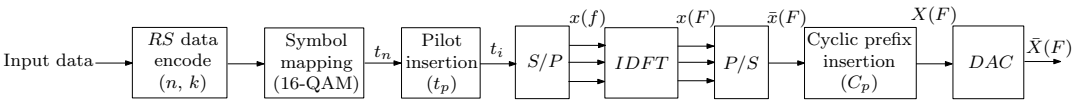

FIGURE 3.1: OFDM transmitter system.

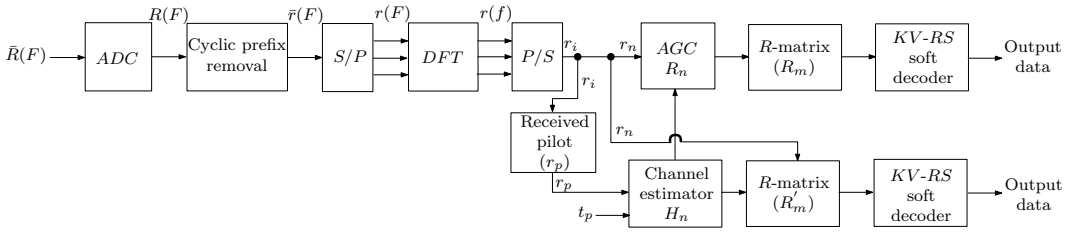

FIGURE 3.2: OFDM receiver system.

The PSAM OFDM transmitter and receiver system models are shown in Fig. 3.1 and Fig. 3.2 respectively. At the transmitter, the input data is first encoded using a (n, k) RS code. The RS codeword is defined by n, and the information symbol length is represented by k. The encoded data is mapped to 16-QAM complex symbols. Pilot symbols are inserted uniformly between the 16-QAM data symbol sequence. The pilot symbols are assumed to take on the same values. The pilot and data sequence (t_i) is divided into frames of equal length F_L, with each frame beginning with a pilot symbol followed by $F_L - 1$ data symbol. The pilot and data sequence of length L is fed into a serial-to-parallel (S/P) converter. The Inverse Discrete Fourier Transform (IDFT) block converts the frequency domain OFDM signal $x(f)$ to the time domain as expressed in Eqn. (3.1):

$$x(F) = \frac{1}{\sqrt{L}} \sum_{f=0}^{L-1} x(f) e^{+j(2\pi f F/L)}. \tag{3.1}$$

The length of the DFT is defined by L. Note that a number of zeros are padded in between the carriers, so that the length of the carriers will be compatible with

the size of filter. The transformed time domain OFDM symbol $x(F)$ is fed into a parallel-to-serial (P/S) converter. Cyclic prefix of C_p sample duration is added to the OFDM symbol in order to combat ISI. Thus, the resulting OFDM symbol is defined as [4]:

$$X(F) = \begin{cases} x(L+F), & F = -C_p, -C_p+1, \ldots, -1, \\ x(F), & F = 0, 1, \ldots, L-1. \end{cases} \tag{3.2}$$

After Digital-to-Analogue Conversion (DAC), the OFDM signal is transmitted over a time-varying frequency-selective Rayleigh fading channel with Additive White Gaussian Noise (AWGN).

At the receiver (Fig. 3.2), the received time domain OFDM signal is defined as:

$$\bar{R}(F) = \bar{X}(F) \otimes \bar{H}(F) + \bar{Z}(F), \tag{3.3}$$

where $\bar{H}(F)$ is the channel impulse response, $\bar{X}(F)$ is the transmitted OFDM signal, and $\bar{Z}(F)$ is the complex AWGN. The $\bar{H}(F)$ is defined in terms of the normalized Doppler frequency F_dT (where F_d is Doppler frequency, and T is the symbol period) as [4]:

$$\bar{H}(F) = \sum_{a=0}^{P-1} \bar{H}_a e^{j(2\pi F_d T F/L)} \delta(\varphi - \tau_a), \tag{3.4}$$

where $\bar{H}_a$ is the complex impulse response of the *a-th* propagation path, φ is the average path gain, P is the number of propagation path, and τ_a is the *a-th* path delay.

After Analogue-to-Digital Conversion (ADC), the cyclic prefix is removed. The received signal $\bar{r}(F)$ passes through the S/P block, and subsequently the DFT block. The DFT block converts the time domain OFDM signal $r(F)$ to the frequency domain as expressed in Eqn. (3.5):

$$r(f) = \frac{1}{\sqrt{L}} \sum_{F=0}^{L-1} r(F) e^{-j(2\pi f F/L)}. \tag{3.5}$$

If the ISI is eliminated by the cyclic prefix, the received signal after the P/S block as shown in Fig. 3.2 can be represented as:

$$r_i = \mathcal{F} t_i H_i + Z_i, \tag{3.6}$$

where H_i is the fading distortion at the data and pilot symbol positions and Z_i is the complex AWGN. The notation $\mathcal{F}$ is the matrix of DFT defined by Eqn. (3.7)[4]:

$$\mathcal{F} = \begin{bmatrix} Z_L^{00} & \cdots & Z_L^{0(L-1)} \\ \vdots & \ddots & \vdots \\ Z_L^{(L-1)0} & \cdots & Z_L^{(L-1)(L-1)} \end{bmatrix}, \tag{3.7}$$

with corresponding weight given as [4]:

$$Z_L^{fF} = \frac{1}{\sqrt{L}} e^{-j(2\pi fF/L)}. \tag{3.8}$$

Note that the fading estimate H_i is only known at the pilot symbol positions. Thus, the frequency domain estimate of the channel state information at the data symbol position is obtained using the properties of the known pilot symbols.

3.3 PSAM Channel Estimation

The pilot symbol is extracted from the data symbol in order to obtain the channel properties at the pilot symbol positions. The observation at the pilot symbol position is defined as:

$$r_p = \mathcal{F} t_p H_p + Z_p, \tag{3.9}$$

where r_p, $\mathcal{F}$, t_p, H_p, and Z_p are defined as above in terms of the pilot symbols. Thus, the frequency domain CSI estimate at the data symbol positions is derived from the pilot symbol observations. In this paper, the LMMSE criterion, and the cubic interpolation channel estimation method are used to derive the fading distortion at the data symbol positions. Note, the channel estimation is based on

block-type pilot channel estimation. Refer to [4] for more details on block-type pilot channel estimation method.

3.3.1 LMMSE Estimator

Provided that the channel vector H_p is Gaussian and uncorrected with the channel noise Z_p, the frequency domain CSI estimate H_n at the data symbol position using the LMMSE estimator is defined as [4, 10]:

$$H_n = \mathcal{F}\mathbf{H}_n^{\dagger} r_p, \tag{3.10}$$

where the † sign denotes the conjugate transpose. The coefficient $\mathbf{H}_n$ is found by solving the Wiener-Hopf equation defined as:

$$\mathcal{R}\mathbf{H}_n = \mathcal{W}_n. \tag{3.11}$$

The autocorrelation matrix $\mathcal{R}$, and the covariance vectors $\mathcal{W}_n$ are defined by Eqn. (3.12) and Eqn. (3.13) respectively as [10]:

$$\mathcal{R} = E\Big[r_p r_p^{\dagger}\Big], \tag{3.12}$$

$$\mathcal{W}_n = E\Big[H_p^{*} r_p\Big]. \tag{3.13}$$

The $*$ sign denotes the complex conjugate. Note that the coefficient $\mathbf{H}_n$ is interpolated to obtain the fading estimates H_n at each data symbol position. Refer to [10] for direct derivations of the LMMSE channel estimator.

3.3.2 Cubic Interpolation Channel Estimator

Given that $(H_p, \ldots, H_{p+3})$ are the four nearest pilot symbol fading estimates to the ρ-th data symbol, and $(\alpha_p, \ldots, \alpha_{p+3})$ are the known positions of these pilot symbols in the frame structure. The frequency domain CSI estimate H_n is derived

using the cubic interpolation channel estimator as [9, 11]:

$$H_n = \mathcal{F}\left(\sum_{\rho=1}^{F_L-1} \Gamma_1 + \Gamma_2(\rho) + \Gamma_3(\rho)^2 + \Gamma_4(\rho)^3\right), \quad \rho = 1, ..., F_L - 1, \tag{3.14}$$

where $(\Gamma_1, \ldots, \Gamma_4)$ are the cubic filter coefficients. The filter coefficients are derived using a sliding window approach as [9, 11]:

$$\begin{bmatrix} \Gamma_1 \\ \Gamma_2 \\ \Gamma_3 \\ \Gamma_4 \end{bmatrix} = \begin{bmatrix} 1 & 1 & 1 & 1 \\ 1 & \alpha_{1+F_L} & \alpha_{1+F_L}^2 & \alpha_{1+F_L}^3 \\ 1 & \alpha_{1+2F_L} & \alpha_{1+2F_L}^2 & \alpha_{1+2F_L}^3 \\ 1 & \alpha_{1+3F_L} & \alpha_{1+3F_L}^2 & \alpha_{1+3F_L}^3 \end{bmatrix}^{\mathbf{-1}} \begin{bmatrix} H_p \\ H_{p+1} \\ H_{p+2} \\ H_{p+3} \end{bmatrix}. \tag{3.15}$$

References [9, 11] give detailed derivations of the cubic interpolation channel estimation technique.

3.4 Reliability Matrix

Conventionally, the derived frequency domain CSI H_n is used to scale the received data signal r_n in a process called Automatic Gain Control (AGC) in order to compensate for the fading distortion. The soft reliability information matrix (R-matrix) is therefore derived from the scaled received frequency domain symbols R_n, and the output signal constellation assumed as the modulation scheme in the OFDM system. Alternatively, we propose in this paper that the R-matrix can be derived from the estimated frequency domain CSI H_n and the scaled frequency domain CSI $H_n^{'}$ in order to further improve the OFDM system performance using soft decision FEC schemes.

3.4.1 Existing Method

Let the received signal r_n and the estimated frequency domain CSI be defined by Eqn. (3.16) and Eqn. (3.17) respectively.

$$r_n = [r_0, r_1, \ldots r_{n-1}], \tag{3.16}$$

$$H_n = [H_0, H_1, \ldots H_{n-1}]. \tag{3.17}$$

Firstly, the estimated frequency domain CSI H_n is used to scale the noisy received signal r_n to derive the scaled received frequency domain symbols defined as:

$$R_n = \frac{r_n}{H_n}. \tag{3.18}$$

Hence, the R-matrix is derived in the form of a DM from the scaled received frequency domain symbols R_n, and the symbols in the output 16-QAM constellation as [8, 9]:

$$\mathcal{D} = \sqrt{(R_{n_x} - \mathcal{Z}_x)^2 + (R_{n_y} - \mathcal{Z}_y)^2}, \tag{3.19}$$

where $\mathcal{Z}_{xy} = (\mathcal{Z}_x, \mathcal{Z}_y)$ are the symbols in the output 16-QAM constellation. The in-phase and quadrature part of the scaled received frequency domain symbols R_n are represented by R_{n_x} and R_{n_y} respectively. In Eqn. (3.19), the distance from the scaled received frequency domain symbols R_n to all the output 16-QAM constellation points $\mathcal{Z}_{xy}$ are measured to form an $M \times n$ R-matrix (R_m) defined as [6-9]:

$$R_m = \begin{bmatrix} \beta_{0,0} & \beta_{0,1} & \cdots & \beta_{0,n-1} \\ \beta_{1,0} & \beta_{1,1} & \cdots & \beta_{1,n-1} \\ \vdots & \vdots & \ddots & \vdots \\ \beta_{M-1,0} & \beta_{M-1,1} & \cdots & \beta_{M-1,n-1} \end{bmatrix}. \tag{3.20}$$

Note, the entries of R_m are normalized and quantized to $\log_2(M)$ bits of precision.

3.4.2 Proposed Method

We propose an improved method of extracting soft reliability information for OFDM systems on time-varying frequency-selective Rayleigh fading channels based on previous work done in [9] for M-QAM in flat fading Rayleigh fading channels. The R-matrix is computed from the estimated frequency domain CSI H_n and the derived scaled frequency domain CSI $H_n^{'}$. The scaled frequency domain CSI $H_n^{'}$ is first derived in a matrix form as:

$$H_n^{'} = \{H_{u,v}\}. \tag{3.21}$$

The notation $H_{u,v}$ is defined in terms of the noisy received signal r_n and the output 16-QAM constellation points $\mathcal{Z}_{xy}$ as:

$$H_{u,v} = \frac{r_{n_v}}{\mathcal{Z}_{xy_u}}, \quad u = 0 \ldots M-1 \quad \text{and} \quad v = 0 \ldots n-1.$$

Therefore, the R-matrix is derived also in the form of a DM from the scaled frequency domain CSI $H_n^{'}$, and the estimated frequency domain CSI H_n as:

$$\mathcal{D}^{'} = \sqrt{(H_{n_x} - H_{n_x}^{'})^2 + (H_{n_y} - H_{n_y}^{'})^2}, \tag{3.22}$$

where the in-phase and quadrature part of the scaled frequency domain CSI $H_n^{'}$ are represented by $H_{n_x}^{'}$ and $H_{n_y}^{'}$ respectively. Similarly, the in-phase and quadrature part of the estimated frequency domain CSI H_n are represented as H_{n_x} and H_{n_y} respectively. In Eqn. (3.22), the distance from the estimated frequency domain CSI H_n to all the entries in the scaled frequency domain CSI $H_n^{'}$ are measured to form an $M \times n$ R-matrix ($R_m^{'}$) defined as:

$$R_m^{'} = \begin{bmatrix} \beta_{0,0}^{'} & \beta_{0,1}^{'} & \cdots & \beta_{0,n-1}^{'} \\ \beta_{1,0}^{'} & \beta_{1,1}^{'} & \cdots & \alpha_{1,n-1}^{'} \\ \vdots & \vdots & \ddots & \vdots \\ \beta_{M-1,0}^{'} & \beta_{M-1,1}^{'} & \cdots & \beta_{M-1,n-1}^{'} \end{bmatrix}. \tag{3.23}$$

The entries in Eqn. (3.23) are also normalized and quantized to $\log_2(M)$ bits of precision.

3.5 Comparative Computational Complexity Analysis

In terms of computational time complexity comparison, the existing DM method will require a total of $n(6M + 1)$ operations. The proposed DM method on the other hand will require a total of $7Mn$ operations as shown in Table 3.1.

TABLE 3.1: Computational complexity per iteration

Operations	Existing	Proposed
$+$	Mn	Mn
$-$	$2Mn$	$2Mn$
$\times$	0	0
$\div$	n	Mn
$\{\}^2$	$2Mn$	$2Mn$
$\surd$	Mn	Mn
Total operations	$n(6M + 1)$	$7Mn$

For $M = 16$, and $n = 15$, the total number of operations required using the existing DM method to produce the R-matrix defined by Eqn. (3.20) is 1455. With the same values for M and n, the total number of operations required using the proposed DM method to produce the R-matrix defined by Eqn. (3.23) is 1680. These analysis show that the proposed DM method displays little increase in the computational time complexity in comparison with the existing DM method. However, it exhibits significant increase in the OFDM system Codeword Error Rate (CER) performance as shown in Fig. 3.3. and Fig. 3.4.

3.6 Simulation Results and Discussion

The OFDM system parameter used in the MATLAB simulation is as shown in Table 3.2.

TABLE 3.2: OFDM simulation parameters

Parameters	Specifications
FFT size	64
Coding rate, k/n	7/15
List Size of KV-RS algorithm, S_L	4
Pilot to data symbol ratio	4/15, 6/15
Sampling rate	$10kHz$
Signal constellation	16-QAM
Channel model	Rayleigh Fading, Multipath

In the simulation, we assume perfect synchronisation in order to prevent ISI and Inter Carrier Interference (ICI). The cyclic prefix is chosen to be 10% of the OFDM symbol's duration. Moreover, we select the maximum average path gain such that it is less than the cyclic prefix. Four taps/multipath are used in the simulation setup with the first tap always assumed to have zero delay which corresponds to a perfect synchronisation.

The Matlab simulation setup was designed to investigate the CER performance of the existing and proposed DM methods. The derived R-matrices (R_m and $R_m^{'}$) defined by Eqn. (3.20) and Eqn. (3.23) are fed into the KV-RS soft decision decoder. The KV-RS soft decision decoder converts this soft reliability information into a choice set of interpolation points along with their multiplicities. The KV-RS decoding algorithm builds upon the Guruswami and Sudan algorithm [12]. A list size S_L=4 is assumed in the KV-RS soft decoder in order to reduce the simulation time complexity. The decoding performance of the KV-RS algorithm depends on the list size chosen in the algorithm. Although, an increase in S_L ($S_L \geq 1$) improves the performance of the KV-RS soft decoding algorithm, it results in increase in the decoding complexity. Refer to [7, 12, 13] for more details on the KV-RS algorithm.

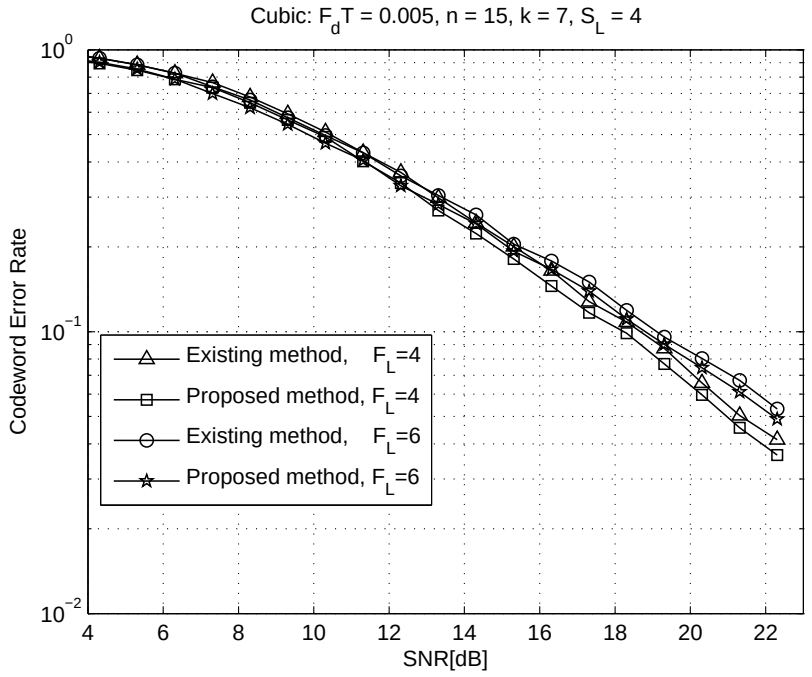

(a) $F_dT = 0.005$

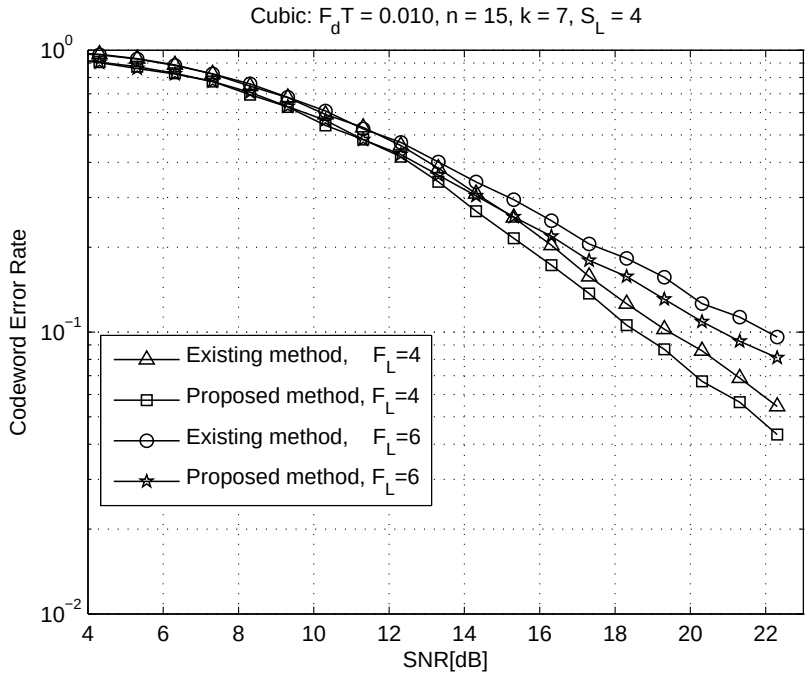

(b) $F_dT = 0.010$

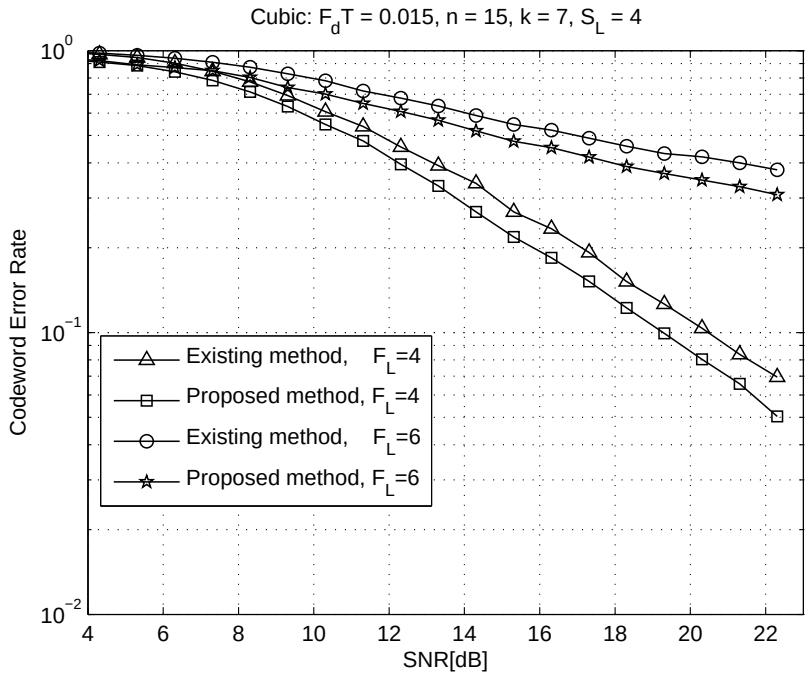

(c) $F_dT = 0.015$

FIGURE 3.3: OFDM system performance in terms of CER versus SNR for Cubic interpolation channel estimation method.

For the same input data, the performance of the R-matrices (R_m and $R_m^{'}$) are documented assuming two different PSAM channel estimation methods. Frame length sizes F_L=4 and F_L=6 are assumed for these channel estimation techniques. Three normalized Doppler frequencies (F_dT) are considered: F_dT=0.005, F_dT=0.010, and F_dT=0.015. Fig. 3.3. and Fig. 3.4 show the CER performance of the proposed DM method compared with the existing DM method for these normalized Doppler frequencies. From the figures, the proposed DM method of extracting soft reliability information in OFDM systems exhibits superior CER performance in comparison to the existing DM method. Although the CER performance of both method of soft extracting reliability information degrades as the fading rate F_dT increases, the proposed DM method still offers significant improvement in the CER performance. In fact, we observe that as the fading rate increases, the proposed DM method displays significant CER performance in comparison to the existing DM method even at moderately low Signal-to-Noise Ratios (SNR). The frequency domain CSI is more difficult to derive in a fast fading channel. Thus, the reliability metric derived in Eqn. (3.20) and Eqn. (3.23) employing the existing

and proposed DM method respectively is not reliable. This results in the degradation in the CER performance as the the fading rate increases from F_dT=0.050 - F_dT=0.015. Also, the CER performance of both method degrades with increase in the frame length size L; notwithstanding, the proposed DM method displays better CER performance compared to the existing DM method.

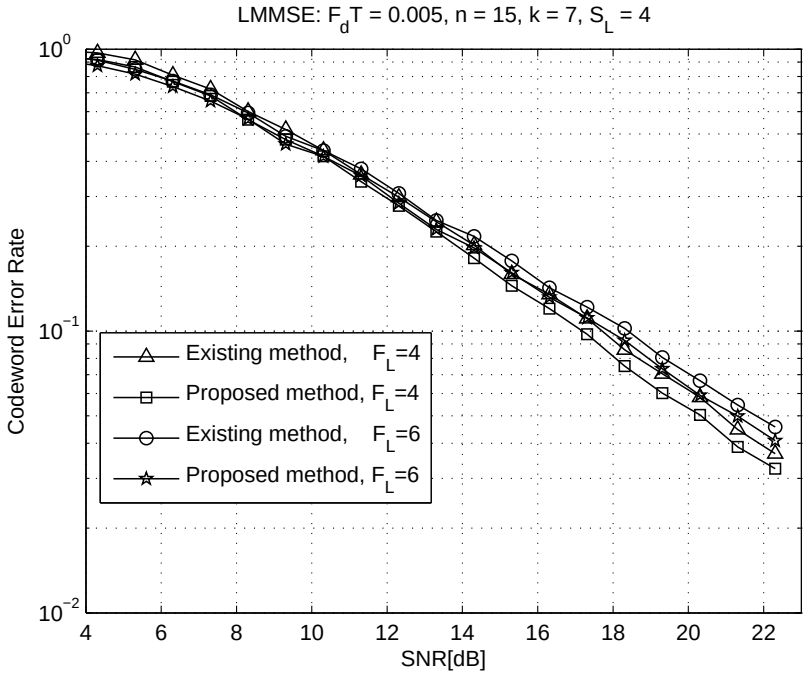

(a) $F_dT = 0.005$

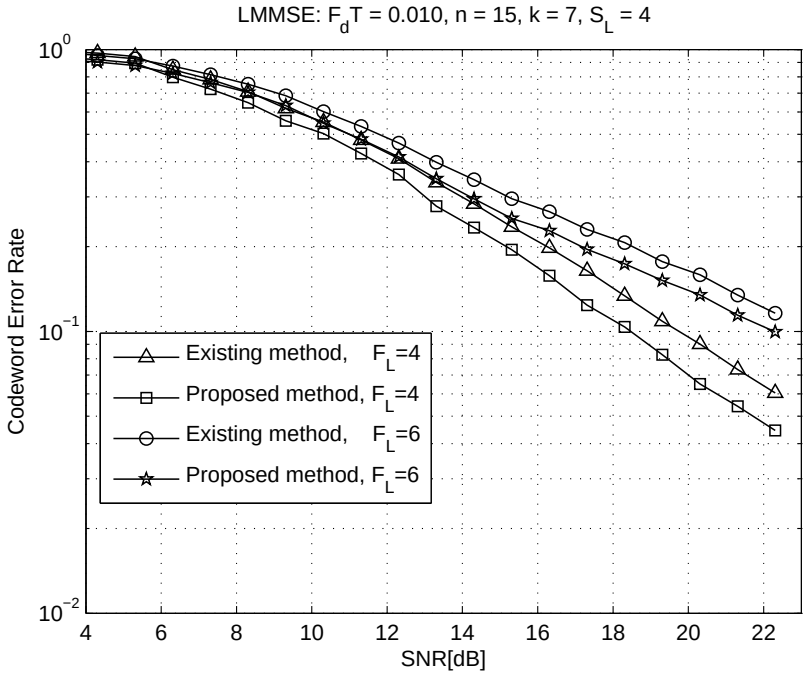

(b) $F_dT = 0.010$

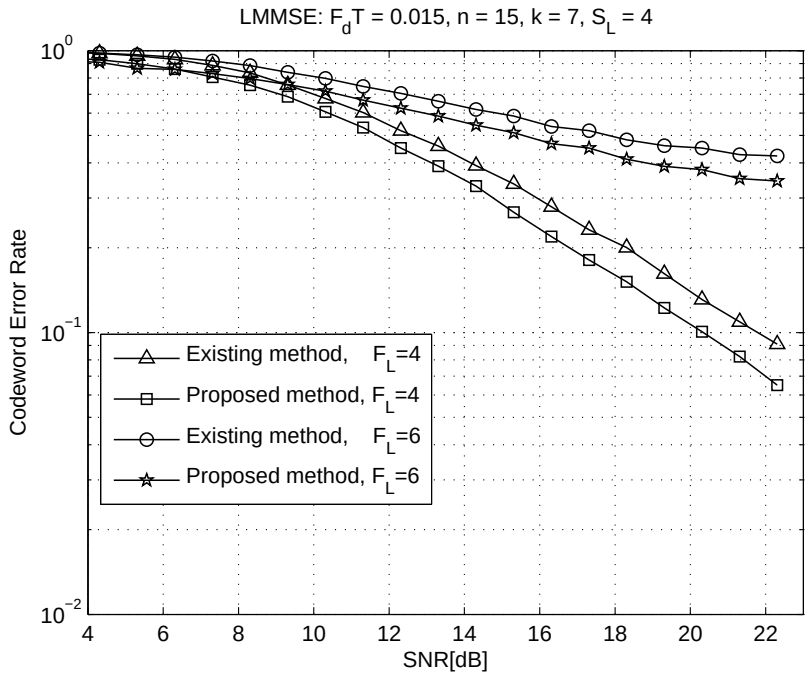

(c) $F_dT = 0.015$

FIGURE 3.4: OFDM system performance in terms of CER versus SNR for LMMSE channel estimation method.

As explained in [9], we also observed that the proposed DM method of extracting soft reliability information from the frequency domain CSI introduces little or no bias in deriving the reliability values for each output symbol. It allocates the nearest symbols to the received constellation points with almost the same reliability values. Therefore, the FEC soft decoder has enough degree to prioritize more symbols with good reliability values. The existing DM method on the other hand allocates high reliability value to potential symbol in comparison to other close-by symbols on the output constellation. If this potential symbol with high reliability value is not the transmitted symbol, it will result in decoding failure. In this case, the FEC soft decoder has less symbols to prioritize; thus, this degrades the decoding performance of the soft FEC decoder.

3.7 Conclusion

In this paper, an improved method of deriving soft reliability information for OFDM systems on time-varying frequency selective Rayleigh fading channels have

been proposed. We derived the soft reliability information in the form of a DM from the estimated frequency domain CSI and the derived scale frequency domain CSI. The OFDM system performance is documented comparing the proposed DM method with the conventionally used DM method. Also, a simple comparative computational time complexities between the existing and the proposed DM method have been presented. Firstly, the proposed DM method exhibits significant CER performance in comparison to the existing DM method. Secondly, as shown in Table 3.1, the the proposed DM method increases the computational time complexity of the overall OFDM system setup in comparison to the existing DM method. However, considering the significant increase in CER performance offered by proposed DM method, this method offers suitable trade-off between the computational time complexity and the OFDM system performance. Finally, the performance of this proposed DM method do not depend on the channel estimation technique used in deriving the frequency domain CSI. Simulation results shown in Fig. 3.3. and Fig. 3.4 confirm our analysis for two different channel estimation techniques.

3.8 References

[1] H. Hafez, Y. A. Fahmy, and M. Khairy, "Iterative channel estimation and Turbo decoding for OFDM systems," in *Wireless and Mobile Computing, Networking and Communications (WiMob), 2011 IEEE 7th International Conference on,* Oct 2011, pp. 428-432.

[2] O. Oyerinde and S. Mneney,"Decision Directed Channel Estimation for OFDM Systems Employing Fast Data Projection Method Algorithm," in *Communications, 2009. ICC '09. IEEE International Conference on,* June 2009, pp. 1-5.

[3] O. Oyerinde and S. Mneney, "Subspace Tracking-Based Decision Directed CIR Estimator and Adaptive CIR Prediction," *Vehicular Technology, IEEE Transactions on,* vol. 61, no. 5, pp. 2097-2107, Jun 2012.

[4] S. Coleri, M. Ergen, A. Puri, and A. Bahai, "Channel estimation techniques based on pilot arrangement in OFDM systems," *Broadcasting, IEEE Transactions on*, vol. 48, no. 3, pp. 223-229, Sep 2002.

[5] A. Khan, V. Jeoti, and M. Zakariya, "Improved pilot-based LS and MMSE channel estimation using DFT for DVB-T OFDM systems," in *Wireless Technology and Applications (ISWTA), 2013 IEEE Symposium on,* Sept 2013, pp. 120-124.

[6] T. K. Moon, *Error Correction Coding: Mathematical Methods and Algorithms.* John Wiley & Sons, 2005.

[7] R. Koetter and A. Vardy, "Algebraic soft-decision decoding of Reed-Solomon codes," *Information Theory, IEEE Transactions on*, vol. 49, no. 11, pp. 2809-2825, Nov 2003.

[8] W. Phoel, J. Pursley, M. Pursley, and J. Skinner, "Frequency-hop spread spectrum with quadrature amplitude modulation and error-control coding," *in Military Communications Conference, 2004. MILCOM 2004. 2004 IEEE*, vol. 2, Oct 2004, pp. 913-919 Vol. 2.

[9] O. Ogundile and D. Versfeld, "Improved reliability information for rectangular 16-QAM over flat Rayleigh fading channels," in *Computational Science and Engineering (CSE), 2014 IEEE 17th International Conference on,* Dec 2014, pp. 345–349.

[10] J. Cavers, "An analysis of pilot symbol assisted modulation for Rayleigh fading channels [mobile radio]," *Vehicular Technology, IEEE Transactions on,* vol. 40, no. 4, pp. 686-693, Nov 1991.

[11] L. Erup, F. M. Gardner, and R. Harris, "Interpolation in digital modems. ii. implementation and performance," *Communications, IEEE Transactions on*, vol. 41, no. 6, pp. 998-1008, Jun 1993.

[12] V. Guruswami and M. Sudan, "Improved decoding of Reed-Solomon and algebraic-geometry codes," *Information Theory, IEEE Transactions on*, vol. 45, no. 6, pp. 1757-1767, Sep 1999.

[13] L. Chen and R. Carrasco, "Soft decoding of algebraic-geometric codes using Koetter-Vardy algorithm," *Electronics Letters*, vol. 45, no. 25, pp. 1334-1336, December 2009.

CHAPTER 4

Decision Directed Iterative Channel Estimation and Reed-Solomon Decoding Over Flat Fading Channels

A decision directed iterative channel estimation and Reed-Solomon decoding over flat Rayleigh fading channels is studied in this chapter. The iterative receiver structure uses the symbol level KV soft decision decoding algorithm as the FEC scheme. Besides, this Chapter develops a DM method of deriving *a priori* information used in refining the previous estimate of the channel in an iterative receiver structure. Results show the importance of RS codes in an iterative channel estimation and decoding receiver structure. Moreover, results indicate that the DM method of deriving *a priori* information is a suitable replacement for the widely used LLR method. The results of this chapter have been published in a peer-reviewed journal paper for publication. This chapter is consequently organised conforming to this published journal paper. The detail of the paper is as follows.

- **O. Ogundile**, O. Oyerinde, and D. Versfeld, "Decision directed iterative channel estimation and Reed #x2013;Solomon decoding over flat fading channels," *Communications, IET* Vol. 9, no. 17 pp. 2077-2084, 2015.

The iterative receiver scheme developed in this journal paper was conceptualised and executed by **O. Ogundile**. Moreover, the results obtained, and the manuscript preparation were accomplished by **O. Ogundile**. The feedback section of the iterative receiver was supervised by O. Oyerinde. The research and manuscript preparation was supervised by D. Versfeld.

Abstract

Iterative channel estimation and decoding over flat Rayleigh fading channels have been shown in literature to improve the performance of receivers in wireless communication systems. Turbo and LDPC codes have mostly been used as the FEC scheme in the iterative receiver structures. This paper proposes a decision directed iterative channel estimation and decoding receiver using Reed-Solomon codes. In particular, the Koetter and Vardy, Reed-Solomon (*KV-RS*) soft decision decoder is adopted in the receiver structure as the FEC scheme. Two methods of deriving *a priori* information in joint iterative channel estimation and decoding receiver structures are also analysed in this paper. The first method derives the *a priori* information employing the Log Likelihood Ratio (LLR) method. *A priori* information derived using the LLR method is mostly used in iterative receiver structures in the literature. The second method derives the *a priori* information employing the Distance Metric (DM) method. The DM method is proposed in this paper as an alternative approach to the LLR method of deriving *a priori* information in iterative receivers. Hard and soft feedback information from the *KV-RS* decoder are considered to verify the performance of these methods. The performance of the two *a priori* information methods are documented through computer simulation assuming a M-QAM system. Simulation results verify the improvement in SER performance in the *KV-RS* iterative receiver structure in comparison with the *KV-RS* receiver without feedback. Also, the proposed DM method exhibits the same SER performance in comparison with the LLR method which is mostly used in the literature. More importantly, the proposed DM method has the advantage of less computational delay and time complexity compared to the LLR method.

4.1 Introduction

Development in wireless communication systems and applications motivated the design of receivers for efficient and reliable data transmission over Rayleigh fading

channels. New techniques are developed to improve the performance of the receiver over fading channels. Pilot Symbol Assisted Modulation (PSAM) has been studied in the literature to combat Rayleigh fading and improve the receiver performance [1-3]. Also, Forward Error Correction (FEC) schemes (Reed-Solomon (RS) codes, Turbo codes, Low Density Parity Check (LDPC) codes, etc) have been extensively investigated to improve the performance of receivers over fading channels. Much recent techniques employ joint iterative channel estimation and decoding schemes to improve the performance of receivers over Rayleigh fading channels with Additive White Gaussian Noise (AWGN) [4-8].

Conventionally, in iterative receivers, the initial Channel State Information (CSI) are derived from known pilot symbols. After each iterative decoding, the CSI are refined using feedback information from the decoder [4-8]. Most studies on joint iterative channel estimation and decoding employ Turbo, and Low Density Parity Check (LDPC) codes as the Forward Error Correction (FEC) scheme in the receiver structure. This paper proposes a joint iterative channel estimation and decoding receiver using the Koetter and Vardy, Reed-Solomon (KV-RS) soft decision decoding algorithm.

Reed-Solomon (RS) codes introduced in [9] have been shown to perform at near capacity over fading channels [10]. However, RS codes have not been widely used over fading channels because it exhibits high decoding complexity. Also, most RS decoding schemes in literature are hard decision decoding algorithms and they are not suitable in iterative receiver structures in order to avoid error propagation. Koetter and Vardy (KV) [10] proposed an RS soft decision decoding algorithm. The KV-RS soft decision decoding algorithm produces a list of codewords whereby extrinsic information can be derived in a decision directed approach, and fed back to refine the initial CSI. Thus, this work utilizes the KV-RS soft decision decoder in an iterative receiver structure as shown in Fig. 4.2 and Fig. 4.3

In Fig. 4.2, the iterative receiver structure employ the Log likelihood Ratio (LLR) method in deriving the *a priori* information which is subsequently remapped into symbols and used to refine the initial CSI. Most studies on joint iterative receivers

that employ Turbo or LDPC codes as the FEC scheme in the receiver structure uses the LLR method in deriving the *a priori* information. In this paper, we propose the Distance Metric (DM) method as an alternative approach to the LLR method of deriving *a priori* information in iterative receiver structures. Fig. 4.3 depicts the iterative channel estimation and decoding receiver structure employing the DM method in deriving the *a priori* information.

M-ary Quadrature Amplitude Modulation (M-QAM) systems is assumed in this work. The initial CSI is derived using the Pilot Symbol Assisted Modulation (PSAM) Linear Minimum Mean Square Error (LMMSE) criterion [1, 11]. The CSI is refined after each iterative decoding by decision directed hard or soft feedback information from the KV-RS soft decision decoder. We compare two types of KV-RS receiver structures: one with feedback, and the other without feedback. The block diagrams (Fig. 4.2 and Fig. 4.3) with the dashed lines represent the KV-RS receiver structure with feedback. Fig. 4.2 and Fig. 4.3 without the dashed lines depict the KV-RS receiver structure with no feedback. Results in Fig. 4.4 and Fig. 4.5 verify the performance of both KV-RS receiver structures. Fig. 4.6 presents the comparative computer simulation of both *a priori* information derivation methods employed in this work. Also, Table 4.2 analyses the computational time complexities the LLR and DM methods impose on the overall iterative receiver structure. We emphasize that the primary aim of this paper is not to compare between codes (RS codes, Turbo codes, LDPC codes, etc), rather, the introduction of RS codes in an iterative receiver structure. More importantly, we propose the DM method as a new and less complex way of deriving *a priori* information for iterative receivers, and a fair comparison with LLR method.

The contribution and relevance of this paper is as follows. Most work in literature on iterative channel estimation uses Turbo and LDPC codes as the FEC scheme in the iterative receiver structure. This paper adopts RS codes as the FEC scheme in an iterative channel estimation receiver structure over flat Rayleigh fading channels. Also, the paper proposes the DM method as an alternative approach to the LLR method of deriving *a priori* information in iterative channel estimation

receiver structures. The proposed DM method has the advantage of low computational delay and time complexity in comparison with the LLR method when used in iterative channel estimation and decoder receiver structures. Furthermore, we use a decision directed approach in the *KV-RS* iterative receiver structure in order to reduce the computational delay and time complexity of the iterative receiver structure, and to avoid error propagation. *RS* codes are used in wireless communication systems such as DAB (Digital Audio Broadcasting), DVB (Digital Video Broadcasting), and satellite communications. The European Telecommunications Standards Institute (ETSI) encourages the use of *RS* codes in DAB and DVB applications [12, 13]. The Consultative Committee for Space Data Systems (CCSDS) also proposed the adoption of *RS* codes in the data link because of its capability of correcting random and burst errors [14, 15]. This paper is useful for these wireless applications because they require efficient channel estimation schemes and *RS* decoding over Rayleigh fading channels.

The remainder of this paper is structured as follows. Section 4.2 gives a brief description of the discrete-time transmitter and channel model. The *KV-RS* iterative receiver structure is explained in detailed in Section 4.3. In particular, the LLR and the DM methods of deriving *a priori* information in iterative receiver structures are analysed. In Section 4.4, the computer simulation results for both the LLR and DM methods are discussed. Computational time complexities, and performance analysis of the DM method in comparison with the LLR method are also presented in this Section. The paper is summarized with concluding remarks in Section 4.5.

4.2 Transmitter and Channel Model

The discrete-time transmitter model of an *RS* coded M-QAM (M=16) system is as shown in Fig. 4.1. The input data $\bar{t}_d$ is encoded using a (n,k) *RS* code. The *RS* codeword and information symbol lengths are defined by n and k respectively. The encoded data $\hat{t}_d$ is mapped to rectangular 16-QAM complex data symbols in which both the real and quadrature parts take values from a set $(\pm 1c, \pm 3c, ...\pm(m-1)c)$,

where m is of the form $M = m^2$ [16, 17]. Known pilot symbols (t_p) are periodically inserted in the QAM symbols t_d. We assume all pilot symbols (t_p) take on the same value. The transmitted data and pilot symbols (t_i) are divided into frames of equal length L, with each frame beginning with a pilot symbol followed by L-1 data symbols. The frame structure is transmitted over a flat Rayleigh fading channel with normalized Doppler f_DT (where f_D is Doppler frequency, and T is the symbol period), and distorted with AWGN. We assume Jakes's isotropic scattering model [18] for the complex Rayleigh fading.

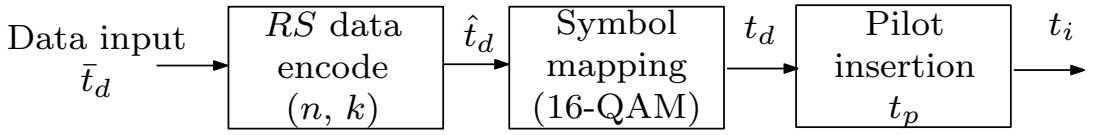

FIGURE 4.1: Transmitter structure

4.3 *KV-RS* Iterative Receiver

The *KV-RS* iterative receiver block diagram is shown in Fig. 4.2 and Fig. 4.3. The received symbol after down-converting and matched filtering is given as:

$$r_i = c\sqrt{E_s}h_i t_i + \bar{z}_i, \qquad i = 0 \ldots n-1, \tag{4.1}$$

where $c \in R^+$, $\bar{z}_i$ is the complex AWGN with σ^2=$N_o/2$, E_s represents the received signal symbol energy, t_i is the transmitted symbol, and h_i is the complex discrete-time zero mean Gaussian variables denoting the fading distortion. In Fig. 4.2 and Fig. 4.3, the initial CSI is obtained from known pilot symbols, after which soft reliability information is derived from the data symbols only. The soft information is fed into the *KV-RS* soft decision decoder which produces a list of codewords. Soft or hard feedback information can therefore be derived in a decision directed approach using the LLR or the DM method in order to refine the initial CSI. The iterative receiver process is thus expatiated as follows.

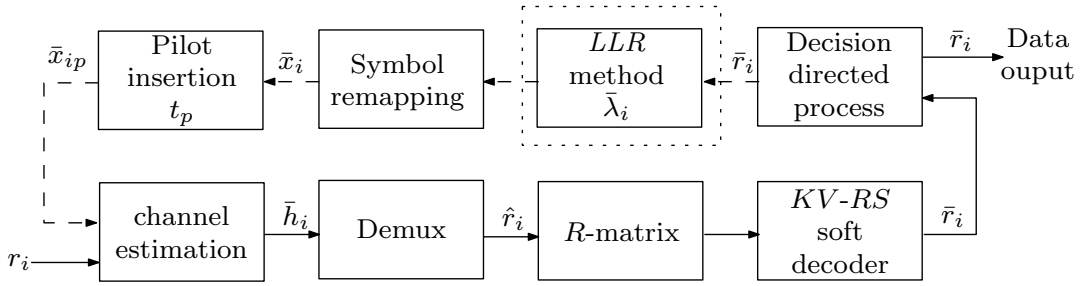

FIGURE 4.2: *KV-RS* iterative receiver structure using LLR *a priori* information method

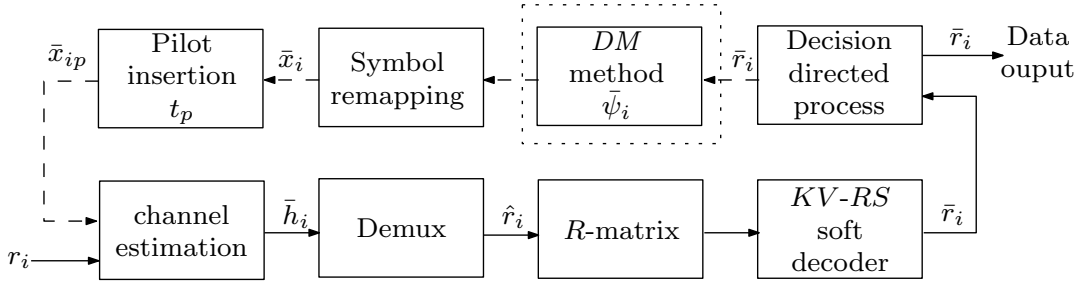

FIGURE 4.3: *KV-RS* iterative receiver structure using DM *a priori* information method

4.3.1 Initial Channel Estimation

Known pilot symbols are used to derive the initial CSI. The observation at the pilot position is given as:

$$r_p = c\sqrt{E_s}h_p t_p + \bar{z}_p, \tag{4.2}$$

thus, the CSI is derived based on the LMMSE criterion as [1, 11]:

$$\bar{h}_i = \mathcal{H}_i^{\dagger} r_p, \tag{4.3}$$

where the † sign denotes the conjugate transpose. The coefficient $\mathcal{H}_i$ is found by solving the Wiener-Hopf equation defined as:

$$\mathcal{R}\mathcal{H}_i = \mathcal{W}_i. \tag{4.4}$$

The autocorrelation matrix $\mathcal{R}$, and the covariance vectors $\mathcal{W}_i$ are given as [1, 11]:

$$\mathcal{R} = E\Big[r_p r_p^{\dagger}\Big] \quad \text{and} \quad \mathcal{W}_i = E\Big[h_p^{*} r_p\Big], \tag{4.5}$$

where the $*$ sign denotes the complex conjugate. Note that the coefficient $\mathcal{H}_i$ is interpolated to obtain the fading estimates $\bar{h}_i$ at each data symbol position. Reference [1] gives straightforward derivations of the LMMSE channel estimation.

4.3.2 R-matrix and KV-RS Soft Decision Decoder

The pilot symbols are separated from the data symbols by the Demultiplexer (Demux). The received signal r_i is thereby scaled by the estimated CSI $\bar{h}_i$ to obtain the scaled received signal $\hat{r}_i$ as:

$$\hat{r}_i = \frac{r_i}{\bar{h}_i}. \tag{4.6}$$

As such, the soft reliability information is derived from the scaled received signal $\hat{r}_i$. The soft reliability information is computed from the scaled received QAM symbols $\hat{r}_i$, and the symbols in the output 16-QAM constellation as [17, 19, 20]:

$$\mathcal{D} = \sqrt{(\hat{r}_{i_{re}} - \mathbb{Z}_{i_{re}})^2 + (\hat{r}_{i_{im}} - \mathbb{Z}_{i_{im}})^2}, \tag{4.7}$$

where $\hat{r}_{i_{re}}$ and $\hat{r}_{i_{im}}$ are the real and quadrature components of the scaled received signal $\hat{r}_i$ respectively, and $\mathbb{Z}_i = (\mathbb{Z}_{i_{re}}, \mathbb{Z}_{i_{im}})$ are the symbols in the output 16-QAM constellation. In Eqn. (4.7), the distance ($\mathcal{D}$) from the scaled received signal $\hat{r}_i$ to all the output 16-QAM constellation points ($\mathbb{Z}_i$) is measured to obtain the reliability matrix (R-matrix) defined as:

$$R\text{-matrix} = \begin{bmatrix} \beta_{0,0} & \beta_{0,1} & \cdots & \beta_{0,n-1} \\ \beta_{1,0} & \beta_{1,1} & \cdots & \beta_{1,n-1} \\ \vdots & \vdots & \ddots & \vdots \\ \beta_{M-1,0} & \beta_{M-1,1} & \cdots & \beta_{M-1,n-1} \end{bmatrix}, \tag{4.8}$$

where $\beta_{M-1,n-1}$ is the reliability value representing the likelihood of receiving a QAM symbol before RS decoding. The entries of the R-matrix are normalized and quantized to $\log_2(M)$ bits of precision. Refer to [10, 17, 20] for direct derivation of Eqn. (4.8). The R-matrix is fed into the KV-RS soft decision decoder. The soft decoder converts the R-matrix into a choice set of interpolation points along with their multiplicities [10]. The KV-RS algebraic soft decision decoding algorithm inherits the interpolation and factorization properties of the Guruswami and Sudan algorithm [21]. A list-size L_s=4 is assumed for the KV-RS soft decision decoder in order to reduce the computational delay and time complexity. The list-size L_s ($L_s \geq 1$) determines the decoding performance of the KV-RS soft decision decoder. The higher the value of L_s the better the decoding performance of the KV-RS decoding algorithm, but at the price of increased decoding time complexity. Refer to [10, 22] for details on the Koetter and Vardy, Reed-Solomon algebraic soft decision decoding algorithm.

4.3.3 Decision Directed Process

The decision directed block decides if the iterative channel estimation process is required in order to refine the previous CSI. The codeword reliability of all the codewords produced by the KV-RS soft decision decoder is first computed. The codeword reliabilities are computed by measuring the distances of the decoded symbols $\bar{r}_i$ to the scaled received symbols $\hat{r}_i$. The most reliable codeword is therefore selected from the list of codewords produced by the KV-RS soft decision decoder. The next step is to determine if it is necessary to refine the previous CSI. In this step, a threshold value obtained through simulations is set to decide if a symbol in the selected codeword is reliable. The iterative estimation process is not carried out if all the symbols in the selected codeword are reliable. We assume that it is most likely that the symbols are received correctly when all the symbols in the selected codeword are reliable. Furthermore, in order to avoid error propagation, no iteration is initiated if all symbols in the selected codeword are unreliable. The iterative estimation process is only performed when the selected

codeword contains both reliable and unreliable symbols. The decision directed block is useful basically to reduce the computational delay and time complexity of the *KV-RS* iterative receiver most especially for high number of iterations, and to avoid error propagation.

4.3.4 *A Priori* Information Derivation

Here, we focus on employing the DM method in deriving *a priori* information which are eventually mapped to symbols, and fed back to refine the previous CSI. The LLR method which is mostly used in iterative receiver structure is first analysed from the literature. The DM method is introduced subsequently as an alternative approach to the LLR method in order to reduce the computational burden the LLR method adds to the overall iterative receiver structure.

4.3.4.1 Log Likelihood Ratio Method

Consider the sequence of information bit to symbol mapping for 16-QAM as shown in Table 4.1. Let $\lambda(b_q \,|\, \bar{r}_i)$ be the LLR of the bit b_q given $\bar{r}_i$

TABLE 4.1: 16-QAM bit to symbol mapping.

$b_1 b_3$	Re	$b_2 b_4$	Im
10	-1	10	-1
11	-3	11	-3
01	+3	01	+3
00	+1	00	+1

$$\lambda(b_q \,|\, \bar{r}_i) = \log \frac{Pr\Big(b_q = 1 \,|\, \bar{r}_i\Big)}{Pr\Big(b_q = 0 \,|\, \bar{r}_i\Big)}. \tag{4.9}$$

The straightforward expression for the LLR of each bit is given as [23]:

$$\lambda(b_1\,|\,\bar{r}_i) = \log\left(\frac{exp\left(-\frac{(\bar{r}_{i_{re}} - c\sqrt{E_s})^2}{N_o}\right) + exp\left(-\frac{(\bar{r}_{i_{re}} - 3c\sqrt{E_s})^2}{N_o}\right)}{exp\left(-\frac{(\bar{r}_{i_{re}} + c\sqrt{E_s})^2}{N_o}\right) + exp\left(-\frac{(\bar{r}_{i_{re}} + 3c\sqrt{E_s})^2}{N_o}\right)}\right), \quad (4.10)$$

$$\lambda(b_2\,|\,\bar{r}_i) = \log\left(\frac{exp\left(-\frac{(\bar{r}_{i_{im}} - c\sqrt{E_s})^2}{N_o}\right) + exp\left(-\frac{(\bar{r}_{i_{im}} - 3c\sqrt{E_s})^2}{N_o}\right)}{exp\left(-\frac{(\bar{r}_{i_{im}} + c\sqrt{E_s})^2}{N_o}\right) + exp\left(-\frac{(\bar{r}_{i_{im}} + 3c\sqrt{E_s})^2}{N_o}\right)}\right), \quad (4.11)$$

$$\lambda(b_3\,|\,\bar{r}_i) = \log\left(\frac{exp\left(-\frac{(\bar{r}_{i_{re}} - c\sqrt{E_s})^2}{N_o}\right) + exp\left(-\frac{(\bar{r}_{i_{re}} + c\sqrt{E_s})^2}{N_o}\right)}{exp\left(-\frac{(\bar{r}_{i_{re}} - 3c\sqrt{E_s})^2}{N_o}\right) + exp\left(-\frac{(\bar{r}_{i_{re}} + 3c\sqrt{E_s})^2}{N_o}\right)}\right), \quad (4.12)$$

$$\lambda(b_4\,|\,\bar{r}_i) = \log\left(\frac{exp\left(-\frac{(\bar{r}_{i_{im}} - c\sqrt{E_s})^2}{N_o}\right) + exp\left(-\frac{(\bar{r}_{i_{im}} + c\sqrt{E_s})^2}{N_o}\right)}{exp\left(-\frac{(\bar{r}_{i_{im}} - 3c\sqrt{E_s})^2}{N_o}\right) + exp\left(-\frac{(\bar{r}_{i_{im}} + 3c\sqrt{E_s})^2}{N_o}\right)}\right), \quad (4.13)$$

where $\bar{r}_{i_{re}}$ and $\bar{r}_{i_{im}}$ are the real and quadrature components of the selected codeword $\bar{r}_i$ respectively.

In order to model the effect of the Rayleigh fading channel, we scale and rotate the LLR ($\lambda(b_q\,|\,\bar{r}_i)$) derived in [23] by the output QAM constellation to obtain the exact LLR ($\bar{\lambda}_i(b_q\,|\,\bar{r}_i)$) of each bit as:

$$\bar{\lambda}_i(b_1\,|\,\bar{r}_i) = \frac{\lambda(b_1\,|\,\bar{r}_i)}{\sum_{i=1}^{M} |c\mathbb{Z}_i|^2}, \quad (4.14)$$

$$\bar{\lambda}_i(b_3\,|\,\bar{r}_i) = \frac{\lambda(b_3\,|\,\bar{r}_i)}{\sum_{i=1}^{M} |c\mathbb{Z}_i|^2}, \tag{4.15}$$

$$\bar{\lambda}_i(b_2\,|\,\bar{r}_i) = \frac{\lambda(b_2\,|\,\bar{r}_i)}{\sum_{i=1}^{M} |c\mathbb{Z}_i|^2}, \tag{4.16}$$

$$\bar{\lambda}_i(b_4\,|\,\bar{r}_i) = \frac{\lambda(b_4\,|\,\bar{r}_i)}{\sum_{i=1}^{M} |c\mathbb{Z}_i|^2}. \tag{4.17}$$

Computing the exact LLR using Eqns. (4.10)-(4.17) is straightforward. The exact LLR ($\bar{\lambda}_i(b_q\,|\,\bar{r}_i)$) obtained in Eqns. (4.14)-(4.17) are used to derive the code bit probability $Pr(t_d = \mathbb{Z}_i)$ defined as [6, 24, 25]:

$$Pr(t_d = \mathbb{Z}_i) = \prod_{q=1}^{Q} \frac{1}{2}\left(1 + \rho.tanh\left(\frac{\bar{\lambda}_i(b_q\,|\,\bar{r}_i)}{2}\right)\right), \tag{4.18}$$

where Q is the number of bits (Q=4 for 16-QAM), and the constant ρ is defined as:

$$\rho = \begin{cases} -1 & b_q = 1 \\ +1 & b_q = 0. \end{cases} \tag{4.19}$$

The code bit probability $Pr(t_d = \mathbb{Z}_i)$ defines the probability that each bit in the symbols on the output 16-QAM constellation equals 1 or 0. Since M represents the number of output signal constellation points and the codeword length is defined by n, substituting Eqns. (4.10)-(4.17) in Eqn. (4.18) will produce an $M \times n$ *a priori* information matrix defined as:

$$Pr(t_d = \mathbb{Z}_i) = Pr(t_{d_n} = \mathbb{Z}_{i_M}) = \begin{bmatrix} \alpha_{0,0} & \alpha_{0,1} & \dots & \alpha_{0,n-1} \\ \alpha_{1,0} & \alpha_{1,1} & \dots & \alpha_{1,n-1} \\ \vdots & \vdots & \ddots & \vdots \\ \alpha_{M-1,0} & \alpha_{M-1,1} & \dots & \alpha_{M-1,n-1} \end{bmatrix}, \tag{4.20}$$

where $\alpha_{M-1,n-1}$ is the probabilistic element of the *a priori* information matrix used in symbol remapping. The $M \times n$ *a priori* information matrix $Pr(t_d = \mathbb{Z}_i)$ is therefore remapped into symbols in order to refine the previous CSI.

4.3.4.2 Distance Metric Method

The distance metric method is proposed as an alternative approach to the LLR method of deriving *a priori* information in the iterative receiver structure. Also, consider the sequence of information bit to symbol mapping for 16-QAM shown in Table 4.1. We derive the *a priori* information from the selected codeword and the 16-QAM output constellation point as:

$$\bar{\psi}_i = c.\left(e^{-\left(\sqrt{(\bar{r}_{i_{re}}-\mathbb{Z}_{i_{re}})^2+(\bar{r}_{i_{im}}-\mathbb{Z}_{i_{im}})^2}\right)}\right), \tag{4.21}$$

where $\bar{r}_i = (\bar{r}_{i_{re}}, \bar{r}_{i_{im}})$ and $\mathbb{Z}_i = (\mathbb{Z}_{i_{re}}, \mathbb{Z}_{i_{im}})$ are defined as above. In Eqn. (4.21), the distance from the selected codeword to all the output 16-QAM symbol constellation points are measured to obtain the code symbol probability $Pr(t_d = \mathbb{Z}_i)^{'}$. Similarly, Eqn. (4.21) will produce an *a priori* information matrix which is defined in terms of the size of the output signal constellation points M and the codeword length n as:

$$Pr(t_d = \mathbb{Z}_i)^{'} = Pr(t_{d_n} = \mathbb{Z}_{i_M})^{'} = \begin{bmatrix} \alpha^{'}_{0,0} & \alpha^{'}_{0,1} & \cdots & \alpha^{'}_{0,n-1} \\ \alpha^{'}_{1,0} & \alpha^{'}_{1,1} & \cdots & \alpha^{'}_{1,n-1} \\ \vdots & \vdots & \ddots & \vdots \\ \alpha^{'}_{M-1,0} & \alpha^{'}_{M-1,1} & \cdots & \alpha^{'}_{M-1,n-1} \end{bmatrix}, \tag{4.22}$$

where $\alpha^{'}_{M-1,n-1}$ is the probabilistic element of the *a priori* information matrix $Pr(t_d = \mathbb{Z}_i)^{'}$ used in symbol remapping. In the same approach, the $M \times n$ *a priori* information matrix $Pr(t_d = \mathbb{Z}_i)^{'}$ derived in Eqn. (4.22) is remapped into symbols in preparation for the next iterative channel estimation process. In comparison with LLR method which computes the *a priori* information by using the bits properties of the selected symbol, the DM method derives the *a priori* information by comparing the distance of the selected symbol to the output QAM constellation. The DM method is not an approximation of the LLR method because it does not require the complex symbol to bit conversion steps of Eqns. (4.10)-(4.17) while computing the *a priori* information. Hence, the *a priori* information derivation step using the DM method is straightforward and less computational intensive.

4.3.5 Symbol Remapping

The *a priori* information derived in Eqns. (4.20) and (4.22) employing the LLR and the DM methods respectively are remapped into symbols. Two types of symbol remapping techniques are considered: the decision directed hard symbol remapping, and decision directed soft symbol remapping.

The decision directed hard symbol remapping technique selects the most reliable point on the output 16-QAM constellation as [6, 24, 25]:

$$\bar{x}_i = c.\left(\max_{i=1,2....16} \Upsilon_i\right), \tag{4.23}$$

where

$$\Upsilon_i = \begin{cases} \Pr(t_d = \mathbb{Z}_i) & \text{LLR method} \\ Pr(t_d = \mathbb{Z}_i)' & \text{DM method.} \end{cases}$$

On the other hand, the decision directed soft symbol remapping technique takes the mean of the probability value $Pr(t_d = \mathbb{Z}_i)$ and $Pr(t_d = \mathbb{Z}_i)'$ over all the output 16-QAM constellation points as [6, 24, 25]:

$$\bar{x}_i = \sum_{i=1}^{16} \mathbb{Z}_i \Upsilon_i. \tag{4.24}$$

The remapped symbols $\bar{x}_i$ are combined with the known pilot symbols t_p for the next iterative channel estimation process.

4.3.6 Iterative Channel Estimation

The iterative channel estimation assumes the same form as the initial channel estimation. In this case, the remapped symbol ($\bar{x}_i$) are combined with the known pilot symbols (t_p) to obtain the refined CSI as:

$$\bar{h}_i^{\gamma} = \mathcal{H}_i^{\dagger} r_i. \tag{4.25}$$

Let γ denote the number of iterative channel estimations, and r_i be defined as:

$$r_i = c\sqrt{E_s}h_i\,\bar{x}_{ip} + \bar{z}_i, \tag{4.26}$$

where $\bar{x}_{ip}$ is the combination of the remapped symbol $\bar{x}_i$ and the known pilot symbol t_p. The autocorrelation matrix $\mathcal{R}$, and covariance vectors $\mathcal{W}_i$ are defined here as:

$$\mathcal{R} = E\Big[r_i r_i^{\dagger}\Big] \quad \text{and} \quad \mathcal{W}_i = E\Big[h_i^{*} r_i\Big]. \tag{4.27}$$

The iterative process is repeated until the stopping criterion is reached. The iterative channel estimate convergences at γ=3 for a list-size L_s=4 in the *KV-RS* soft decision decoder (refer to results in Section 4.4). We emphasize that the stopping condition is only investigated for the list-size (L_s=4) assumed in this work. The performance of the *KV-RS* soft decision decoder is a function of L_s; thus, the maximum number of iterative estimates (γ_{max}) might vary as L_s increases. The L_s should tend to infinity ($L_s \rightarrow \infty$) in order to effectively investigate the optimum stopping criterion for the *KV-RS* iterative receiver. However, as L_s increases, the decoding complexity of the *KV-RS* algorithm also increase.

The *KV-RS* iterative receiver process is hereby summarized into the following steps:

Step 1: Initial channel estimation - The initial CSI is derived from know pilot symbols using LMMSE channel estimation.

Step 2: Reliability information - Soft reliability information is extracted from the data symbols only using Eqn. (4.7) after compensating for the channel fading errors.

Step 3: *KV-RS* soft decoder - The *KV-RS* soft decision decoder utilizes the soft information derived in Step 2 to produce a list of codewords.

Step 4: Decision directed process - Codeword and symbol reliabilities are derived from the list of codewords produced in Step 3 in order to decide if the next iterative channel estimation process is required.

Step 5: *A priori* information derivation - Extrinsic information is derived from the selected codeword in Step 4 using either the LLR method (Eqns. (4.9)-(4.20))

or the proposed DM method (Eqns. (4.21)-(4.22)).

Step 6: Symbol remapping - The *a priori* information derived in Step 5 is mapped into symbols using Eqns. (4.23)-(4.24). The remapped symbols are combined with the known pilot symbols and used to refine the initial CSI.

Step 7: Repeat iterative process - Steps 1-6 are repeated until the stopping criterion is reached (in Step 1, the CSI is derived from the remapped symbols combined with the known pilot symbols). Otherwise, output the resulting codeword in Step 4.

4.4 Performance Analysis

4.4.1 Simulation Result for LLR and DM *A Priori* Information Methods

This Section presents the computer simulation results of the KV-RS receiver without feedback, and with feedback employing the LLR and the proposed DM methods. In the simulation set-up, a low rate (15,7) RS code is used. We focus our attention on a 16-QAM constellation with the bit to symbol mapping illustrated in Table 4.1. The maximum number of iterations (γ=3) is set assuming a list-size L_s=4 in the KV-RS soft decision decoding algorithm. Two normalized Doppler frequencies (f_DT) are considered: f_DT=0.015 and f_DT=0.020.

Fig. 4.4 and Fig. 4.5 show the SER performance for normalized Doppler f_DT=0.015 and f_DT=0.020 using the LLR method and the proposed DM method respectively. Each figure compares the performance of the perfect CSI with no pilot symbols, the performance using known pilot symbols without feedback, and the performance using known pilot symbols with hard and soft decision feedback. As shown in the figures, the KV-RS iterative receiver structure offers significant improvement in the SER performance compared to the KV-RS receiver structure with no feedback. More so, as we reduce the fading rate (f_DT), the performance of the KV-RS receiver structure improves. The CSI is more difficult to derive in a

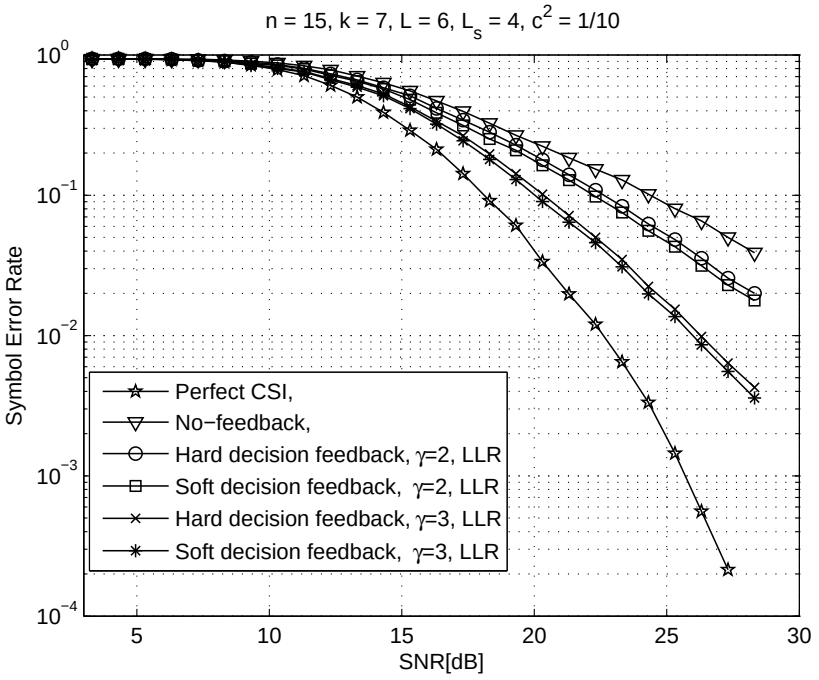

(a) $f_D T$=0.015

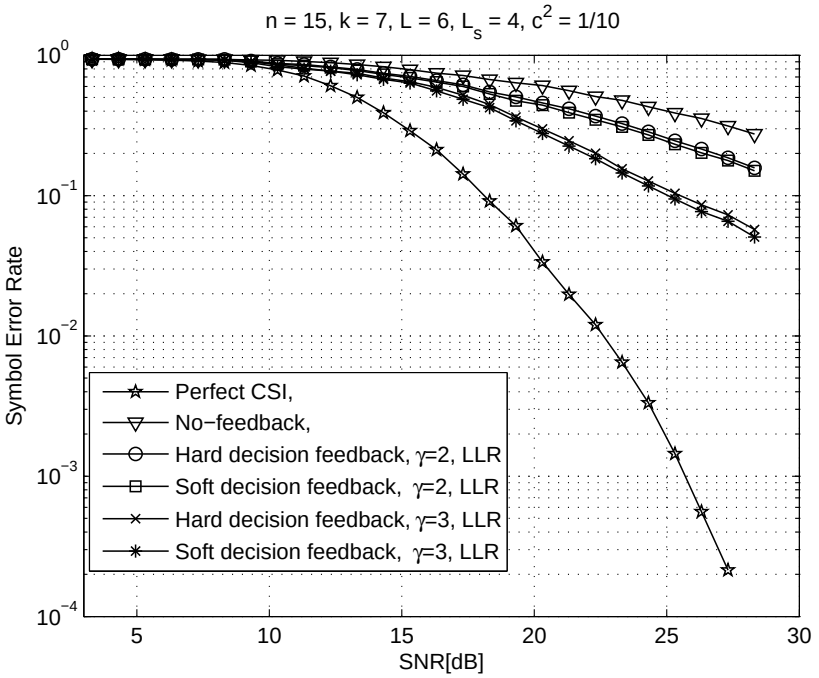

(b) $f_D T$=0.020

FIGURE 4.4: Receiver performance in terms of SER versus SNR using the LLR method

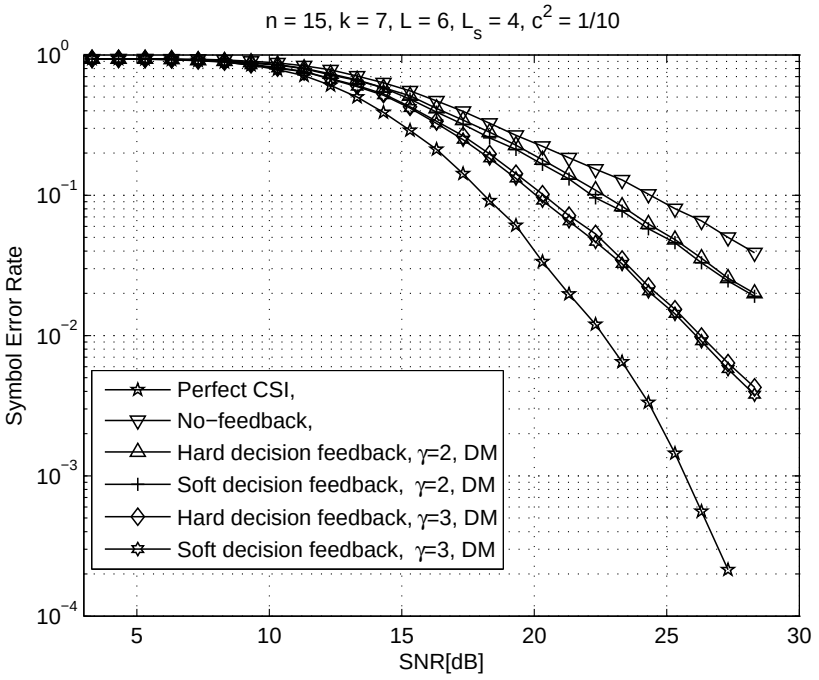

(a) $f_D T$=0.015

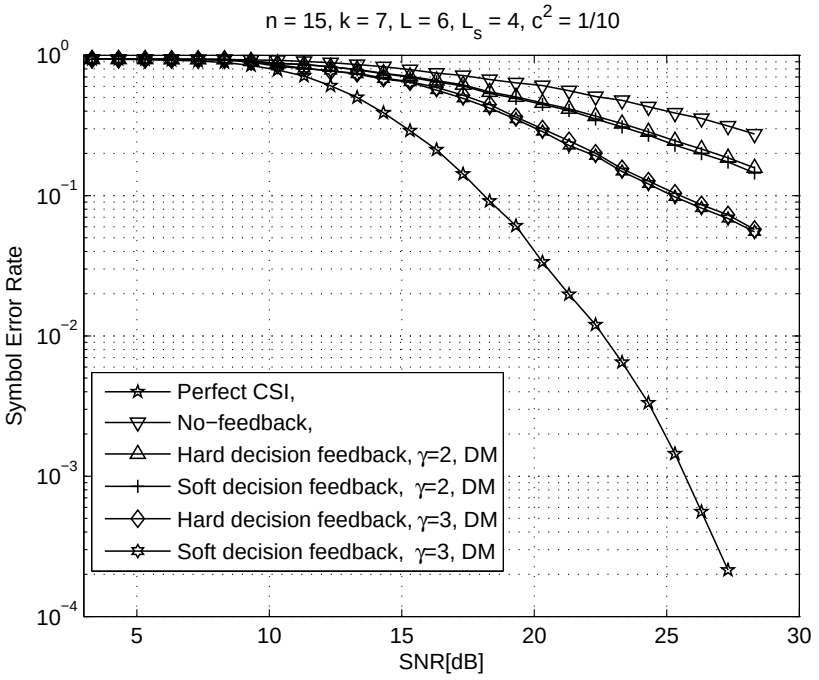

(b) $f_D T$=0.020

FIGURE 4.5: Receiver performance in terms of SER versus SNR using the DM method

fast Rayleigh fading channel. This results in the significant gap in performance between the perfect CSI without pilot symbols and the estimated CSI using known pilot symbols in Fig. 4.4b and Fig. 4.5b. Furthermore, the decision directed soft symbol remapping method edges the hard symbol remapping method in terms of SER performance at no significant computational time complexity. Also, note that as the number of iterations (γ) increases, the SER performance of the *KV-RS* iterative receiver improves but with increase in computational delay and time complexity.

4.4.2 Computational Complexity Analysis and Comparative Simulation Results of the LLR and DM *A Priori* Information Methods

We analyses the SER performance of the LLR and the DM *a priori* information method for the same input data using the aforementioned parameters. Also, a computational time complexity analysis of the DM method in comparison with the LLR method is discussed in this Section. Fig. 4.6a and Fig. 4.6b show the SER performance using both *a priori* information method for normalized Doppler f_DT=0.015 and f_DT=0.020 respectively. From the figures, the proposed DM method exhibits the same SER performance in comparison with the widely used LLR method for hard and soft decision feedback. Thus, the proposed DM method can be a suitable alternative to the LLR method to derive *a priori* information for real time iterative receiver systems. The use of DM *a priori* information derivation method is not limited to only RS codes, it can be used with other FEC codes such as Turbo codes, LDPC codes, most especially when symbol decoding is adopted at the receiver.

In terms of computational time complexity comparison, the *a priori* information matrix defined by Eqn. (4.20) employing the LLR method will require the complex symbol to bit conversion steps of Eqns. (4.10)-(4.17). Also, the LLR method will require the code bit probability conversion steps of Eqns. (4.18)-(4.19) whereby

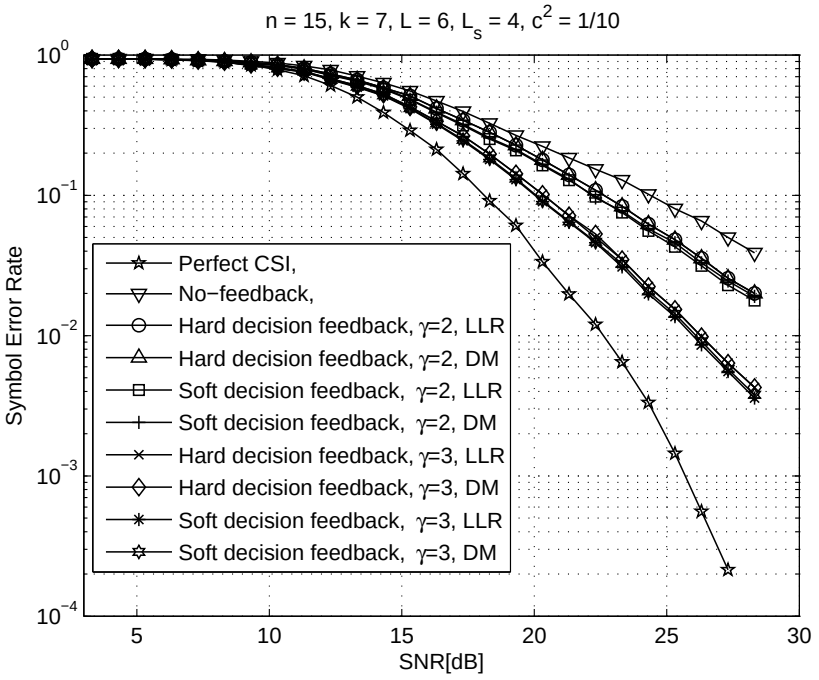

(a) f_DT=0.015

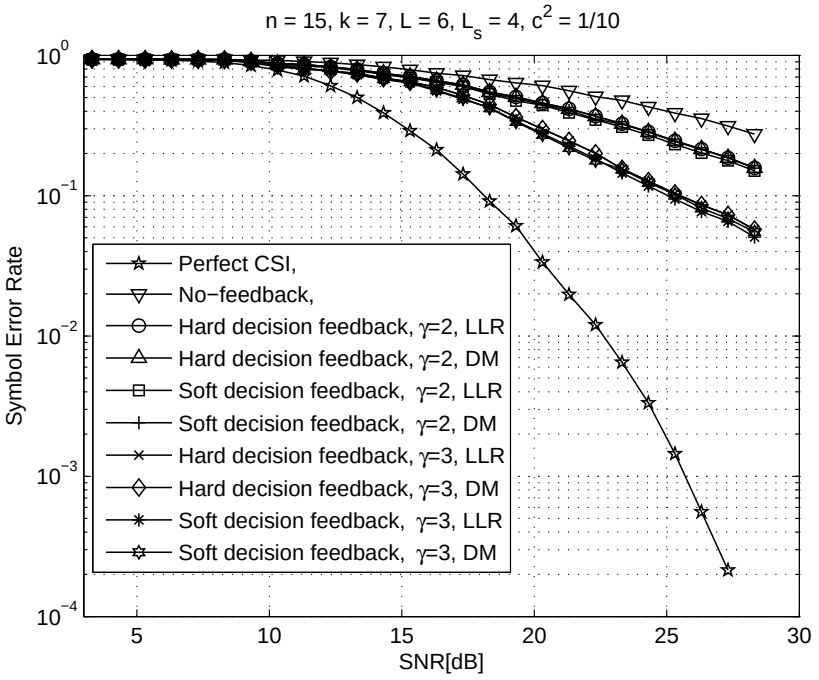

(b) f_DT=0.020

FIGURE 4.6: *A priori* information SER versus SNR performance comparison

the derived log likelihood ratio are converted back to probability values (*a priori* information) in preparation for symbol remapping. On the other hand, the *a priori* information matrix defined by Eqn. (4.22) employing the DM method is derived using only Eqn. (4.21). In this case, Eqn. (4.21) derives directly the probability values (*a priori* information) in preparation for symbol remapping. With this in mind, we analyse the computational time complexity for both *a priori* information derivation methods based on these equations. Therefore, working through Eqns. (4.10)-(4.19), the LLR *a priori* information derivation method will require a total of $MnQ(M+10)$ addition/subtraction operations, $MnQ(M+14)$ multiplication/division operations, and other functions. In comparison, the proposed DM *a priori* information derivation method defined by Eqn. (4.21) will require a total of $4Mn$ addition/subtraction operations, Mn multiplication/division operations with other functions as shown in Table 4.2.

TABLE 4.2: Computational complexity per iteration

Operations	LLR	LLR ($M=16$, $n=15$, $Q=4$)	DM	DM ($M=16$, $n=15$, $Q=4$)
$+/-$	$MnQ(M+10)$	24960	$4Mn$	960
$\times/\div$	$MnQ(M+14)$	28800	Mn	240
$\{\}^2$	$MnQ(M+4)$	19200	$2Mn$	480
$\surd$	$4MnQ$	3840	Mn	240
exp	$4MnQ$	3840	Mn	240
log	MnQ	960	0	0
$\|\ \|$	M^2nQ	15360	0	0
$tanh$	MnQ	960	0	0

As shown in Table 4.2, for $M=16$, $Q=4$, and $n=15$, the number of operations and functions required using the LLR method to produce Eqn. (4.20) is much higher in comparison to the number of operations and functions required using the DM method to produce Eqn. (4.22). From these analysis, it can be concluded that the DM method displays lower computational delay and time complexity in comparison with the LLR method; thus, it is suitable for use in real time iterative channel estimation systems. The lower computational delay and time complexity offered by the DM method makes it more suitable in iterative receiver structure in order to reduce the overall computational burden of the receiver.

Furthermore, the *KV-RS* algorithm guarantees soft decoding convergence. Theorems (12) and (17) in [10] proves how quickly the *KV-RS* decoding algorithm converges to the asymptotic performance as a function of the list-size L_s. As such, the *KV-RS* algorithm will guarantee convergence when used in iterative receiver structure employing either the LLR or DM *a priori* information method, even with small list-size L_s. Fig. 4.7 and Fig. 4.8 show the SER performance for L_s =4 employing both the LLR or DM *a priori* derivation information method. From Fig. 4.7, it can be seen that the LLR *a priori* information method converges with the third iteration. At iteration $\gamma = 4$ and 5, there is no significant improvement in the SER performance despite the increase in computational delay and time complexity as γ increases. Likewise, in Fig. 4.8, the DM *a priori* information derivation method convergences with the third iteration. This showcase that the proposed DM *a priori* information derivation method will maintain the asymptotic performance of the *KV-RS* algorithm as γ tends to infinity ($\gamma \rightarrow \infty$). However, as earlier said, the asymptotic performance of the *KV-RS* algorithm is a function of the list-size L_s. As list-size L_s increases, the convergence point of the *KV-RS* iterative receiver might also vary, most especially for large L_s.

4.5 Conclusion

In this paper, a decision directed iterative channel estimation and decoding receiver using Reed-Solomon codes has been studied. We adopted the *KV-RS* soft decision decoding algorithm assuming a list-size L_s=4 in the iterative receiver structure. This paper also proposed the DM method as a new and less complex way of deriving *a priori* information in iterative receiver structure, and a fair comparison with the LLR method. Performance evaluation is undertaken comparing the *KV-RS* iterative receiver with the *KV-RS* receiver without iteration. Furthermore, comparative computational delay and time complexity analysis are carried out to compare the proposed DM method with the widely used LLR method. Firstly, the *KV-RS* iterative receiver achieves significant SER performance improvement compared to the *KV-RS* receiver without feedback. Results shown in Fig. 4.4

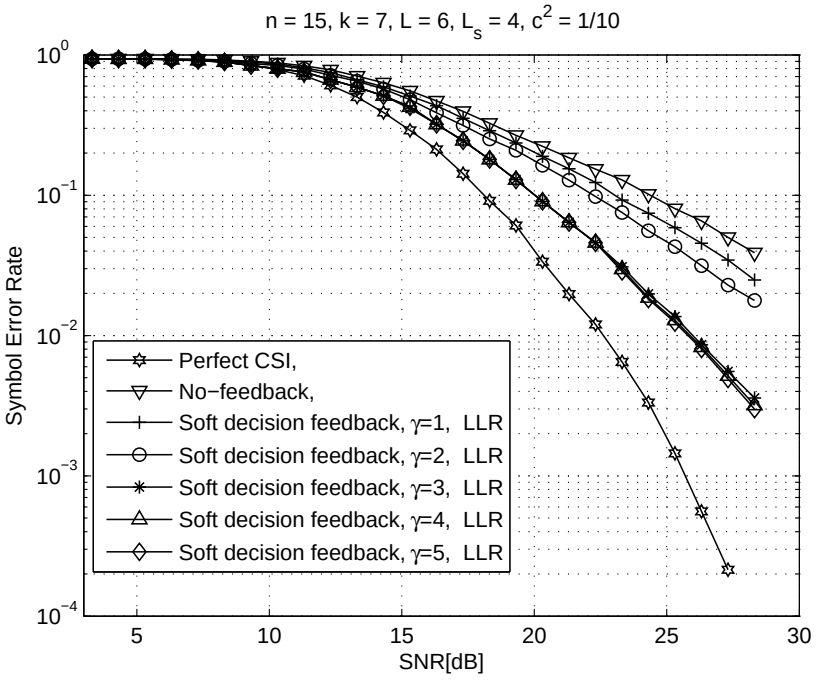

(a) Soft feedback

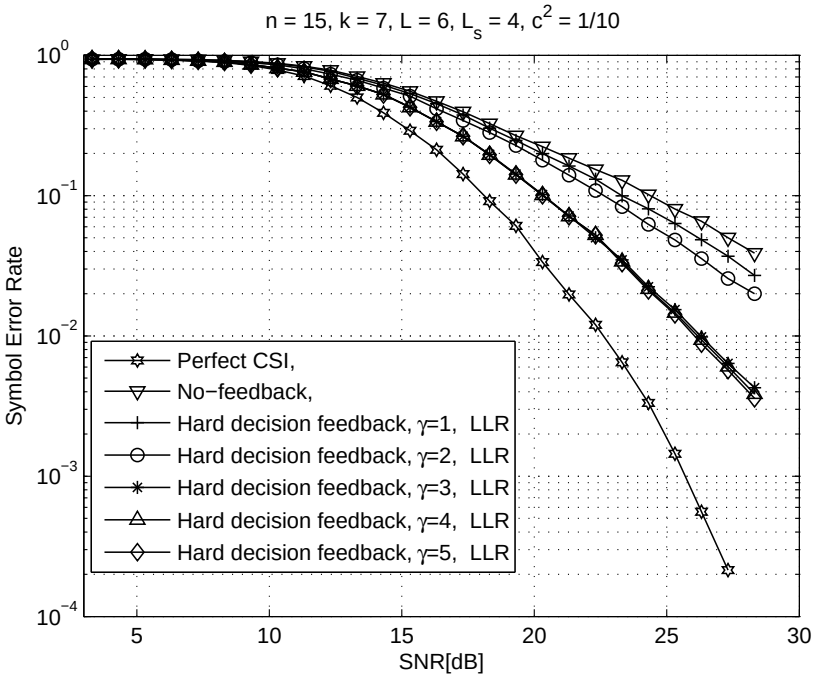

(b) Hard feedback

FIGURE 4.7: LLR *a priori* information method SER performance for $\gamma = 1, \ldots, 5$, and normalized Doppler $f_D T$=0.015

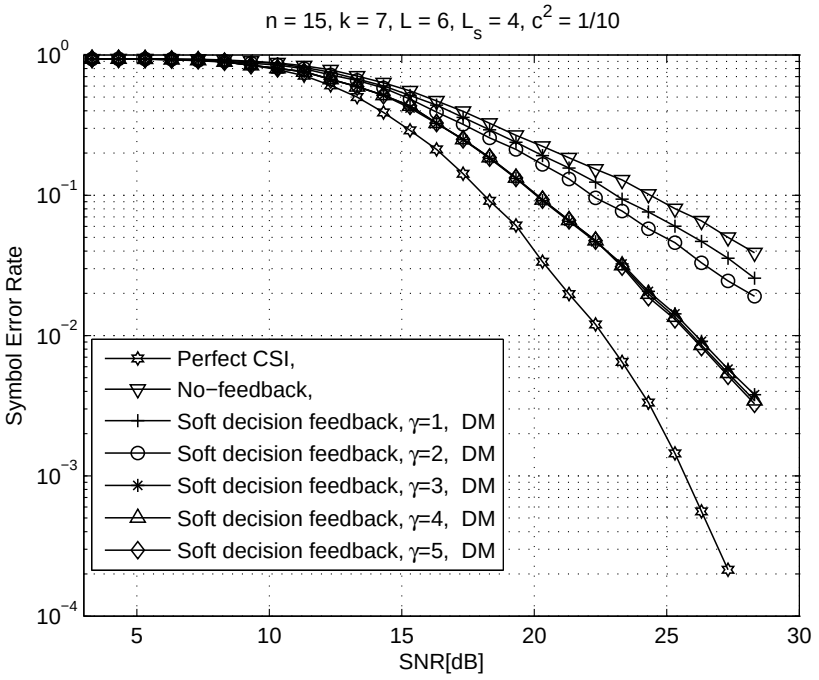

(a) Soft feedback

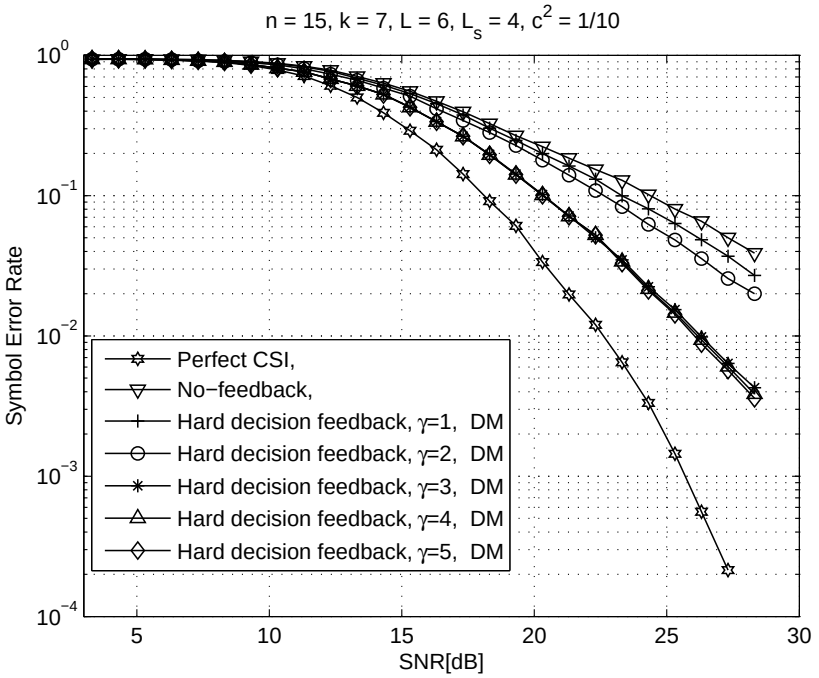

(b) Hard feedback

FIGURE 4.8: DM *a priori* information method SER performance for $\gamma = 1, \ldots, 5$, and normalized Doppler $f_D T$=0.015

and Fig. 4.5 confirm our analysis. The results indicate that *RS* codes can be used in iterative channel estimation receiver structure over flat Rayleigh fading channels. Secondly, the proposed DM method achieves the same SER performance in comparison with the LLR method for both decision directed hard and soft feedback at lower computational delay and time complexity. Table 4.2, and Fig. 4.6 confirm our analysis of the computational delay and time complexities of the LLR and proposed DM methods, and the SER performance respectively. The results presented show that the proposed DM method is a suitable replacement for the LLR method because it offers the same performance as the LLR method and it has the advantage of lower computational delay and time complexity. Although, results are shown for rectangular 16-QAM, the *KV-RS* iterative receiver structure can be extended to higher rectangular QAM signal constellations (M) and Reed-Solomon codes.

4.6 References

[1] J. Cavers, "An analysis of pilot symbol assisted modulation for Rayleigh fading channels [mobile radio]," *Vehicular Technology, IEEE Transactions on,* vol. 40, no. 4, pp. 686-693, Nov 1991.

[2] L. Erup, F. M. Gardner, and R. Harris, "Interpolation in digital modems. ii. implementation and performance," *Communications, IEEE Transactions on*, vol. 41, no. 6, pp. 998-1008, Jun 1993.

[3] Y.-S. Kim, C.-J. Kim, G.-Y. Jeong, *et al.*, "New Rayleigh fading channel estimator based on PSAM channel sounding technique," in *Communications, 1997. ICC '97 Montreal, Towards the Knowledge Millennium. 1997 IEEE International Conference on*, vol. 3, Jun 1997, pp. 1518-1520 vol.3.

[4] M. Valenti and B. Woerner, "Iterative channel estimation and decoding of pilot symbol assisted Turbo codes over flat-fading channels," *Selected Areas in Communications, IEEE Journal on,* vol. 19, no. 9, pp. 1697-1705, Sep 2001.

[5] T. Zemen, M. Loncar, J. Wehinger, C. Mecklenbrauker, and R. Muller, "Improved channel estimation for iterative receivers," in *Global Telecommunications Conference, 2003. GLOBECOM '03. IEEE,* vol. 1, Dec 2003, pp. 257–261 Vol.1.

[6] H. Niu and J. Ritcey, "Iterative channel estimation and decoding of pilot symbol assisted LDPC coded QAM over flat fading channels," in *Signals, Systems and Computers, 2004. Conference Record of the Thirty-Seventh Asilomar Conference on,* vol. 2, Nov 2003, pp. 2265-2269 Vol.2.

[7] M.-K. Oh, H. Kwon, D.-J.Park, and Y. H. Lee, "Iterative Channel Estimation and LDPC Decoding With Encoded Pilots," *Vehicular Technology, IEEE Transactions on,* vol. 57, no. 1, pp. 273-285, Jan 2008.

[8] K. Takeuchi, R. Muller, and M. Vehkapera, "Iterative LMMSE channel estimation and decoding based on probabilistic bias," *Communications, IEEE Transactions on,* vol. 61, no. 7, pp. 2853-2863, July 2013.

[9] I. G. Reed and G. Solomon, "Polynomial codes over certain finite fields," J. Soc.Ind. Appl. Maths., 8:300-304, June 1960.

[10] R. Koetter and A. Vardy, "Algebraic soft-decision decoding of Reed-Solomon codes," *Information Theory, IEEE Transactions on,* vol. 49, no. 11, pp. 2809-2825, Nov 2003.

[11] F. Kadrija, M. Simko, and M. Rupp, "Iterative channel estimation in LTE systems," in *Smart Antennas (WSA), 2013 17th International ITG Workshop on,* March 2013, pp. 1-7

[12] ETSI EN 300 744 V1.6.1 (2009-01), "DVB; Framing structure, channel coding, and modulation for digital terrestrial television".

[13] ETSI TS 102 563 V1.2.1 (2010-05), "DAB; Transport of AAC audio".

[14] CCSDS, "TM Synchronization and Channel Coding, Recommendation for Space Data Systems Standards." CCSDS 131.0-B-1, Blue Book, Issue 1, September 2003.

[15] Y. Liu, Y. Guan, J. Zhang, *et al.*, "Reed-Solomon Codes for Satellite Communications," in *Control, Automation and Systems Engineering, 2009. CASE 2009. IITA International Conference on*, July 2009, pp. 246-249.

[16] M. K. Simon and J. Smith, "Carrier Synchronization and Detection of QASK Signal Sets," *Communications, IEEE Transactions on*, vol. 22, no. 2, pp. 98-106, Feb 1974.

[17] W.C Jakes, *Mobile microwave communication.* New York: Wiley, 1974.

[18] W. Phoel, J. Pursley, M. Pursley, and J. Skinner, "Frequency-hop spread spectrum with quadrature amplitude modulation and error-control coding," *in Military Communications Conference, 2004. MILCOM 2004. 2004 IEEE*, vol. 2, Oct 2004, pp. 913-919 Vol. 2.

[19] T. K. Moon, *Error Correction Coding: Mathematical Methods and Algorithms.* John Wiley & Sons, 2005.

[20] O. Ogundile and D. Versfeld, "Improved reliability information for rectangular 16-QAM over flat Rayleigh fading channels," *in Computational Science and Engineering (CSE), 2014 17th IEEE International Conference on,* Dec 2014, pp. 345-349.

[21] V. Guruswami and M. Sudan, "Improved decoding of Reed-Solomon and algebraic-geometry codes," *Information Theory, IEEE Transactions on*, vol. 45, no. 6, pp. 1757-1767, Sep 1999.

[22] L. Chen and R. Carrasco, "Soft decoding of algebraic-geometric codes using Koetter-Vardy algorithm," *Electronics Letters,* vol. 45, no. 25, pp. 1334-1336, December 2009.

[23] S. Allpress, C. Luschi, and S. Felix, "Exact and approximated expressions of the log-likelihood ratio for 16-QAM signals," in *Signals, Systems and Computers, 2004. Conference Record of the Thirty-Eighth Asilomar Conference on*, vol. 1, Nov 2004, pp. 794-798 Vol.1.

[24] M. Tüchler, A. Singer, and R. Koetter, "Minimum mean squared error equalization using a priori information," *Signal Processing, IEEE Transactions on*, vol. 50, no. 3, pp. 673-683, Mar 2002.

[25] O. Oyerinde and S. Mneney, "Iterative receiver with soft-input-based-channel estimation for orthogonal frequency division multiplexing-interleave division multiple access systems" *Communications, IET,* vol. 8, no. 14, pp. 2445-2457, Sept 2014.

CHAPTER 5

Symbol Level Iterative Soft Decision Decoder for Reed-Solomon Codes Based on Parity-Check Equations

A symbol level iterative soft decision algorithm for Reed-Solomon codes based on parity-check equations is developed in this chapter. This algorithm is based on the soft reliability information derived from the channel output in order to perform syndrome checks in an iterative process. Performance analysis verifies that the developed algorithm outperforms the conventional *RS* hard decision decoding algorithms and the symbol level *KV* soft decision decoding algorithm. The developed algorithm have been published in a peer-reviewed journal paper. Accordingly, this chapter is organised conforming to this published journal paper. The detail of this journal paper is as follows.

- **O. Ogundile**, Y. Genga, and D. Versfeld, "Symbol level iterative soft decision decoder for Reed-Solomon codes based on parity-check equations," *Electronics Letters*, vol. 51, no. 17, pp. 1332–1333, 2015.

In this journal paper, the *RS* decoding algorithm was conceptualised and implemented by **O. Ogundile**. The results presented in this paper, and the manuscript preparation were developed by **O. Ogundile**. Y.Genga was involved with the result verification and performance comparison analysis of the developed *RS* decoding algorithm. The research was supervised by D. Versfeld, as well as manuscript preparation. Refer to Appendices A and B for the computational complexity and detailed performance analysis of the algorithm presented in this paper.

Abstract

A symbol level iterative Soft Decision (SD) algorithm for Reed-Solomon (RS) codes based on parity-check equations is developed. This is achieved by transforming the systematic parity-check matrix according to some rules. The rules are based on the soft reliability information matrix derived from the received vector. The performance of the resulting algorithm is documented through computer simulation in comparison with the hard decision Berlekamp-Massey (B-M) algorithm, and the Koetter-Vardy - Guruswami-Sudan (KV-GS) algorithm. Result verifies that the iterative SD algorithm outperforms the KV-GS and B-M algorithms by significant margin while maintaining a reasonable decoding time complexity level.

5.1 Introduction

Reed-Solomon (RS) codes introduced in [1] are very popular codes, due to this class of codes meeting the Singleton bound. This makes RS code maximum distance separable. Therefore, a (n, k) RS code can correct up to $\lfloor (n-k)/2 \rfloor$ errors, when a Hard-Decision (HD) decoder based on the minimum distance principle is employed. The RS codeword and information lengths are defined by n and k respectively. Efficient HD symbol level decoders are found in [2, 3]

Guruswami-Sudan (GS) [4] developed a list decoder for RS codes that can find all codewords with Hamming distance (d) within $n - \sqrt{n(n-d)}$ from the received word. In contrast, with minimum distance decoding we are guaranteed to either find only one codeword with d less than or equal to $((n-k)/2)$, or no codeword at all. The latter constitutes a decoding failure. However, HD decoding discards the real-valued information available from the channel by quantizing the real-valued information into HD. By performing HD decoding, it is shown that a penalty of approximately 2-3 dB in coding gain is paid [5] assuming an Additive White Gaussian Noise (AWGN) channel. In this regard, Koetter-Vardy (KV) [6] then developed a symbol level decoding algorithm that translates the Soft Decision (SD) reliability information provided by the channel into a modified multiplicity

matrix fed into the GS algorithm, effectively rendering the GS decoder as a SD decoder. KV proved that their algorithm effectively outperforms all the previous HD decoding algorithm for RS codes.

In this letter, we develop a simple symbol level iterative SD decoder for RS codes based on Parity-Check Equations (PCE). This Parity-check matrix Transformation Algorithm (PTA) is based on the soft reliability information derived from the channel output in order to perform syndrome checks in an iterative process. The performance of this proposed soft decoding algorithm is documented through computer simulations assuming an AWGN channel.

5.2 PTA for RS Codes

Assume we transmit a codeword $c \in C$, of length n. The codeword c is first passed through the modulator, where the symbols are mapped onto signals to be transmitted. The channel introduces AWGN, and we receive the vector r at the receiver. As a precursor to the PTA, we derive the soft reliability information matrix (β) using Distance Metric (DM) method proposed in [7]. Thus, we now directly operate on β, using the following algorithm. At the lth iteration, the PTA performs the following steps.

1. Determine the k most reliable received signals, according to some rules. The indices of these signals are denoted as $\mathcal{R}$, and the indices of the $n-k$ remaining signals are denoted as $\mathcal{U}$. (For the purpose of this letter, we will simply use the first k columns which contain the highest maximum values to determine the most reliable signals.)
2. Transform the systematic PCE H, such that $H^{(l)}$ contains a partitioned identity matrix where the indices of the unit column vectors u_i are equal to $\mathcal{U}$, and the indices of the parity column vectors are equal to $\mathcal{R}$.
3. Calculate the $n-k$ PCE using $H^{(l)}$. This is done by performing HD detection on β to obtain the vector r, and then doing the dot product $r \cdot H_q^{(l)}$, where $H_q^{(l)}$ is the qth row of matrix $H^{(l)}$. Due to the systematic structure of $H^{(l)}$,

one symbol with index in $\mathcal{U}$ and k symbols with indices in $\mathcal{R}$ will be used in the dot product. If the dot product is zero, we increment all $\beta_{v,j}$ (where $j \in u_q \cup \mathcal{R}$ and v such that $\beta_{v,j}$ is the largest element in column β_j) with some δ. If the dot product is not zero, we decrement all $\beta_{v,j}$ with some δ.

If all the PCE are satisfied, the process is halted, otherwise, the updated decision matrix $\beta^{(l)}$ is used as input, and the steps are repeated until the matrix $\beta^{(l)}$ seats an element $-\beta^{(l)}_{u,i}$ (where u and i denotes the row and column of matrix $\beta^{(l)}$ respectively). The PTA is hereby demonstrated by way of an example.

Consider the RS code with the following parameters:

- $n = 7$, $k = 2$, $\delta = 0.005$,
- $GF(2^3)$ constructed with primitive polynomial $p(z) = z^3 + z + 1$.

Assume that the codeword $c = (\alpha^5, \alpha^2, 0, \alpha, \alpha^3, \alpha^4, 1)$ with PCE defined by Eqn. (2) is modulated, and transmitted through a noisy channel.

$$H = \begin{pmatrix} \alpha^6 & \alpha^2 & 1 & 0 & 0 & 0 & 0 \\ \alpha & \alpha^3 & 0 & 1 & 0 & 0 & 0 \\ \alpha^2 & \alpha^6 & 0 & 0 & 1 & 0 & 0 \\ \alpha^5 & \alpha^4 & 0 & 0 & 0 & 1 & 0 \\ \alpha^3 & \alpha & 0 & 0 & 0 & 0 & 1 \end{pmatrix}. \tag{5.1}$$

Let β derived using the DM method [7] as:

$$\beta = \begin{pmatrix} 0.257 & 0.214 & 0.749 & 0.253 & 0.059 & 0.034 & 0.038 \\ 0.019 & 0.009 & 0.000 & 0.004 & 0.034 & 0.086 & 0.702 \\ 0.236 & 0.081 & 0.023 & 0.021 & 0.164 & 0.009 & 0.002 \\ 0.015 & 0.408 & 0.006 & 0.251 & 0.172 & 0.190 & 0.052 \\ 0.007 & 0.127 & 0.006 & 0.049 & 0.014 & 0.000 & 0.122 \\ 0.005 & 0.049 & 0.021 & 0.120 & 0.183 & 0.321 & 0.064 \\ 0.052 & 0.026 & 0.048 & 0.017 & 0.005 & 0.331 & 0.005 \\ 0.408 & 0.086 & 0.147 & 0.286 & 0.370 & 0.030 & 0.015 \end{pmatrix}, \tag{5.2}$$

Firstly, we determine the k columns with the highest maximum values, which constitute $\mathcal{R}$. For β, the set of indices for the reliable symbols are $\mathcal{R} = \{3, 7\}$, while $\mathcal{U} = \{1, 2, 4, 5, 6\}$.

Following Step 2, the PCE H is transformed to $H^{(1)}$ as

$$H^{(1)} = \begin{pmatrix} 1 & 0 & \alpha^4 & 0 & 0 & 0 & \alpha^5 \\ 0 & 1 & \alpha^6 & 0 & 0 & 0 & \alpha^2 \\ 0 & 0 & \alpha^3 & 1 & 0 & 0 & \alpha \\ 0 & 0 & \alpha & 0 & 1 & 0 & \alpha^3 \\ 0 & 0 & \alpha^5 & 0 & 0 & 1 & \alpha^4 \end{pmatrix}. \tag{5.3}$$

As shown in Eqn. (A), the indices of parity-check columns coincide with $\mathcal{R}$, and the indices of the partitioned identity matrix coincide with $\mathcal{U}$. There are various ways of transforming H to $H^{(1)}$. For a computationally efficient way, see for instance [8].

Using the HD outputs, we now calculate the various parity-checks. The received vector is determined as $r = (\alpha^5, \alpha^3, 0, \alpha^5, \alpha^5, \alpha^4, 1)$, by assuming that the rows correspond to $\{0, 1, \alpha, \alpha^3, \alpha^2, \alpha^6, \alpha^4, \alpha^5\}$. Next, the syndromes is calculated as

$$r \cdot H_1^{(1)} = (\alpha^5, \alpha^3, 0, \alpha^5, \alpha^5, \alpha^4, 1) \cdot (1, 0, \alpha^4, 0, 0, 0, \alpha^5) = 0 \tag{5.4}$$

$$r \cdot H_2^{(1)} = (\alpha^5, \alpha^3, 0, \alpha^5, \alpha^5, \alpha^4, 1) \cdot (0, 1, \alpha^6, 0, 0, 0, \alpha^2) = \alpha^5 \tag{5.5}$$

$$r \cdot H_3^{(1)} = (\alpha^5, \alpha^3, 0, \alpha^5, \alpha^5, \alpha^4, 1) \cdot (0, 0, \alpha^3, 1, 0, 0, \alpha) = \alpha^6 \tag{5.6}$$

$$r \cdot H_4^{(1)} = (\alpha^5, \alpha^3, 0, \alpha^5, \alpha^5, \alpha^4, 1) \cdot (0, 0, \alpha, 0, 1, 0, \alpha^3) = \alpha^2 \tag{5.7}$$

$$r \cdot H_5^{(1)} = (\alpha^5, \alpha^3, 0, \alpha^5, \alpha^5, \alpha^4, 1) \cdot (0, 0, \alpha^5, 0, 0, 1, \alpha^4) = 0 \tag{5.8}$$

The first PCE (Eqn. (4)) checks, therefore the corresponding $\mathcal{U}$ element is incremented by δ, and the $\mathcal{R}$ elements by $\delta/2$, yielding:

$$\beta_1^{(1)} = \begin{pmatrix} 0.257 & 0.214 & 0.752 & 0.253 & 0.059 & 0.034 & 0.038 \\ 0.019 & 0.009 & 0.000 & 0.004 & 0.034 & 0.086 & 0.705 \\ 0.236 & 0.081 & 0.023 & 0.021 & 0.164 & 0.009 & 0.002 \\ 0.015 & 0.408 & 0.006 & 0.251 & 0.172 & 0.190 & 0.052 \\ 0.007 & 0.127 & 0.006 & 0.049 & 0.014 & 0.000 & 0.122 \\ 0.005 & 0.049 & 0.021 & 0.120 & 0.183 & 0.321 & 0.064 \\ 0.052 & 0.026 & 0.048 & 0.017 & 0.005 & 0.331 & 0.005 \\ 0.413 & 0.086 & 0.147 & 0.286 & 0.370 & 0.030 & 0.015 \end{pmatrix}. \tag{5.9}$$

Similarly, we verify if the second PCE (Eqn. (4)) checks. In this case, Eqn. (4) fails the parity-check test. Therefore, the corresponding $\mathcal{U}$ element is decremented by δ, and the $\mathcal{R}$ elements by $\delta/2$, yielding:

$$\beta_2^{(1)} = \begin{pmatrix} 0.257 & 0.214 & 0.749 & 0.253 & 0.059 & 0.034 & 0.038 \\ 0.019 & 0.009 & 0.000 & 0.004 & 0.034 & 0.086 & 0.702 \\ 0.236 & 0.081 & 0.023 & 0.021 & 0.164 & 0.009 & 0.002 \\ 0.015 & 0.404 & 0.006 & 0.251 & 0.172 & 0.190 & 0.052 \\ 0.007 & 0.127 & 0.006 & 0.049 & 0.014 & 0.000 & 0.122 \\ 0.005 & 0.049 & 0.021 & 0.120 & 0.183 & 0.321 & 0.064 \\ 0.052 & 0.026 & 0.048 & 0.017 & 0.005 & 0.331 & 0.005 \\ 0.413 & 0.086 & 0.147 & 0.286 & 0.370 & 0.030 & 0.015 \end{pmatrix}. \tag{5.10}$$

Using similar approach, the final β after the first iteration is given as:

$$\beta^{(1)} = \begin{pmatrix} 0.257 & 0.214 & 0.747 & 0.253 & 0.059 & 0.034 & 0.038 \\ 0.019 & 0.009 & 0.000 & 0.004 & 0.034 & 0.086 & 0.700 \\ 0.236 & 0.081 & 0.023 & 0.021 & 0.164 & 0.009 & 0.002 \\ 0.015 & 0.404 & 0.006 & 0.251 & 0.172 & 0.190 & 0.052 \\ 0.007 & 0.127 & 0.006 & 0.049 & 0.014 & 0.000 & 0.122 \\ 0.005 & 0.049 & 0.021 & 0.120 & 0.183 & 0.321 & 0.064 \\ 0.052 & 0.026 & 0.048 & 0.017 & 0.005 & 0.336 & 0.005 \\ 0.413 & 0.086 & 0.147 & 0.281 & 0.365 & 0.030 & 0.015 \end{pmatrix}, \tag{5.11}$$

The iterative process is repeated until all the PCE are satisfied or any entry of the updated decision matrix $\beta^{(l)}$ is less than zero $\left(\beta_{u,i}^{(l)} < 0\right)$. In this example, the PCE are satisfied after 172 iterations. Thus, the resulting β is given as:

$$\beta^{(172)} = \begin{pmatrix} 0.257 & 0.124 & 1.467 & 0.018 & 0.059 & 0.034 & 0.038 \\ 0.019 & 0.009 & 0.000 & 0.004 & 0.034 & 0.086 & 1.467 \\ 0.236 & 0.081 & 0.023 & 0.026 & 0.164 & 0.009 & 0.002 \\ 0.015 & 0.123 & 0.006 & 0.021 & 0.822 & 0.190 & 0.052 \\ 0.007 & 0.617 & 0.006 & 0.019 & 0.014 & 0.000 & 0.122 \\ 0.005 & 0.049 & 0.021 & 0.020 & 0.168 & 0.321 & 0.064 \\ 0.052 & 0.026 & 0.048 & 0.017 & 0.005 & 1.196 & 0.005 \\ 1.216 & 0.086 & 0.147 & 0.021 & 0.170 & 0.030 & 0.015 \end{pmatrix}. \tag{5.12}$$

The reliability matrix defined by Eqn. (5.12) has an all zero syndrome and it yields the correctly decoded vector $\hat{c} = c = (\alpha^5, \alpha^2, 0, \alpha, \alpha^3, \alpha^4, 1)$.

5.3 Performance Comparison Analysis for Different δ

A simulation study was carried out to test the performance of the PTA. In the simulation, a (15, 7) *RS* code is used. The underlying modulation scheme is a rectangular 16-QAM constellation, with AWGN. For the same input data, we compare the performance of the proposed algorithm for different values of δ. Fig. A.2 shows

the Symbol Error Rate (SER) performance for the values of δ assumed. As a key note from the figure, δ determines the performance of the algorithm. The smaller the value of δ, the better the performance of the algorithm. As shown, δ=0.001 yields the best performance on the SER curve of Fig. A.2. However, the smaller the value of δ, the more iterations the algorithm will need. To emphasize, if δ=0.001 is assumed in the algorithm for the above example, the PCE are only satisfied after 792 iterations $\left(\beta^{(792)}\right)$. The number of iterations required to satisfy the PCE for δ=0.001 $\left(\beta^{(792)}\right)$ is much greater than the number of iterations required for δ=0.005 $\left(\beta^{(172)}\right)$, so the former increases the decoding time complexity of the algorithm. Thus, there is a trade-off between the algorithm decoding performance, and its computational delay and time complexity while selecting the value of δ.

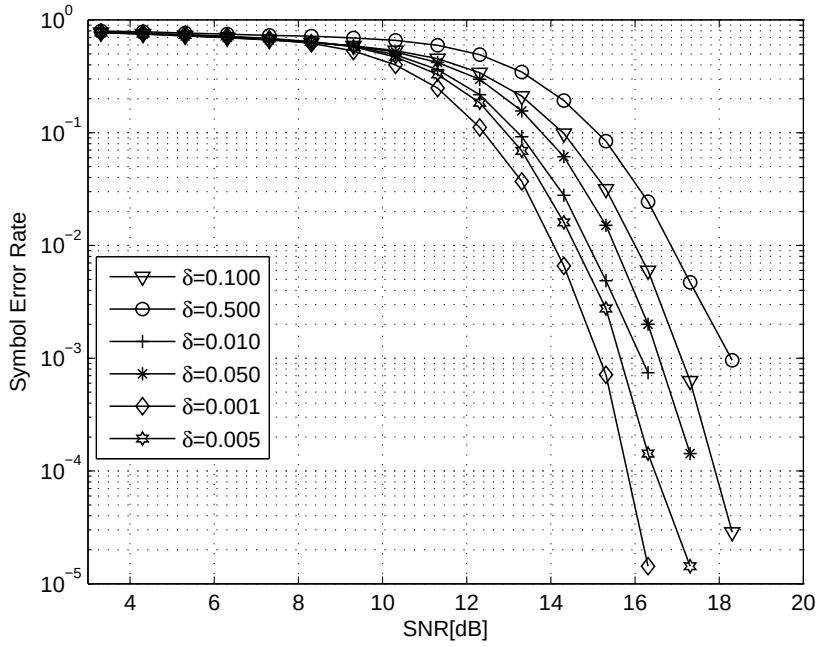

FIGURE 5.1: Performance comparison of the PTA for different values of δ.

5.4 Performance Comparison Analysis with other Symbol Level Soft Decoding Algorithms

Assuming the same computer simulation parameters, we compare the performance of HD *B-M* [2, 3] algorithm, the *KV-GS* SD decoder with a list-size $L = 4$, and

the proposed PTA. Fig. A.3 shows the SER performance of this *RS* decoding algorithms. From the figure, it can be seen that the proposed algorithm outperforms the *KV-GS* SD decoder and the HD *B-M* decoder. This portrays the proposed PTA for *RS* codes as a robust symbol level Forward Error Correction (FEC) decoding scheme and it can be implemented on real time coding systems.

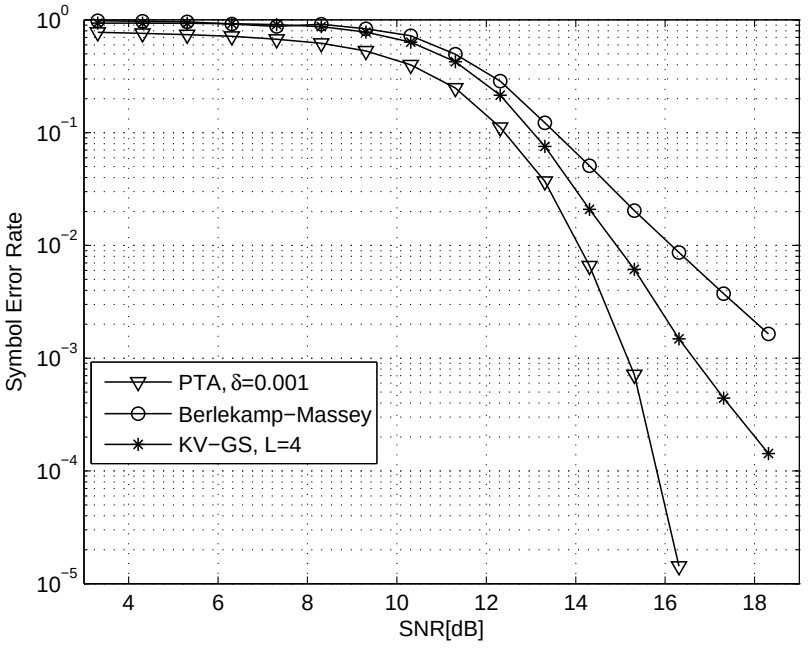

FIGURE 5.2: Performance comparison of the PTA with the *KV-GS* and *B-M* algorithms.

5.5 Conclusion

In this letter, we show that PCE can be used to implement SD decoding for *RS* codes. The proposed PTA surpasses the HD *B-M* algorithm, and the *KV-GS* SD algorithm with significant gap. Besides, we show that the SER performance of the algorithm can be improved by making δ as small as possible; though, this increase the decoding complexity.

5.6 References

[1] I. S. Reed and G. Solomon, "Polynomial codes over Certain Finite fields," J. Soc.Ind. Appl. Maths., 8:300-304, June 1960.

[2] E. R. Berlekamp, *Algebraic Coding Theory.* New York: McGraw-Hill, Inc., 1968.

[3] J. Massey, "Shift-register synthesis and bch decoding," *Information Theory, IEEE Transactions on,* vol. 15, no. 1, pp. 122-127, Jan 1969.

[4] V. Guruswami and M. Sudan, "Improved decoding of Reed-Solomon and algebraic-geometry codes," *Information Theory, IEEE Transactions on*, vol. 45, no. 6, pp. 1757-1767, Sep 1999.

[5] S. Wicker and V. Bhargava, *Reed-Solomon Codes and Their Applications.* New York: IEEE Press, 1994.

[6] R. Koetter and A. Vardy, "Algebraic soft-decision decoding of Reed-Solomon codes," *Information Theory, IEEE Transactions on*, vol. 49, no. 11, pp. 2809-2825, Nov 2003.

[7] O. Ogundile and D. Versfeld, "Improved reliability information for rectangular 16-QAM over flat Rayleigh fading channels," in *Computational Science and Engineering (CSE), 2014 IEEE 17th International Conference on,* Dec 2014, pp. 345–349.

[8] J. Cavers, "An analysis of pilot symbol assisted modulation for Rayleigh fading channels [mobile radio]," *Vehicular Technology, IEEE Transactions on,* vol. 40, no. 4, pp. 686-693, Nov 1991.

[9] D. Versfeld, J. Ridley, H. Ferreira, and A. Helberg, "On systematic generator matrices for Reed-Solomon codes," *Information Theory, IEEE Transactions on,* vol. 56, no. 6, pp. 2549–2550, June 2010.

CHAPTER 6

An Iterative Channel Estimation and Decoding Receiver Based on Reed-Solomon PTA

In this chapter, a low complexity iterative channel estimation and decoding receiver is developed based on the Reed-Solomon parity-check matrix transformation algorithm. The PTA provides design ease and flexibility, and lesser computational time complexity in comparison with the KV algorithm when deployed in a joint iterative receiver structure. Besides, a key feature of this iterative receiver structure is the simple symbol remapping process used to refine the previous estimate of the channel after each iterative Reed-Solomon PTA decoding. Simulation results show that the PTA iterative receiver structure outperforms the first Reed-Solomon KV iterative receiver structure. The study and results of this chapter have been submitted in a peer-reviewed journal for publication. As such, this chapter is structured in line with this submitted journal paper. The paper submission detail is as follows.

- **O. Ogundile**, and D. Versfeld, "An Iterative Channel Estimation and Decoding Receiver Based on Reed-Solomon PTA", -*Submitted to IET Communications (under review), March 2016.*

The concept, model and results presented in this journal paper (under review) was developed by **O. Ogundile**. As well, this manuscript was prepared by **O. Ogundile**. The research and manuscript preparation was supervised by D. Versfeld.

Abstract

A low complexity iterative channel estimation and Reed-Solomon (RS) decoding receiver is developed. The joint channel estimation and decoding receiver is based on the Linear Minimum Mean Square Error (LMMSE) channel estimation technique and the recently proposed RS Parity-check Transformation Algorithm (PTA). A key feature of this joint receiver is the simple symbol remapping process used to refine the initial LMMSE estimate of the channel after each iterative RS-PTA decoding. The performance of the joint iterative receiver is compiled through computer simulation assuming a rectangular M-ary Quadrature Amplitude Modulation (M-QAM) as the underlying modulation scheme. Simulation results show significant Symbol Error Rate (SER) improvement in the iterative receiver in comparison with the receiver without iterative feedback. Besides, the RS-PTA iterative receiver outperforms the recently proposed RS Koetter and Vardy (RS-KV) iterative receiver structure both in terms of the SER performance and the computational time complexity. Of particular interest, results verify that the computational time complexity of the RS-PTA iterative receiver can be reduced without compromising the SER performance of the receiver.

6.1 Introduction

Recently, the Parity-check Transformation Algorithm (PTA) [1] was proposed as a soft decision decoding Forward Error Correction (FEC) scheme for Reed-Solomon (RS) codes. The PTA is a symbol level RS soft decoder that iteratively transforms the parity-check matrix in order to perform a syndrome check. With each iteration, the RS-PTA fine-tune the derived soft reliability information from the channel output based on some rules. The RS-PTA has an adjustable decimal parameter δ which specifies the decoding Symbol Error Rate (SER) performance, and the decoding time complexity of the algorithm. In all cases, the smaller the degree of δ the better the SER performance of the RS-PTA, which in turns increase the decoding time complexity of the algorithm. For reference, see Fig. 6.1.

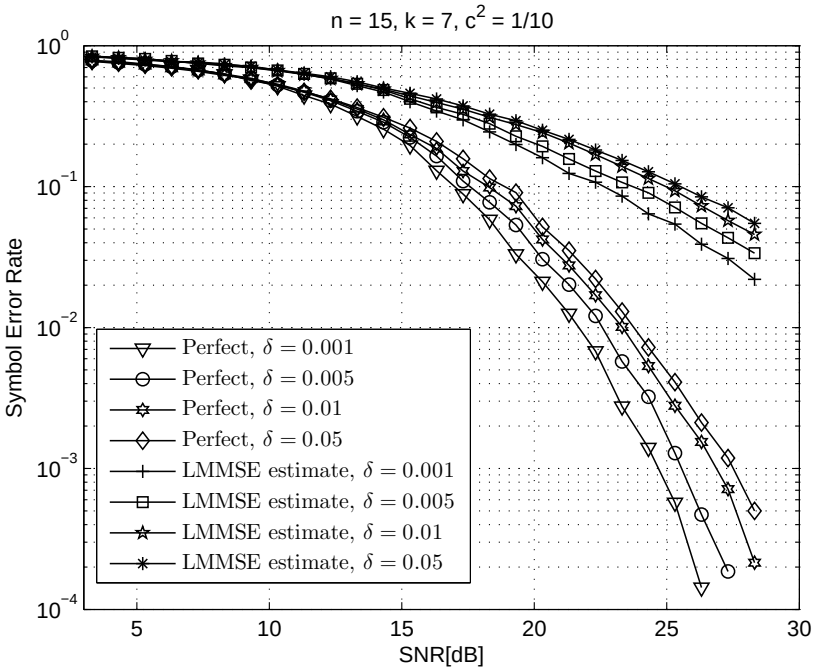

FIGURE 6.1: SER performance of the RS-PTA over flat Rayleigh fading channel, $F_dT = 0.015$.

In Fig. 6.1, it is conspicuous that the performance of the decoder plummets as a result of the fast Rayleigh fading channel. Note, F_dT specifies the normalized Doppler frequency (where F_d is the Doppler frequency and T is the symbol period), and rectangular M-ary Quadrature Amplitude Modulation (M-QAM) is adopted as the underlying modulation scheme, where $M = 16$. One way of solving this problem; that is, improving the SER performance of this RS-PTA over Rayleigh fading channels is by iteratively combining the RS-PTA decoder with an optimal channel estimation technique. Joint iterative channel estimation and decoding receivers have been the subject of recent research, whereby different FEC schemes are adapted in the receiver structure. Traditionally, in iterative receiver structures, the initial Channel State Information (CSI) are computed using the properties of the known pilot symbols. The quality of the CSI is improved after each iterative decoding using the feedback information from the decoder. In literature, most iterative receiver structures uses Turbo, and Low Density Parity Check (LDPC) codes as the FEC scheme in the receiver structure. See for instances [2-6].

With attention to RS codes, we recently provided a survey and proposed the

first joint iterative channel estimation and RS decoding receiver using the RS Koetter and Vardy (RS-KV) soft decision decoder [8] as the FEC scheme in the receiver structure [7]. The importance of deploying RS codes in an iterative receiver structure was emphasized in [7]. In addition, we divulged in [7] that RS codes are suitable in iterative receiver structures as in the case with Turbo and LDPC codes. The main drawback of the joint iterative receiver structure in [7] is the computational delay and time complexity of the receiver, majorly due to the RS-KV algorithm used in the receiver structure. The RS-KV decoder applied to the Guruswami and Sudan algorithm (GS) [9] standing alone can provide a practical $\mathcal{O}(M^2n^2I^4)$ complexity to the receiver structure, where M is defined as above, n is the codeword length and I is the adjustable interpolation multiplicity specified in the GS algorithm [10].

In this regard, we propose a low complexity iterative channel estimation and decoding receiver structure based on the RS-PTA [1] [2]. Firstly, as shown in Fig. 6.8, this proposed iterative receiver structure offers better SER perform than the recently proposed RS-KV iterative receiver structure in [7]. Secondly, as expounded in [1], the RS-PTA is a much less computationally intensive decoding algorithm in comparison with the RS-KV algorithm. Consequently, it exhibits low computational delay and time complexity when deployed in a joint iterative receiver structure as shown in Table 6.1. Besides, the proposed RS-PTA iterative receiver structure showcases a simple symbol remapping technique in comparison with most iterative receiver structures found in the literature. Thus, the RS-PTA iterative receiver structure can be deployed in real time communication systems. Note that the primary purpose of this paper is not to compare between codes (RS codes, Turbo codes or LDPC codes), rather, the proposal of a less complex and performance efficient iterative receiver structure based on Reed-Solomon codes and a fair comparison with existing RS iterative receiver structure.

[1] Note in passing that we proposed the Reed-Solomon Parity Transformation Algorithm (RS-PTA) in [1].

[2] The RS-PTA iterative receiver is a low complexity and performance efficient modification of the RS-KV iterative receiver we proposed in [7].

The remainder of this paper is organised as follows. The discrete-time transmitter and channel model is described in Section 6.2. Section 6.3 explains the proposed *RS*-PTA iterative receiver structure in a block-wise fashion. Results with discernible comments are presented in Section 6.4. In particular, Section 6.4 presents a comparative SER simulation result and computational time complexity analysis between the *RS*-KV iterative receiver structure and this proposed *RS*-PTA iterative receiver structure. This paper is summarised with notable remarks in Section 6.5.

6.2 Transmitter and Channel Model

Fig. 6.2 depicts the discrete-time transmitter model of a *RS* coded 16-QAM system. The generated input symbol g is encoded using a (n, k) *RS* code, where k is the length of the information symbol, and n is defined as above. The encoded symbol $\hat{g}$ of length n is mapped to rectangular 16-QAM (M=16) complex data symbols in which the in-phase and quadrature parts both assume values from a set $(\pm 1c, \pm 3c, ... \pm (m-1)c)$, where m is defined as $M = m^2$ [11, 12]. In order to efficiently track the effect of the fading channel, pilot symbols p are intermittently inserted to the mapped symbols x_u. In this paper, we assumed that all the pilot symbols have uniform value. The pilot and data sequence x_v is divided into frames of equal length F_L with the assumption that each frame starts with a pilot symbol. This frame structure is transmitted over a flat Rayleigh fading channel with normalized Doppler F_dT, and it is contorted with Additive White Gaussian Noise (AWGN). The Jakes's isotropic scattering model [13] is assumed for the complex Rayleigh fading.

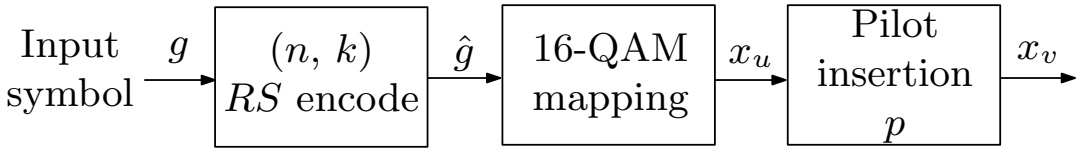

FIGURE 6.2: Transmitter model of an *RS* coded 16-QAM system.

6.3 *RS*-PTA Iterative Receiver Structure

The proposed *RS*-PTA iterative receiver structure is as illustrated in Fig. 6.3. The input of length (n + number of p) to the iterative receiver after down-converting and matched filtering is defined as:

$$y_v = cx_v z_v + \phi_v, \tag{6.1}$$

where y_v is the noisy received symbol, ϕ_v is the complex AWGN with variance $\sigma^2 = N_o/2$, c is a positive real number, and z_v is the complex discrete-time zero mean Gaussian variable representing the fading distortion at both the data and pilot symbol positions. In practice, z_v is only known at the pilot symbol positions. In order to derive the CSI (z_{i_u}) at the data symbol positions, the known properties of the pilot symbols are used.

In Fig. 6.3, the known properties of the pilot symbols are firstly used to derive the initial CSI. Afterwards, the pilot symbols are separated from the data symbols. Therefore, a soft reliability information matrix is initially derived from the data symbols. The initial soft reliability information is fed into the *RS*-PTA decoder which iteratively operate on this matrix to produce a final reliability information matrix. The output of the *RS*-PTA decoder (the final reliability information matrix) is simply remapped into symbols in order to fine-tune the initial CSI. The *RS*-PTA iterative receiver process is further explained as follows.

Given that the properties at the pilot symbol position only is defined as:

$$y_p = cx_p z_p + \phi_p, \tag{6.2}$$

where y_p, x_p, and ϕ_p are defined as above but in terms of the pilot symbols. The initial CSI is derived using the optimal Linear Minimum Mean Square Error (LMMSE) estimator proposed in [14, 15]. Hence, the LMMSE estimate of the

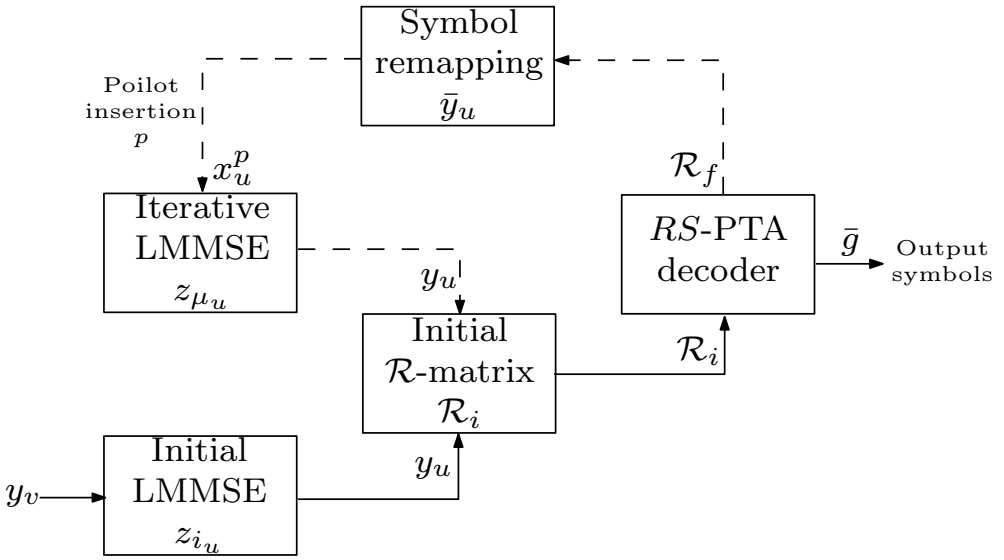

FIGURE 6.3: *RS*-PTA iterative receiver structure.

fading distortion at the data symbol positions is expressed as [14,15]:

$$z_{i_u} = \psi_{i_u}^{\dagger} y_p. \tag{6.3}$$

The notation ψ_{i_u} is derived using the Wiener-Hopf equation defined as [14, 15]:

$$\mathcal{C}_{i_u} = \mathcal{A}\psi_{i_u}, \tag{6.4}$$

where $\mathcal{A}$ and $\mathcal{C}_{i_u}$ are the autocorrelation matrix and covariance vectors respectively defined as [14, 15]:

$$\mathcal{A} = E\Big[y_p y_p^{\dagger}\Big] \quad \text{and} \quad \mathcal{C}_{i_u} = E\Big[z_p^* y_p\Big]. \tag{6.5}$$

The sign † and $*$ denotes the conjugate transpose and the complex conjugate respectively. As a key note, ψ_{i_u} is interpolated to derive the CSI at the each data symbol position. See [14, 15] for straightforward derivations of the LMMSE estimator.

6.3.1 Initial $\mathcal{R}$-matrix

As a precursor to the *RS*-PTA decoder, the initial reliability matrix ($\mathcal{R}$-matrix) is derived from the received symbol as [11, 16, 17]:

$$\mathcal{D} = c.\left(e^{-\sqrt{(y_{u_{in}} - q_{u_{in}}) + (y_{u_{im}} - q_{u_{im}})}}\right), \tag{6.6}$$

where $q_u = (q_{u_{in}}, q_{u_{im}})$ is the symbol in the output 16-QAM constellation, and $y_u = (y_{u_{in}}, y_{u_{im}})$ is the in-phase and quadrature parts of the received symbol. Literally, Equation (6.6) measures the distance from y_u to all the output 16-QAM constellation points q_u to form a $\mathcal{R}$-matrix defined as:

$$\mathcal{R}_i = \begin{pmatrix} \alpha_{0,0} & \alpha_{0,1} & \alpha_{0,2} & \dots & \alpha_{0,n-1} \\ \alpha_{1,0} & \alpha_{1,1} & \alpha_{1,2} & \dots & \alpha_{1,n-1} \\ \alpha_{2,0} & \alpha_{2,1} & \alpha_{2,2} & \dots & \alpha_{2,n-1} \\ \vdots & \vdots & \vdots & \ddots & \vdots \\ \alpha_{n,0} & \alpha_{n,1} & \alpha_{n,2} & \dots & \alpha_{n,n-1} \end{pmatrix}. \tag{6.7}$$

The notation $\alpha_{n,n-1}$ is the reliability value denoting the likelihood of receiving a QAM symbol. Also, the entries of $\mathcal{R}_i$ are normalized and quantized to $\log_2(n+1)$ bits of precision. For a performance efficient way of obtaining Equation (6.7), refer to [11].

6.3.2 *RS*-PTA Decoder

As explained in Section 6.1, the *RS*-PTA decoder iteratively operate on the derived $\mathcal{R}$-matrix (in this case $\mathcal{R}_i$) to produce a final $\mathcal{R}$-matrix $\mathcal{R}_f$ defined as:

$$\mathcal{R}_f = \begin{pmatrix} \alpha'_{0,0} & \alpha'_{0,1} & \alpha'_{0,2} & \dots & \alpha'_{0,n-1} \\ \alpha'_{1,0} & \alpha'_{1,1} & \alpha'_{1,2} & \dots & \alpha'_{1,n-1} \\ \alpha'_{2,0} & \alpha'_{2,1} & \alpha'_{2,2} & \dots & \alpha'_{2,n-1} \\ \vdots & \vdots & \vdots & \ddots & \vdots \\ \alpha'_{n,0} & \alpha'_{n,1} & \alpha'_{n,2} & \dots & \alpha'_{n,n-1} \end{pmatrix}. \tag{6.8}$$

Therefore, the decoded symbol $\bar{g}$ is obtained from the hard decoding decision of $\mathcal{R}_f$ (by selecting the most reliable symbols in each column of $\mathcal{R}_f$). However, for more reliable symbol decoding over fading channels, the entries of $\mathcal{R}_f$ are remapped into symbols in order to improve the quality of the previous CSI.

6.3.3 Symbol Remapping

The output of the *RS*-PTA decoder ($\mathcal{R}_f$) prior to the hard decoding decisions, is simply remapped into symbols as defined by Equation (6.9):

$$\bar{y}_{u_j} = \sum_{l=1}^{n+1} q_u \mathcal{R}_{f_{l,j}}, \tag{6.9}$$

where l and j denotes the row and column of $\mathcal{R}_f$ respectively. The remapped symbols $\bar{y}_u$ are subsequently fused with the pilot symbols p in preparation for the next iterative estimate. Key remark, the *RS*-PTA iterative receiver structure do not require the log-likelihood ratio and the code bit probability calculation steps to derive the *a priori* information which is used in the symbol remapping process. Accordingly, the symbol remapping process of the *RS*-PTA iterative receiver structure is far much less time complex in comparison with most iterative receiver structures in the literature. For more details on the Log-Likelihood Ratio

(LLR) and the code bit probability calculation steps of iterative receiver structures, see references [4-7].

6.3.4 Iterative LMMSE Estimate

The iterative CSI estimate is derived using a similar approach as the initial CSI estimate. Thus, it is derived as:

$$z_{\mu_u} = \psi^{\dagger}_{\mu_u} y_u, \tag{6.10}$$

where μ represents the number of iterative estimates, and y_u is defined as:

$$y_u = c x^p_u z_u + \phi_u. \tag{6.11}$$

The combination of the remapped symbol $\bar{y}_u$ and the pilot symbol p is denoted as x^p_u. In this case, the autocorrelation matrix $\mathcal{A}$ and the covariance vector are defined in terms of the received data symbols as:

$$\mathcal{A} = E\Big[y_u y^{\dagger}_u\Big] \quad \text{and} \quad \mathcal{C}_{i_u} = E\Big[z^*_u y_u\Big]. \tag{6.12}$$

The iterative process continues until the set number of iterative estimates is reached. Thus, we summarise the RS-PTA iterative receiver structure with the following algorithm.

6.4 Performance Analaysis

6.4.1 Performance Comparison of the RS-PTA Iterative Receiver Structure for Different δs

In this Section, the computer simulation results of the RS-PTA receiver without feedback (Fig. 6.3 without the dashed lines) and with feedback (Fig. 6.3 with the dashed lines) are presented for different adjustable decimal parameter δ. A low

Algorithm 1: *RS*-PTA iterative receiver structure

Input: *RS*-PTA parameters, y_v, p, μ.
Output: Decoded vector $\bar{g}$.
derive: z_{i_u}, $\mathcal{R}_i$;
repeat
  RS-PTA, $\mathcal{R}_f$;
  $\mu = false$;
  repeat
    derive: $\bar{y}_u$, x_u^p, z_{μ_u}, $\mathcal{R}_i$;
    RS-PTA, $\mathcal{R}_f$;
  until $\mu = true$;
until $\mu = true$;
$\mathcal{R}_f = \bar{g}$

rate (15, 7) *RS* code is assumed in the computer simulation set-up. A rectangular 16-QAM constellation is used as the underlying modulation scheme over a flat Rayleigh fading channel with normalized Doppler frequency $F_dT = 0.015$. In addition, a maximum number of iterative channel estimation $\mu = 5$ is set.

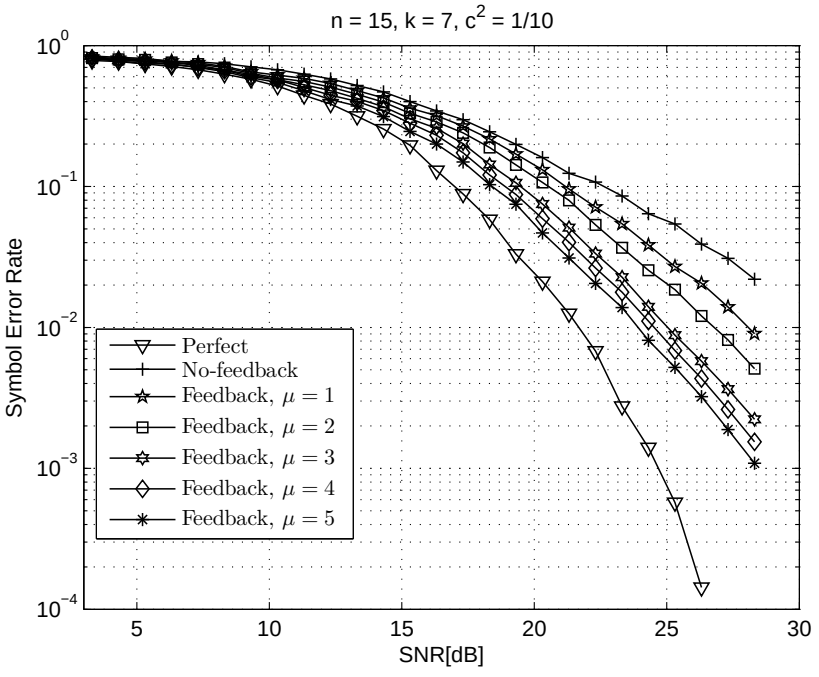

FIGURE 6.4: SER performance of the *RS*-PTA iterative receiver structure for $\delta = 0.001$, $F_dT = 0.015$.

Fig. 6.4 and Fig. 6.5 verify the SER performance of the *RS*-PTA iterative receiver structure for $\delta = 0.001$ and $\delta = 0.005$ respectively. The figures compare the SER performance of the iterative receiver assuming perfect channel estimation, the

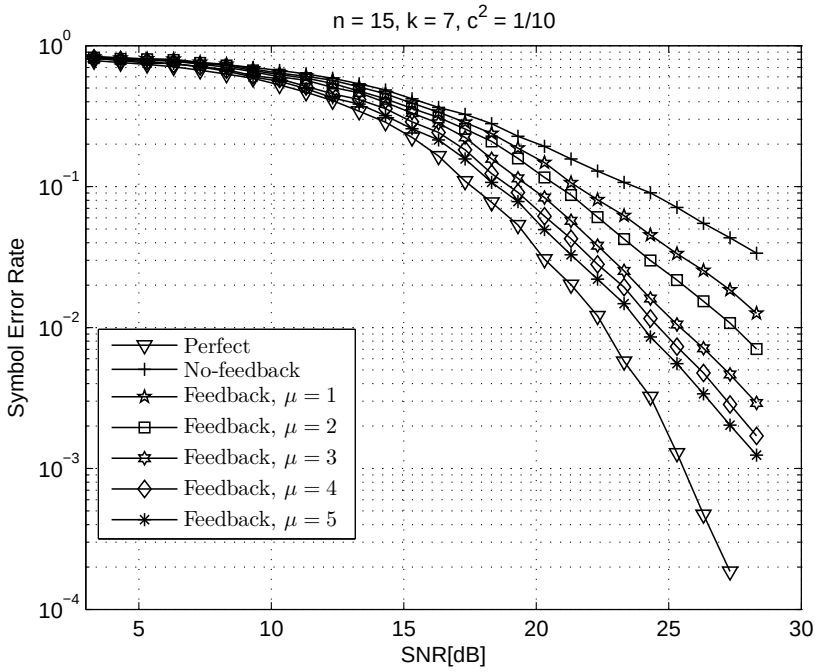

FIGURE 6.5: SER performance of the *RS*-PTA iterative receiver structure for $\delta = 0.005$, $F_dT = 0.015$.

SER performance using pilot symbols without feedback, and the SER performance using pilots symbol with feedback. From the figures, it is observable that the *RS*-PTA iterative receiver structure exhibits good SER performance improvement in comparison with the *RS*-PTA receiver without feedback.

Of particular interest, Fig. 6.6 shows the SER performance of the *RS*-PTA iterative receiver structure at $\mu = 4$ and $\mu = 5$ for adjustable decimal parameters $\delta = 0.001$ and $\delta = 0.005$. Clearly, both δs offer similar SER performance as μ increases. Thus, we note that it is possible to reduce the degree of δ in order for the receiver to evince a moderate time complexity level while maintaining a comparable SER performance with δs of the same decimal digit. To buttress, as expounded in [1], a $\delta = 0.001$ exhibits more than four times the decoding time complexity of $\delta = 0.005$. Consequently, this means we can greatly reduce the computational time complexity of the *RS*-PTA iterative receiver by selecting a higher δ without compromising the SER performance of receiver.

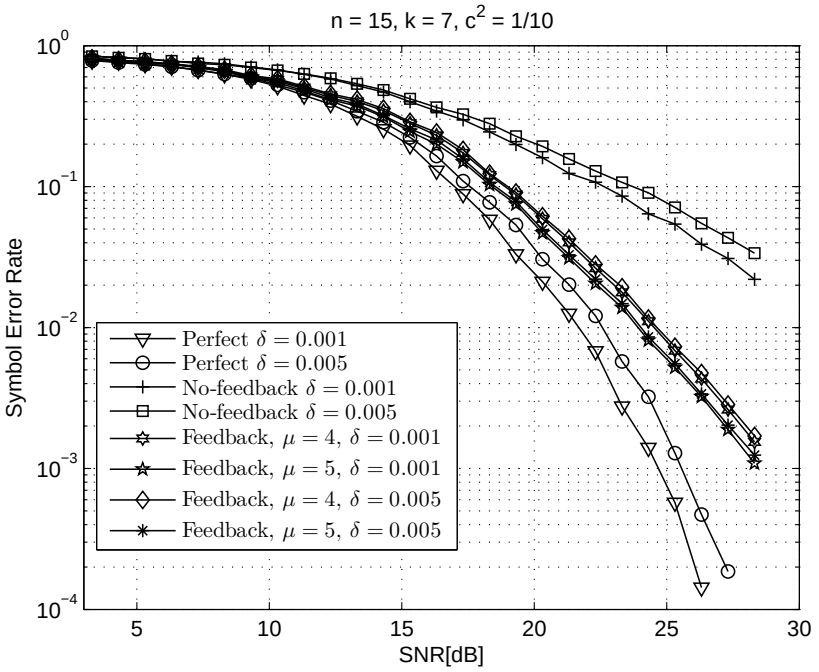

FIGURE 6.6: SER performance comparison of the *RS*-PTA iterative receiver structure for $\delta = 0.005$ and $\delta = 0.001$, $F_dT = 0.015$.

6.4.2 Performance Comparison of the *RS*-PTA and *RS*-KV Iterative Receiver Structures

6.4.2.1 Computational Complexity Performance Analysis

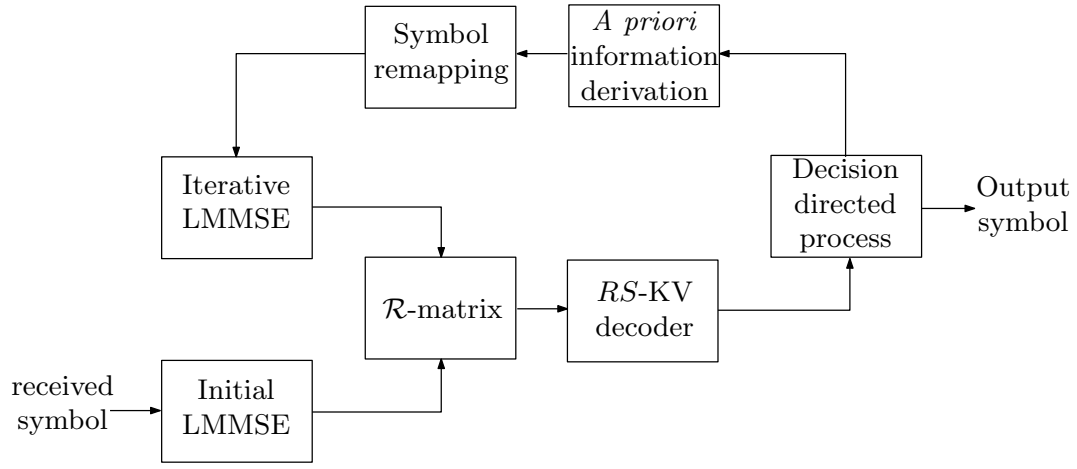

FIGURE 6.7: *RS*-KV iterative receiver structure.

Fig. 6.7 depicts the *RS*-KV iterative receiver structure proposed in [7]. In comparison with the *RS*-PTA iterative receiver structure in Fig. 6.3, the *RS*-KV iterative

receiver structure require extra blocks such as the decision directed process block, and the *a priori* information derivation block to complete the iterative process. These additional blocks increase the computational time complexity of the *RS*-KV iterative receiver structure, most especially the *a priori* information derivation block. However, in order to reduce the computational time complexity incurred by the *a priori* information derivation block, we assume the Distance Metric (DM) *a priori* information derivation method proposed in [7]. Besides, the *RS*-KV decoder is more complex in comparison with the *RS*-PTA decoder as explained in [1]. Thus, the proposed *RS*-PTA iterative receiver structure is characterised to exhibit lower computational time complexity in comparison to the *RS*-KV iterative receiver structure. The computational time complexity of the *RS*-PTA and the *RS*-KV iterative receiver structures for each block is therefore shown in Table 6.1 as follows.

Table 6.1: Computational complexity analysis per iteration

Blocks	*RS*-PTA Iterative Receiver	*RS*-KV Iterative Receiver
Initial LMMSE	$\mathcal{O}(n^2)$	$\mathcal{O}(n^2)$
Iterative LMMSE	$\mathcal{O}(n^2)$	$\mathcal{O}(n^2)$
$\mathcal{R}$-matrix	$\mathcal{O}(Mn)$	$\mathcal{O}(Mn)$
Symbol remapping	$\mathcal{O}(Mn)$	$\mathcal{O}(Mn)$
RS-PTA decoder	$\mathcal{O}(Mn+(n-k)(n^2+(n-k)+1))$	0
RS-KV decoder	0	$\mathcal{O}(M^2n^2I^4)$
Decision directed process	0	$\mathcal{O}(n)$
A priori information derivation	0	$\mathcal{O}(Mn)$

As presented in Table 6.1, the extra blocks in the *RS*-KV iterative receiver generates a minimum of $\mathcal{O}(Mn)$ and $\mathcal{O}(n)$ additional computational time complexity in comparison to the *RS*-PTA iterative receiver. Furthermore, the *RS*-KV decoder experiences a higher complexity of $\mathcal{O}(M^2n^2I^4)$ in comparison to the $\mathcal{O}(Mn+(n-k)(n^2+(n-k)+1))$ complexity experienced by the *RS*-PTA decoder. For example, given $M = 16$, $n = 15$, $k = 7$, and $I = 1$, the *RS*-KV decoder will experienced a minimum of 57600 complexity compared to the 2112 complexity experienced by the *RS*-PTA decoder. Note that this example assumes $I = 1$. In real time *RS*-KV decoding, the value of I varies from one to infinity depending on the list size L used in the algorithm. From this analysis, it can be concluded

that the *RS*-PTA iterative receiver structure exhibits lower computational time complexity in comparison to the *RS*-KV iterative receiver structure.

6.4.2.2 SER Performance Comparison

In terms of the SER performance of both iterative receiver structures, we assume the same computer simulation parameters as in Section 6.4.1. In the *RS*-KV iterative receiver structure, a list size L=4 is assumed in the *RS*-KV algorithm [8], and a maximum possible iterative estimate of $\mu = 3$ is set. Note, as demonstrated in [7], the *RS*-KV iterative receiver structure converges after $\mu = 3$ for a list size L=4. Fig. 6.8 verifies the SER performance of both iterative receiver structures. As shown in the figure, the *RS*-PTA iterative receiver structure outperforms the *RS*-KV iterative receiver structure. This delineates the *RS*-PTA iterative receiver structure as a less complex and performance efficient alternative to the *RS*-KV iterative receiver structure when *RS* codes are deployed in joint iterative channel estimation and decoding receiver structures.

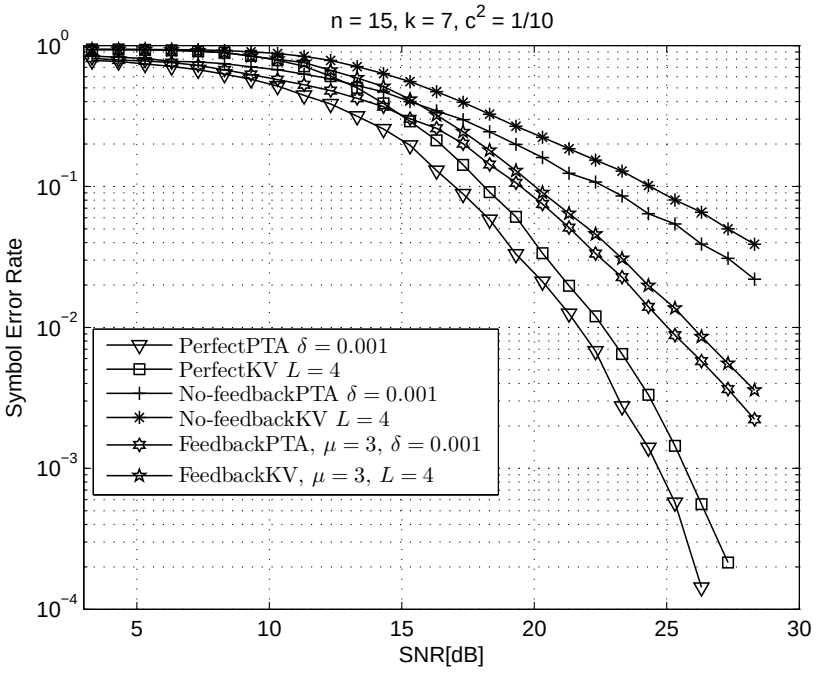

FIGURE 6.8: SER performance comparison of the *RS*-PTA and *RS*-KV iterative receiver structures, $F_dT = 0.015$.

6.5 Conclusion

A joint iterative channel estimation and *RS*-PTA decoding receiver has been developed in this paper. The performance of the *RS*-PTA iterative receiver structure was compared with the *RS*-KV iterative receiver structure. Firstly, it was established that the *RS*-PTA iterative receiver structure outperforms the *RS*-KV iterative receiver structure as shown in Fig. 6.8. Secondly, we demonstrated that the *RS*-KV iterative receiver structure exhibits much higher computational time complexity in comparison with the *RS*-PTA iterative receiver structure as presented in Table 6.1. Finally, we revealed in Fig. 6.6 that the complexity of the *RS*-PTA iterative receiver structure can be reduced by increasing the adjustable decimal parameter δ without compromising the SER performance of the receiver.

6.6 References

[1] O. Ogundile, Y. Genga, and D. Versfeld, "Symbol level iterative soft decision decoder for Reed-Solomon codes based on parity-check equations," *Electronics Letters*, vol. 51, no. 17, pp. 1332–1333, 2015.

[2] M. Valenti and B. Woerner, "Iterative channel estimation and decoding of pilot symbol assisted turbo codes over flat-fading channels," *Selected Areas in Communications, IEEE Journal on,* vol. 19, no. 9, pp. 1697–1705, Sep 2001.

[3] T. Zemen, M. Loncar, J. Wehinger, C. Mecklenbrauker, and R. Muller, "Improved channel estimation for iterative receivers," in *Global Telecommunications Conference, 2003. GLOBECOM '03. IEEE,* vol. 1, Dec 2003, pp. 257–261 Vol.1.

[4] H. Niu and J. Ritcey, "Iterative channel estimation and decoding of pilot symbol assisted LDPC coded QAM over flat fading channels," in *Signals, Systems and Computers, 2004. Conference Record of the Thirty-Seventh Asilomar Conference on,* vol. 2, Nov 2003, pp. 2265-2269 Vol.2.

[5] M.-K. Oh, H. Kwon, D.-J.Park, and Y. H. Lee, "Iterative Channel Estimation and LDPC Decoding With Encoded Pilots," *Vehicular Technology, IEEE Transactions on,* vol. 57, no. 1, pp. 273-285, Jan 2008.

[6] O. Oyerinde and S. Mneney, "Iterative receiver with soft-input-based-channel estimation for orthogonal frequency division multiplexing-interleave division multiple access systems" *Communications, IET,* vol. 8, no. 14, pp. 2445-2457, Sept 2014.

[7] O. Ogundile, O. Oyerinde, and D. Versfeld, "Decision directed iterative channel estimation and Reed #x2013;Solomon decoding over flat fading channels," *Communications, IET* Vol. 9, no. 17 pp. 2077-2084, 2015.

[8] R. Koetter and A. Vardy, "Algebraic soft-decision decoding of Reed-Solomon codes," *Information Theory, IEEE Transactions on*, vol. 49, no. 11, pp. 2809-2825, Nov 2003.

[9] V. Guruswami and M. Sudan, "Improved decoding of Reed-Solomon and algebraic-geometry codes," *Information Theory, IEEE Transactions on*, vol. 45, no. 6, pp. 1757-1767, Sep 1999.

[10] R. McEliece, "The Guruswami-Sudan Decoding Algorithm for Reed-Solomon Codes," 16th April 2003. [Online].
Available: http://www.ee.caltech.edu/EE/Faculty/rjm/papers/RSD-JPL.pdf

[11] O. Ogundile and D. Versfeld, "Improved reliability information for rectangular 16-QAM over flat Rayleigh fading channels," in *Computational Science and Engineering (CSE), 2014 IEEE 17th International Conference on,* Dec 2014, pp. 345–349.

[12] M. K. Simon and J. Smith, "Carrier Synchronization and Detection of QASK Signal Sets," *Communications, IEEE Transactions on*, vol. 22, no. 2, pp. 98-106, Feb 1974.

[13] W.C. Jakes, Mobile microwave communication. New York: Wiley, 1974.

[14] J. Cavers ,"An analysis of pilot symbol assisted modulation for Rayleigh fading channels [mobile radio]," *Vehicular Technology, IEEE Transactions on,* vol. 40, no. 4, pp. 686-693, Nov 1991.

[15] F. Kadrija, M. Simko, and M. Rupp, "Iterative channel estimation in LTE systems," in *Smart Antennas (WSA), 2013 17th International ITG Workshop on,* March 2013, pp. 1-7.

[16] W. Phoel, J. Pursley, M. Pursley,*et al.*, "Frequency-hop spread spectrum with quadrature amplitude modulation and error-control coding." in *Military Communications Conference, 2004. MILCOM 2004. 2004 IEEE*, vol. 2, Oct 2004, pp. 913-919 Vol. 2.

[17] T. K. Moon, Error Correction Coding: Mathematical Methods and Algorithms. John Wiley & Sons, 2005.

CHAPTER 7

Conclusion

As the final and concluding chapter of this thesis, Chapter 7 delineates the overall contribution of this study. An overview of the aim and achievement of this study is first abridged. Afterwards, the findings of each chapter is summarised to give a general view of the exact contribution of each chapter. Recommendations and suggestions for future research possibilities are also presented in this chapter. Chapter 7 finally ends with the closing remarks.

7.1 Thesis Summary and Key Results

This thesis titled "Symbol Level Decoding of Reed-Solomon Codes with Improved Reliability Information Over Fading Channels" expounds the overall goal of this study. More realistically, the thesis aims at improving the message reliability over Rayleigh fading channels using FEC schemes, in particular, *RS* codes. The challenges facing the transmission reliability over Rayleigh fading channels are introduced in Chapter 1. Chapter 1 also explains the importance of using *RS* codes in this thesis. Besides, the previous closely related work done supporting the aim and accomplishment of this thesis are explained in Chapter 1. The contributions in Chapters 2-6 of this thesis were presented as conference and journal papers.

In Chapter 2, an improved distance metric method of deriving soft reliability information over flat Rayleigh fading channels for combined demodulation with symbol level *RS* soft decision decoding algorithms is developed. Performance analysis verify that the proposed metric offers a significant gain improvement in comparison to the conventional method in [1-3]. The study in Chapter 2 further

improves the transmission reliability of combined demodulation with symbol level *RS* soft decision decoding algorithms over flat Rayleigh fading channels. Although, in the Chapter 2, the performance of the developed DM method of deriving soft reliability information over Rayleigh fading channels is only verified for symbol level *RS* soft decision decoders, it is applicable to any symbol level soft decision decoding FEC scheme.

Chapter 3 extended the findings in Chapter 2 to OFDM systems on time-varying frequency-selective fading channels. OFDM systems are deployed in different wireless communication applications and standards. For example, DAB, DVB, Long-Term Evolution (LTE), high-rate wireless LAN standard (IEEE 802.11a) [4], WiMAX, and IEEE 802.16a metropolitan area network standard. Therefore, the results in Chapter 3 proffer solutions in enhancing the performance of OFDM systems with combined symbol level soft decision decoding algorithms when used in these aforementioned applications over Rayleigh fading channels.

A decision directed iterative channel estimation and Reed-Solomon decoding over flat Rayleigh fading channels is presented in Chapter 4. The results in Chapter 4 showcase the importance of *RS* codes in a joint iterative channel estimation and decoding receiver structure. In literature, joint iterative channel estimation and decoding receiver structures were only deployed using Turbo and LDPC codes as the FEC schemes. Chapter 4 develops the first joint iterative channel estimation and decoding receiver structure based on the symbol level *KV* soft decision decoding algorithm [2]. *RS* codes are important class of linear block codes capable of correcting random symbol and burst errors [1, 5], and are used in important wireless applications. Accordingly, the results in Chapter 4 offer solutions in improving the message reliability over Rayleigh fading channels using *RS* codes. Once again, this study emphasize that the primary aim of deploying *RS* codes in an iterative receiver structure is not to compare between codes (*RS* codes, Turbo codes, or LDPC codes), rather, the introduction of *RS* codes in an iterative receiver structure because of its numerous and important advantages in wireless applications.

Chapter 5 develops a novel symbol level iterative soft decision algorithm for Reed-Solomon codes based on parity-check equations. The results in Chapter 5 verify that this developed PTA for *RS* codes outperform the conventional *RS* hard decision decoding algorithms and the symbol level Koetter and Vardy *RS* soft decision decoding algorithm [2]. This portrays the developed PTA in Chapter 5 as a robust symbol level *RS* soft decision decoding FEC scheme, and it can be implemented on real time coding systems to improve the message reliability of communication links. Equally, the developed, less computationally intensive, and performance efficient symbol level decoding algorithm for *RS* codes can be used in consumer technologies like compact disc and digital versatile disc.

In Chapter 6, a low complexity iterative channel estimation and decoding receiver is developed based on the Reed-Solomon PTA proposed in Chapter 5. Results show that the Reed-Solomon PTA is suitable in an iterative receiver structure both in terms of the SER performance and the computational time complexity in comparison with the *KV* algorithm. Thus, the message reliability of communication links can be improved more efficiently using the Reed-Solomon PTA.

Essentially, this study proffer solutions in improving the message reliability over Rayleigh fading channels. While some of the results in this thesis are useful in improving the performance of most symbol level soft decision decoding FEC schemes over Rayleigh fading channels, the majority of the findings of this study are peculiar to *RS* codes. The results presented in Chapters 2, 3, 4, 5, and 6 answer this thesis research question. In general, the following key points are deduced from the results obtained in this study:

- *The performance of combined demodulation with symbol level soft decision decoding FEC schemes can be improved over Rayleigh fading channels if the estimated CSI is adequately taken into account during the symbol decoding process.*
- *The performance of combined demodulation with symbol level RS soft decision decoder over Rayleigh fading channels depend on the symbol level RS*

soft decision decoding algorithm employed. Thus, the more dependable the symbol level RS soft decision decoding algorithm, the better the performance of RS codes over Rayleigh fading channels.

- *Reed-Solomon codes is suitable in a joint iterative channel estimation and decoding receiver structure to improve the message reliability over Rayleigh fading channels.*

Lastly, all analysis and results of this study can be implemented on real time coding systems, most especially in wireless application like DAB, DVB, LTE, and long distance satellite communications.

7.2 Recommendation and Future Research Possibilities

In order to completely utilize the analysis and results presented in this thesis, the following recommendations can be considered as useful guidance for future research possibilities.

1. *The results in Chapters 2 and 3 of this thesis can be verified for other symbol level soft decision decoding FEC schemes, such as LDPC codes.*

2. *Extensive analysis on the results in Chapters 4-6 of this thesis should be carried out on time-varying frequency-selective fading channels, where OFDM systems can be deployed as the modulation scheme.*

3. *Research can be carried out to extend the Reed-Solomon PTA developed in Chapter 5 to a bit level decoding algorithm. In this case, performance comparisons should be carried out with important bit level RS algorithms such as the algorithms in [6, 7].*

4. *Fair performance comparison can be carried out between RS codes with other FEC schemes such as Turbo and LDPC codes in a joint iterative channel estimation and decoding receiver structure over Rayleigh fading channels.*

5. *Finally, the work in this thesis can be verified for other realistic fading channel models such as the Nakagami fading channel models, and Rician fading channel models.*

7.3 Final Remarks

Although FEC schemes have been used extensively over fading channels to improve the message reliability of communication links, *RS* codes have not been widely used. *RS* codes introduced in [8] form an important class of linear block codes capable of correcting random symbol errors, as well as burst errors [1, 5]. Before this study, only few works are published in literature on improving the performance of *RS* codes over Rayleigh fading channels, most especially in a joint iterative channel estimation and decoding receiver structure. In order to showcase the good error correcting capability of *RS* codes over fading channels, this thesis firstly proposes an improved DM method of deriving soft reliability information over Rayleigh fading channels as shown in Chapters 2 and 3. Although, this newly proposed DM method can be used in other symbol level soft decision decoding FEC schemes. Secondly, as shown in Chapter 5, the thesis proposes a novel soft decision decoding algorithm for *RS* codes which outperforms other efficient symbol level *RS* soft decision decoding algorithms. Furthermore, as a final measure of improving the performance of *RS* codes over fading channels, the thesis deployed *RS* codes in a joint iterative channel estimation and decoding receiver structure for the first time as presented in Chapters 4 and 6. Most of the results presented in this thesis have been peer-reviewed and published in different conference and journal papers.

7.4 References

[1] T. K. Moon, *Error Correction Coding: Mathematical Methods and Algorithms.* John Wiley & Sons, 2005.

[2] R. Koetter and A. Vardy, "Algebraic soft-decision decoding of Reed-Solomon codes," *Information Theory, IEEE Transactions on*, vol. 49, no. 11, pp. 2809-2825, Nov 2003.

[3] W. Phoel, J. Pursley, M. Pursley, and J. Skinner, "Frequency-hop spread spectrum with quadrature amplitude modulation and error-control coding," *in Military Communications Conference, 2004. MILCOM 2004. 2004 IEEE*, vol. 2, Oct 2004, pp. 913-919 Vol. 2.

[4] IEEE, Std. 802.11a-1999, Wireless LAN Medium Access Control (MAC) and Physical Layer (PHY) Specification: Highspeed Physical Layer in the 5GHz Band. The Institute of Electrical and Electronics Engineers, Inc.

[5] S. Lin and D. J. Costello, *Error Control Coding,* 2nd ed. Prentice Hall, June 2005.

[6] J. Jiang and K. Narayanan, "Iterative Soft-Input Soft-Output Decoding of Reed amp; #8211;Solomon Codes by Adapting the Parity-Check Matrix," *Information Theory, IEEE Transactions on,* vol. 52, no. 8, pp. 3746–3756, Aug 2006.

[7] O. Ur-rehman and N. Zivic, "Soft decision iterative error and erasure decoder for Reed #8211;Solomon codes," *Communications, IET,* vol. 8, no. 16, pp. 2863–2870, 2014.

[8] I. S. Reed and G. Solomon, "Polynomial codes over Certain Finite fields," J. Soc.Ind. Appl. Maths., 8:300-304, June 1960.

Appendix A

Performance Analysis of the Parity Transformation Algorithm

The Parity Transformation Algorithm (PTA) is a symbol level Reed-Solomon (RS) as described in Chapter 5. With most soft decision forward error correction decoders, the PTA operates on the derived reliability information from the channel output to obtain the valid transmitted codeword. Therefore, given the derived reliability information β, and the systematic Parity Check Equation (PCE) H, the PTA performs the following steps at the lth iteration.

1. Determine the k most reliable received signals, according to some rules. The indices of these signals are denoted as $\mathcal{R}$, and the indices of the $n-k$ remaining signals are denoted as $\mathcal{U}$. (For the purpose of this letter, we will simply use the first k columns which contain the highest maximum values to determine the most reliable signals.)
2. Transform the systematic PCE H, such that $H^{(l)}$ contains a partitioned identity matrix where the indices of the unit column vectors u_i are equal to $\mathcal{U}$, and the indices of the parity column vectors are equal to $\mathcal{R}$.
3. Calculate the $n-k$ PCE using $H^{(l)}$. This is done by performing HD detection on β to obtain the vector r, and then doing the dot product $r \cdot H_q^{(l)}$, where $H_q^{(l)}$ is the qth row of matrix $H^{(l)}$. Due to the systematic structure of $H^{(l)}$, one symbol with index in $\mathcal{U}$ and k symbols with indices in $\mathcal{R}$ will be used in the dot product. If the dot product is zero, we increment all $\beta_{v,j}$ (where $j \in u_q \cup \mathcal{R}$ and v such that $\beta_{v,j}$ is the largest element in column β_j) with some δ. If the dot product is not zero, we decrement all $\beta_{v,j}$ with some δ.

If all the PCE are satisfied, the process is halted, otherwise, the updated decision matrix $\beta^{(l)}$ is used as input, and the steps are repeated until the matrix $\beta^{(l)}$ seats an element $-\beta_{u,i}^{(l)}$ (where u and i denotes the row and column of matrix $\beta^{(l)}$ respectively). The PTA is hereby demonstrated by way of an example.

Consider the Reed-Solomon code with the following parameters:

- $n = 7$ (Code length)
- $k = 2$ (Number of data elements)
- $h = n - k = 5$ (Number of redundant elements)
- $d_{min} = n - k + 1 = 6$
- $GF(2^3)$ constructed with primitive polynomial $p(z) = z^3 + z + 1$
- $g(z) = (z-\alpha^1)(z-\alpha^2)\cdots(z-\alpha^5) = z^6+\alpha^2 z^5+\alpha^3 z^4+\alpha^3 z^3+\alpha^6 z^2+\alpha^4 z+\alpha^1$
- $\delta = 0.005$

Assume that the codeword $c = (\alpha^5, \alpha^2, 0, \alpha, \alpha^3, \alpha^4, 1)$ is modulated, and transmitted through a noisy channel. Let the reliability matrix β be given as:

$$\beta = \begin{pmatrix} 0.257 & 0.214 & 0.749 & 0.253 & 0.059 & 0.034 & 0.038 \\ 0.019 & 0.009 & 0.000 & 0.004 & 0.034 & 0.086 & 0.702 \\ 0.236 & 0.081 & 0.023 & 0.021 & 0.164 & 0.009 & 0.002 \\ 0.015 & 0.408 & 0.006 & 0.251 & 0.172 & 0.190 & 0.052 \\ 0.007 & 0.127 & 0.006 & 0.049 & 0.014 & 0.000 & 0.122 \\ 0.005 & 0.049 & 0.021 & 0.120 & 0.183 & 0.321 & 0.064 \\ 0.052 & 0.026 & 0.048 & 0.017 & 0.005 & 0.331 & 0.005 \\ 0.408 & 0.086 & 0.147 & 0.286 & 0.370 & 0.030 & 0.015 \end{pmatrix}.$$

First, we determine the k columns with the highest maximum values, which constitute $\mathcal{R}$. For β, the set of indices for the reliable symbols are $\mathcal{R} = \{3, 7\}$, while $\mathcal{U} = \{1, 2, 4, 5, 6\}$.

Now, given that the parity check matrix H is given as:

$$H = \begin{pmatrix} \alpha^6 & \alpha^2 & 1 & 0 & 0 & 0 & 0 \\ \alpha & \alpha^3 & 0 & 1 & 0 & 0 & 0 \\ \alpha^2 & \alpha^6 & 0 & 0 & 1 & 0 & 0 \\ \alpha^5 & \alpha^4 & 0 & 0 & 0 & 1 & 0 \\ \alpha^3 & \alpha & 0 & 0 & 0 & 0 & 1 \end{pmatrix}.$$

We now transform H to $H^{(1)}$ such that the indices of parity-check columns coincide with $\mathcal{R}$, and the indices of the partitioned identity matrix coincide with $\mathcal{U}$. Various ways can be used to transform H to $H^{(1)}$. One way is to use row operations similar to Gauss reduction. For a computationally efficient way, see reference [9] in Chapter 5.

$$H^{(1)} = \begin{pmatrix} 1 & 0 & \alpha^4 & 0 & 0 & 0 & \alpha^5 \\ 0 & 1 & \alpha^6 & 0 & 0 & 0 & \alpha^2 \\ 0 & 0 & \alpha^3 & 1 & 0 & 0 & \alpha \\ 0 & 0 & \alpha & 0 & 1 & 0 & \alpha^3 \\ 0 & 0 & \alpha^5 & 0 & 0 & 1 & \alpha^4 \end{pmatrix}.$$

Using the hard-decision outputs (indicated by the highlighted entries of β), we now calculate the various parity checks. The received vector is determined as $r = (\alpha^5, \alpha^3, 0, \alpha^5, \alpha^5, \alpha^4, 1)$, by assuming that the rows correspond to $\{0, 1, \alpha, \alpha^3, \alpha^2, \alpha^6, \alpha^4, \alpha^5\}$.

We now perform the $n-k$ dot products $r \cdot H_q^{(1)}$ (effectively calculating the syndrome S):

$$
\begin{aligned}
r \cdot H_1^{(1)} &= (\alpha^5, \alpha^3, 0, \alpha^5, \alpha^5, \alpha^4, 1) \cdot (1, 0, \alpha^4, 0, 0, 0, \alpha^5) \\
&= 0 \\
r \cdot H_2^{(1)} &= (\alpha^5, \alpha^3, 0, \alpha^5, \alpha^5, \alpha^4, 1) \cdot (0, 1, \alpha^6, 0, 0, 0, \alpha^2) \\
&= \alpha^5 \\
r \cdot H_3^{(1)} &= (\alpha^5, \alpha^3, 0, \alpha^5, \alpha^5, \alpha^4, 1) \cdot (0, 0, \alpha^3, 1, 0, 0, \alpha) \\
&= \alpha^6 \\
r \cdot H_4^{(1)} &= (\alpha^5, \alpha^3, 0, \alpha^5, \alpha^5, \alpha^4, 1) \cdot (0, 0, \alpha, 0, 1, 0, \alpha^3) \\
&= \alpha^2 \\
r \cdot H_5^{(1)} &= (\alpha^5, \alpha^3, 0, \alpha^5, \alpha^5, \alpha^4, 1) \cdot (0, 0, \alpha^5, 0, 0, 1, \alpha^4) \\
&= 0
\end{aligned}
$$

The first parity-check equation checks, therefore we increment the corresponding $\mathcal{U}$ element by $\delta = 0.005$, and the corresponding $\mathcal{R}$ elements by $\delta/2$, yielding

$$
\beta_1^{(1)} = \begin{pmatrix}
0.257 & 0.214 & 0.752 & 0.253 & 0.059 & 0.034 & 0.038 \\
0.019 & 0.009 & 0.000 & 0.004 & 0.034 & 0.086 & 0.705 \\
0.236 & 0.081 & 0.023 & 0.021 & 0.164 & 0.009 & 0.002 \\
0.015 & 0.408 & 0.006 & 0.251 & 0.172 & 0.190 & 0.052 \\
0.007 & 0.127 & 0.006 & 0.049 & 0.014 & 0.000 & 0.122 \\
0.005 & 0.049 & 0.021 & 0.120 & 0.183 & 0.321 & 0.064 \\
0.052 & 0.026 & 0.048 & 0.017 & 0.005 & 0.331 & 0.005 \\
0.413 & 0.086 & 0.147 & 0.286 & 0.370 & 0.030 & 0.015
\end{pmatrix}.
$$

(The affected values are highlighted).

The second parity-check equation fails, therefore we decrement the corresponding $\mathcal{U}$ element by δ, and the corresponding $\mathcal{R}$ elements by $\delta/2$, yielding

$$\beta_2^{(1)} = \begin{pmatrix} 0.257 & 0.214 & 0.749 & 0.253 & 0.059 & 0.034 & 0.038 \\ 0.019 & 0.009 & 0.000 & 0.004 & 0.034 & 0.086 & 0.702 \\ 0.236 & 0.081 & 0.023 & 0.021 & 0.164 & 0.009 & 0.002 \\ 0.015 & 0.404 & 0.006 & 0.251 & 0.172 & 0.190 & 0.052 \\ 0.007 & 0.127 & 0.006 & 0.049 & 0.014 & 0.000 & 0.122 \\ 0.005 & 0.049 & 0.021 & 0.120 & 0.183 & 0.321 & 0.064 \\ 0.052 & 0.026 & 0.048 & 0.017 & 0.005 & 0.331 & 0.005 \\ 0.413 & 0.086 & 0.147 & 0.286 & 0.370 & 0.030 & 0.015 \end{pmatrix}. \tag{A.1}$$

The final reliability matrix β after the first iteration is

$$\beta^{(1)} = \begin{pmatrix} 0.257 & 0.214 & 0.747 & 0.253 & 0.059 & 0.034 & 0.038 \\ 0.019 & 0.009 & 0.000 & 0.004 & 0.034 & 0.086 & 0.700 \\ 0.236 & 0.081 & 0.023 & 0.021 & 0.164 & 0.009 & 0.002 \\ 0.015 & 0.404 & 0.006 & 0.251 & 0.172 & 0.190 & 0.052 \\ 0.007 & 0.127 & 0.006 & 0.049 & 0.014 & 0.000 & 0.122 \\ 0.005 & 0.049 & 0.021 & 0.120 & 0.183 & 0.321 & 0.064 \\ 0.052 & 0.026 & 0.048 & 0.017 & 0.005 & 0.336 & 0.005 \\ 0.413 & 0.086 & 0.147 & 0.281 & 0.365 & 0.030 & 0.015 \end{pmatrix},$$

where we have again highlighted the affected values.

The iterative process is repeated until all the PCE are satisfied or any entry of the updated decision matrix $\beta^{(l)}$ is less than zero $\left(\beta_{u,i}^{(l)} < 0\right)$. In this example, the PCE are satisfied after 172 iterations. Thus, the resulting β is given as:

$$\beta^{(172)} = \begin{pmatrix} 0.257 & 0.124 & 1.467 & 0.018 & 0.059 & 0.034 & 0.038 \\ 0.019 & 0.009 & 0.000 & 0.004 & 0.034 & 0.086 & 1.467 \\ 0.236 & 0.081 & 0.023 & 0.026 & 0.164 & 0.009 & 0.002 \\ 0.015 & 0.123 & 0.006 & 0.021 & 0.822 & 0.190 & 0.052 \\ 0.007 & 0.617 & 0.006 & 0.019 & 0.014 & 0.000 & 0.122 \\ 0.005 & 0.049 & 0.021 & 0.020 & 0.168 & 0.321 & 0.064 \\ 0.052 & 0.026 & 0.048 & 0.017 & 0.005 & 1.196 & 0.005 \\ 1.216 & 0.086 & 0.147 & 0.021 & 0.170 & 0.030 & 0.015 \end{pmatrix},$$

which yields a syndrome of zero and the correctly decoded vector $\hat{c} = c = (\alpha^5, \alpha^2, 0, \alpha, \alpha^3, \alpha^4, 1)$.

The iterative process is summarized in a simple flow chart as shown in Fig. A.1.

Performance Comparison Analysis for Different δ

A simulation study was carried out to test the performance of the PTA. In the simulation, a (15, 7) *RS* code is used. The underlying modulation scheme is a rectangular 16-QAM constellation, with AWGN. For the same input data, we compare the performance of the proposed algorithm for different values of δ. Fig. A.2 shows the Symbol Error Rate (SER) performance for the values of δ assumed. As a key note from the figure, δ determines the performance of the algorithm. The smaller the value of δ, the better the performance of the algorithm. As shown, δ=0.001 yields the best performance on the SER curve of Fig. A.2. However, the smaller the value of δ, the more iterations the algorithm will need. To emphasize, if δ=0.001 is assumed in the algorithm for the above example, the PCE are only satisfied after 792 iterations $\left(\beta^{(792)}\right)$. The number of iterations required to satisfy the PCE for δ=0.001 $\left(\beta^{(792)}\right)$ is much greater than the number of iterations required for δ=0.005 $\left(\beta^{(172)}\right)$, so the former increases the decoding time complexity of the algorithm. Thus, there is a trade-off between the algorithm decoding performance, and its computational delay and time complexity while selecting the value of δ.

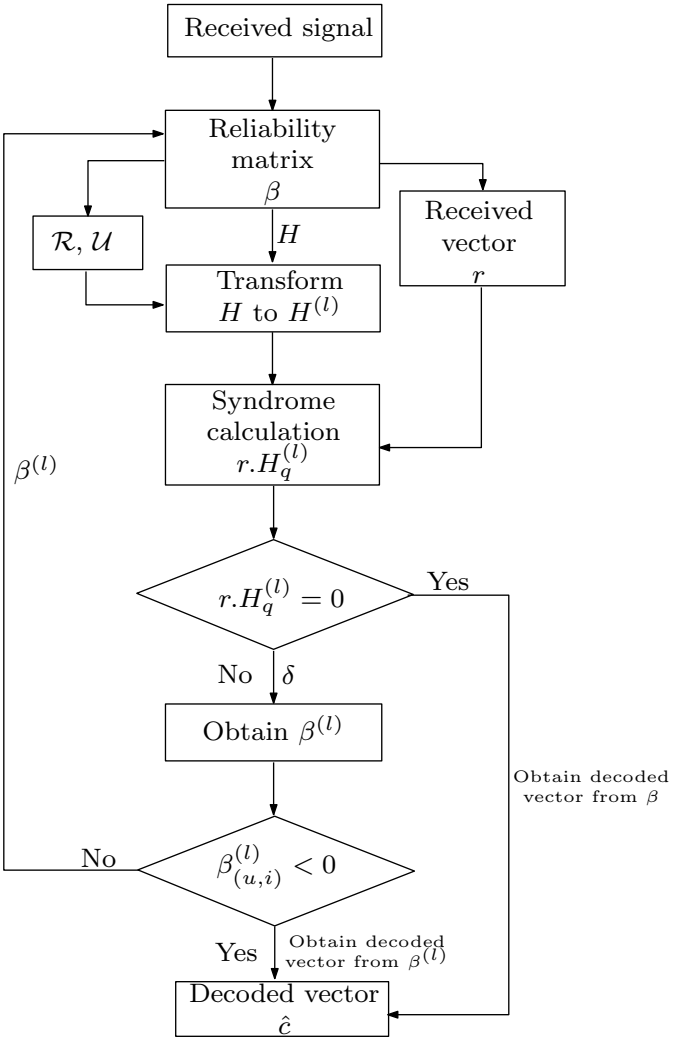

FIGURE A.1: The *RS* PTA soft decoder.

Performance Comparison Analysis with other Symbol Level Soft Decoding Algorithms

Assuming the same computer simulation parameters, we compare the performance of HD *B-M* algorithm (See [2, 3] in Chapter 5), the *KV-GS* SD decoder with a list-size $L = 4$ (see [6] in Chapter 5), and the proposed PTA. Fig. A.3 shows the SER performance of this *RS* decoding algorithms. From the figure, it can be seen that the proposed algorithm outperforms the *KV-GS* SD decoder and the HD *B-M* decoder. This portrays the proposed PTA for *RS* codes as a robust symbol level forward error correction decoding scheme and it can be implemented on real time coding systems.

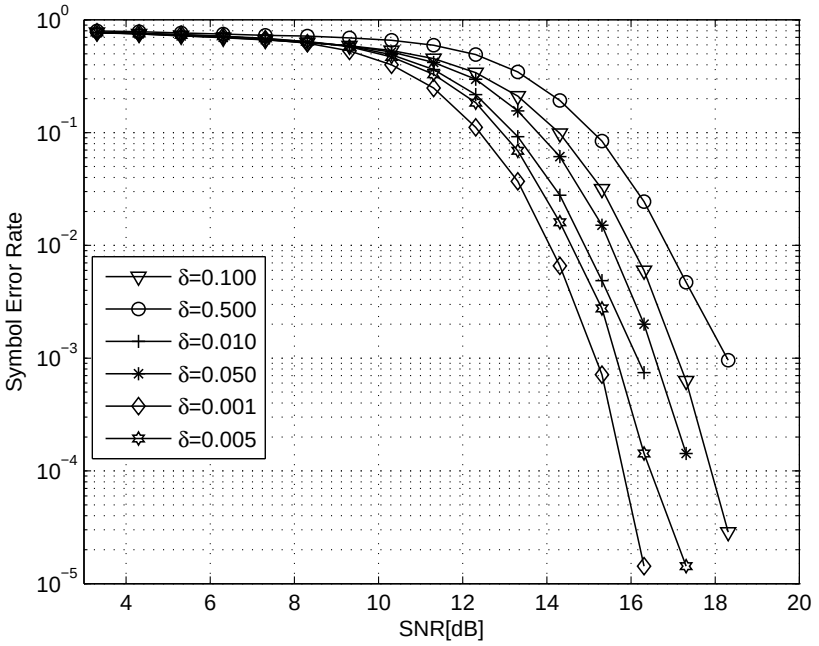

FIGURE A.2: Performance comparison of the PTA for different values of δ.

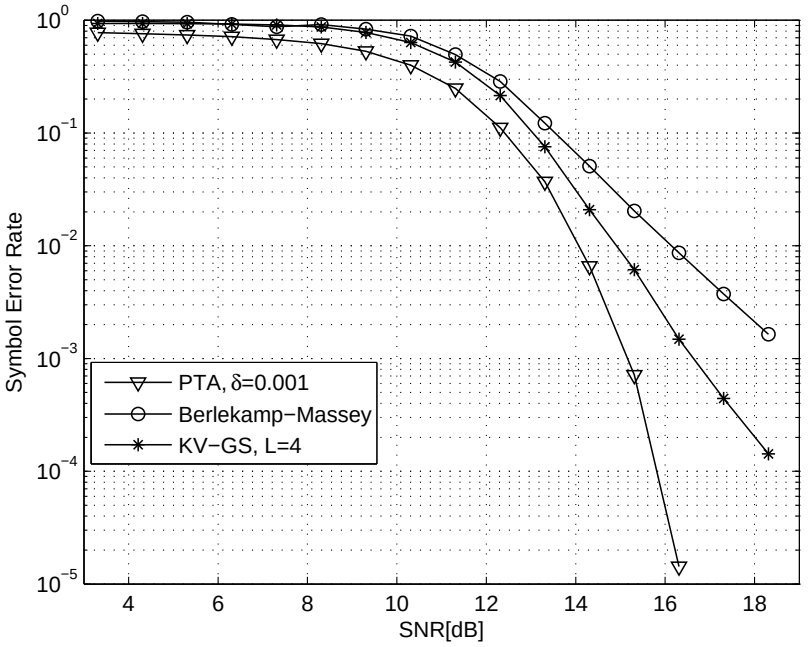

FIGURE A.3: Performance comparison of the PTA with the *KV-GS* and *B-M* algorithms.

Appendix B

Computational Complexity Analysis of the Parity Transformation Algorithm

A breakdown of the computational complexity analysis of the Reed-Solomon (RS) Parity Transformation Algorithm (PTA) presented in Chapter 5 is provided for one iteration. The same notation is used as in Chapter 5, that is:

- H = Parity check equation matrix.
- n = The codeword length (the number of columns in the H).
- k = The message length.
- $h = n - k$ = The parity symbols length (The number of rows in the H matrix).
- M = Number of constellation points (for example, M= 16 for 16-QAM).

Thus, the computational complexity of the RS PTA is analysed for each stage of the algorithm as follows:

1. The first step in the RS PTA presented in Chapter 5 is to determine the k most reliable symbol denoted as $\mathcal{R}$ and the remaining $(n - k)$ symbols denoted as $\mathcal{U}$ from the derived reliability matrix β as shown in Eqn. (5.2).

$$\beta = \begin{pmatrix} 0.257 & 0.214 & 0.749 & 0.253 & 0.059 & 0.034 & 0.038 \\ 0.019 & 0.009 & 0.000 & 0.004 & 0.034 & 0.086 & 0.702 \\ 0.236 & 0.081 & 0.023 & 0.021 & 0.164 & 0.009 & 0.002 \\ 0.015 & 0.408 & 0.006 & 0.251 & 0.172 & 0.190 & 0.052 \\ 0.007 & 0.127 & 0.006 & 0.049 & 0.014 & 0.000 & 0.122 \\ 0.005 & 0.049 & 0.021 & 0.120 & 0.183 & 0.321 & 0.064 \\ 0.052 & 0.026 & 0.048 & 0.017 & 0.005 & 0.331 & 0.005 \\ 0.408 & 0.086 & 0.147 & 0.286 & 0.370 & 0.030 & 0.015 \end{pmatrix},$$

where β is a matrix of dimension $M \times n$. A sorting function is performed to determine the indices of these values from β. Since β is of dimension $M \times n$, a complexity of $\mathcal{O}(Mn)$ is experienced at this stage.

2. Secondly, the parity check equation matrix H as defined by Eqn. (5.3) is transformed such that $H^{(l)}$ contains a partitioned identity matrix where the indices of the unit column vectors u_i are equal to $\mathcal{U}$, and the indices of the parity column vectors are equal to $\mathcal{R}$. In this case, a row reduction technique is used as stated in [9] of Chapter 5. From [9], the complexity experienced using this technique is $\mathcal{O}(h^2)$.

$$H = \begin{pmatrix} \alpha^6 & \alpha^2 & 1 & 0 & 0 & 0 & 0 \\ \alpha & \alpha^3 & 0 & 1 & 0 & 0 & 0 \\ \alpha^2 & \alpha^6 & 0 & 0 & 1 & 0 & 0 \\ \alpha^5 & \alpha^4 & 0 & 0 & 0 & 1 & 0 \\ \alpha^3 & \alpha & 0 & 0 & 0 & 0 & 1 \end{pmatrix}.$$

3. A hard decision detection is performed to determine the most reliable symbol in each column of β in order to produce a received vector r of dimension $1 \times n$. This step incurs a complexity of $\mathcal{O}(Mn)$.

4. A syndrome check is performed as shown in Eqns. (5.4)-(5.8)

$$r \cdot H_1^{(1)} = (\alpha^5, \alpha^3, 0, \alpha^5, \alpha^5, \alpha^4, 1) \cdot (1, 0, \alpha^4, 0, 0, 0, \alpha^5) = 0$$

$$r \cdot H_2^{(1)} = (\alpha^5, \alpha^3, 0, \alpha^5, \alpha^5, \alpha^4, 1) \cdot (0, 1, \alpha^6, 0, 0, 0, \alpha^2) = \alpha^5$$

$$r \cdot H_3^{(1)} = (\alpha^5, \alpha^3, 0, \alpha^5, \alpha^5, \alpha^4, 1) \cdot (0, 0, \alpha^3, 1, 0, 0, \alpha) = \alpha^6$$

$$r \cdot H_4^{(1)} = (\alpha^5, \alpha^3, 0, \alpha^5, \alpha^5, \alpha^4, 1) \cdot (0, 0, \alpha, 0, 1, 0, \alpha^3) = \alpha^2$$

$$r \cdot H_5^{(1)} = (\alpha^5, \alpha^3, 0, \alpha^5, \alpha^5, \alpha^4, 1) \cdot (0, 0, \alpha^5, 0, 0, 1, \alpha^4) = 0.$$

As shown from the equations, the dot product of the hard decision vector r, of dimension $1 \times n$, and each row of the H matrix is performed. This step incurs a complexity of $\mathcal{O}(n^2 h)$.

5. A search function is performed to find out if all the syndrome equations checks. That is the function checks if Eqns. (5.4)-(5.8) for example satisfies the syndrome check. A complexity of $\mathcal{O}(h)$ is incurred at this stage.

6. Finally, if all the syndrome check equations are satisfied, the process is halted. Otherwise, addition and subtraction operations are performed on β based on the outcome of the syndrome check. A complexity of $\mathcal{O}(Mn)$ is incurred at this stage.

Therefore, the complexity of the RS PTA is the total number of operations performed as computed as:

$$\mathcal{O}_{total} = \mathcal{O}(Mn)+\mathcal{O}(h^2)+\mathcal{O}(Mn)+\mathcal{O}(n^2 h)+\mathcal{O}(h)+\mathcal{O}(Mn)$$

$$\mathcal{O}_{total} = \mathcal{O}(3Mn + 2h + n^2 + h^2)$$

$$\mathcal{O}_{total} = \mathcal{O}(3Mn + h(n^2 + h + 1))$$

Note that this computational complexity analysis derived for the RS PTA is for a single iteration.